# Cellulose/polyaniline hybrid nanocomposites

Rana, Ashvinder K.; Scarpa, Fabrizio; Thakur, Vijay Kumar

*Published in:*
Industrial Crops and Products

*DOI:*
10.1016/j.indcrop.2022.115356

Print publication: 01/11/2022

*Document Version*
Publisher's PDF, also known as Version of record

Industrial Crops & Products 187 (2022) 115356

Contents lists available at ScienceDirect

Industrial Crops & Products

journal homepage: www.elsevier.com/locate/indcrop

# Cellulose/polyaniline hybrid nanocomposites: Design, fabrication, and emerging multidimensional applications

Ashvinder K. Rana [a], Fabrizio Scarpa [b], Vijay Kumar Thakur [c,d,e,*]

[a] Department of Chemistry, Sri Sai University, Palampur 176061 India
[b] Bristol Composites Institute, University of Bristol, Bristol BS8 1TR, UK
[c] Biorefining and Advanced Materials Research Center, Scotland's Rural College (SRUC), Kings Buildings, West Mains Road, Edinburgh, UK
[d] School of Engineering, University of Petroleum & Energy Studies (UPES), Dehradun 248007, Uttarakhand, India
[e] Department of Biotechnology, Graphic Era Deemed to be University, Dehradun 248002, Uttarakhand, India

ARTICLE INFO

*Keywords:*
Polyaniline
Water treatment
Tissue engineering
Electromagnetic shielding
Fuel cells

ABSTRACT

Polyaniline, a special class of intrinsic conducting polymers, has a wide range of potential applications in multiple fields, such as in biosensors, electronics devices and biomedical applications. Polyaniline possesses high electrical conductivity, low toxic contents, hydrophilic character, better environmental stability and nano-structured surface characteristics. Polyaniline has however a current limited set of applications because of its low degradation rate and poor processibility; for this reason, polyaniline has been blended with different nano/micro cellulosic biomaterials (i.e. cellulose nano crystals and nano fibers, bacterial cellulose and macro cellulose). Furthermore, cellulose-reinforced polyaniline matrices have shown significant potential for antibacterial agents, antioxidants, sensors, electromagnetic shielding device, adsorbent in water treatment, fuel cells, electrochromic and in biomedical applications. These biodegradable and environmentally benign conducting polymers have also been used in tissue engineering, biosensors, and drug delivery. In the present review article we have surveyed recent advancements in the synthesis process and progress of polyaniline/cellulose based bio-composites for water treatment, electrical devices, biosensors, biomedical application and other areas. The article aims at providing a comprehensive background on the topic, as well as at proposing innovative strategies among investigators for the use of these biobased polymers in future work. The various factors and conditions that impact the adsorption/deterioration behavior of cellulose/PANI composites during the removal of heavy metals, dyes, and other effluents from waste water have also been discussed. Additionally, a comparative view of various fuel cells, electrochromic devices and the electrical and magnetic properties of different cellulose/polyaniline composites has also been provided.

*Abbreviations:* DPPH, 2, 2-diphenyl-1-picryhydrazyl; TEMPO, 2,2,6,6-tetramethylpiperidine-1-oxyl radical; TOCNFs, 6,6-tetramethylpiperidine-1-oxyl oxidized cellulose nano fibrils; AR 4, Acid red 4 dyes; AR-G, Acid Red G; Qm, Adsorption capacities; AD, Alzheimer's disease; AmG, Amino functionalized graphene; APS, Ammonium persulfate; BC, Bacterial cellulose; BH, Berberine hydrochloride; CF, Carbon fiber; CNFIB, Carbonylated nano fibers; CMC, Carboxymethyl cellulose; CF, Cellulose fibers; CNCs, Cellulose nano crystals; CNFs, Cellulose nano fibers; CNWs, Cellulose nano whiskers; CNWs, Cellulose nanowhiskers; CS, Chitosan; CV, Cycling voltammetry; DR23, Direct red 23; SDBS, Dodecylbenzene sulfonate; DBSA, Dodecylbenzene sulfonic acid; ICPs, Electrically conductive polymers; ECG, Electrocardiogram; ECD, Electrochromic devices; EMS, Electromagnetic shielding; EMI, Electromagnetic shielding interference; EDB, Emeraldine base; EDS, Emeraldine-salt; FA, Formic acid; GPE, Gel polymeric electrolyte; GO, Graphene oxide; HEC, Hydroxylethyl cellulose; ITO, Indium tin oxide; ICPs, Inherently conducting polymers; LPG, Liquid petroleum gas; PABS, m-aminobezenesulfonate monomer; MB, Methyl Blue dye; MFC, Microbial fuel cells; MCC, Microcrystalline cellulose; NC, Nanocellulose; NFC, Nanofibrillated cellulose; OD, Optical density; PD, Parkinson's disease; PDS, Peroxydisulfate; PAMPS, Poly(2-acrylamido-2-methyl-1-propane sulfonic acid); PEDOT, Poly(3,4-ethylenedioxythiophene); PVAN, Poly(4-vinylaniline) or polyvinylaniline; PNEANI, Poly(N-ethylaniline); PNMANI, Poly(N-methylaniline); PANI, Polyaniline; PCNFIBA, Polyaniline/carbonylated nano fibers aerogel; MMA, Polymethylmethacrylate; PPA, Polyphenylacetylene; PSS, Polystyrene sulfonate; PVA, Polyvinyl alcohol; PHCFT, Potassium hexacyanoferrate (II) trihydrate; KPS, Potassium persulfate; RL, Reflection loss; RH, Relative humidity; SEM, Scanning electron microscope; SWCNTs, Single-wall carbon nano tubes; AOT, Sodium bis (2 −ethyl hexyl) sulfosuccinate; SDS, Sodium dodecyl sulfate; SDBS, Sodium dodecylbenzene-sulfonate; SVZ, Subventricular zone; SSA, Sulfosalicylic acid; TTAB, Tetradecyltrimethylammonium bromide; TEA, Triethylamine.

* Corresponding author at: Biorefining and Advanced Materials Research Center, Scotland's Rural College (SRUC), Kings Buildings, West Mains Road, Edinburgh, UK.

*E-mail addresses:* ranaashvinder2020@gmail.com, ranaashvinder@gmail.com (A.K. Rana), Vijay.Thakur@sruc.ac.uk (V.K. Thakur).

https://doi.org/10.1016/j.indcrop.2022.115356
Received 13 May 2022; Received in revised form 29 June 2022; Accepted 10 July 2022
Available online 20 July 2022

## 1. Introduction

The majority of polymers behave as insulating materials because of the absence of free moveable electrons or ions. However, some form a conductive path when electrical stress is applied, and their ability to conduct electricity varies depending upon applied conditions. To express the electrical properties of materials/polymers, some most commonly utilized parameters are conductivity, resistivity, dielectric constant, capacitance, dissipation factor, etc. (Das and Prusty, 2012; Shahadat et al., 2017). Inherently conducting polymers (ICPs) are a specific type of synthetic polymers which possess distinctive electro-optic properties because of the presence of conjugated chains with alternating single and double bonds (Skotheim and Reynolds, 2006; Zare et al., 2019). Delocalized and easily polarizable π-electrons heavily influence the electro-optic properties of ICPs. The inherent quasi-one-dimensional character of electrons and the degree of both inter- and intra-chain delocalization of electrons govern a variety of physiochemical properties such as electrical, structural, optical, and antioxidant/antibacterial capabilities.

Until now, a large number of $ICP_S$ such as polypyrrole (Dzulkurnain et al., 2021), polyacetylene (Foyle et al., 2021), polyfuran (Kherroub et al., 2021), polyaniline (PANI) (El-Bery et al., 2021), polythiophene (Oberhaus and Frense, 2021), have been extensively studied and employed in a variety of fields including biomedical (Palza et al., 2019), biosensors (Prajapati and Kandasubramanian, 2019), fuel cell batteries (Mahato et al., 2020), removal of dyes or heavy metals from water (Skotheim and Reynolds, 2006; Thomas and Visakh, 2011a) and electrochromic devices. Their use in these applications has been motivated by their smart responses,. (Skotheim and Reynolds, 2006; Thomas and Visakh, 2011a) Among various ICPs, PANI has received considerable attention because of its low density, ease of preparation, low cost, high electrical conductivity, biocompatibility, low toxicity, and environmental stability (Gong et al., 2020).

However, certain disadvantages such as insolubility or low/partial solubility in common solvents, long chain polymer aggregates, poor processability and infusibility limit the role of PANI in diverse fields. In addition, its electrical conductivity also decreases over a long cycle time (Norouzian et al., 2014). To diminish the aforementioned disadvantages, various approaches like graft copolymerization with derivatives of PANI or other polymers, synthesis in the presence of functionalized organic acids, and preparation of nanocomposites or blends with other natural or synthetic materials have been developed (Abu Hassan Shaari et al., 2021; Najafi Moghadam and Nazarzadeh Zareh, 2010). Materials made from a blend of natural components are preferred because of their eco-friendly and biodegradable nature, and also easy recyclability after use (Hasanin et al., 2021; Vaghela et al., 2016).

Among various natural materials, cellulose, due to its highly hydrophilic and most abundant nature, has drawn considerable attention from researchers working in both industry and research fields (Rana et al., 2021a, 2021b; Rana et al., 2021; Singha and Thakur, 2009; Singha and Thakur, 2009a; Thakur et al., 2013). Different forms of cellulose (C) are available, such as nano crystals (CNCs) (Rana et al., 2021), nano fibers (CNFs) (Shaghaleh et al., 2018; Zhou et al., 2020), bacterial (BC) (Kim et al., 2019), nano whiskers (CNWs) and microcrystalline cellulose (MCC) (Dufresne, 2020; Pradhan et al., 2020). All these forms have been successfully employed in various fields because of their low density, renewable, biodegradable nature and high mechanical properties. Further, the different forms of cellulose can be easily functionalized because of the presence of bulk –OH groups on cellulose backbone and have been successfully blended with other polymers, such as ICPs, poly (caprolactone), poly (acid-lactic), and epoxy to obtain the materials of desired properties (Blaker et al., 2014; Le Hoang et al., 2018; Pappu et al., 2019; Sheng et al., 2014). Extensive work has been done by researchers on the surface functionalization of cellulose and their further blending with different polymer matrices (Singha and Kumar Thakur, 2008; Singha and Thakur, 2008, 2009a) reinforcing agents including PANI. Cellulose is an interesting material to be blended with PANI since it has the potential to exploit the conductive properties or water contaminants adsorbing properties of PANI and also possesses high specific mechanical properties (Hu et al., 2011; Liu et al., 2014).

Cellulose/PANI based nanocomposites are the most alluring ICPs nanocomposites, showing an electrical conductivity due to the combined approach of PANI matrix and cellulose nano fillers (Shahadat et al., 2017). These nanocomposites, with improved conductive, electrical, mechanical, and adsorbing properties, are extensively used in the water treatment industries, electronics devices, and biomedical fields, such as tissue regeneration, drug delivery, and antimicrobial/antioxidant activities (Fu et al., 2015; Shahadat et al., 2017; Zare et al., 2019). In current review articles, we will describe a state-of-the-art update on the water purification, biological/biomedical activities, electrochromic, fuel cells, biosensors, electromagnetic radiation shielding activities of conductive cellulose/PANI based nanocomposites to provide a background for future research (Fig. 1). Moreover, no specific review article about the various synthesis methods and multifunctional applications of cellulose/PANI nano composites have been recently published. This article will be of significant interest to researchers who are working in the water purification industries, as well as in the electronic and biomedical fields. Shahadat et al. (2017) have critically assessed the potential of PANI/biomaterials (chitosan, gelatine, cellulose, proteins and other synthetic biodegradable polymers) in 2017, but in this work we have specially focused our investigation on the prospective of cellulose/PANI nanocomposites.

## 2. Synthesis, structure, and physicochemical properties of polyaniline

### 2.1. Synthesis of polyaniline and their derivatives

PANI is one of the most efficient ICPs and was discovered in the mid of 19th century (Nezakati et al., 2018). The polymeric chain of PANI may contain either quinonoid or benzenoid units or both at the same time, in varying amounts (Visakh, 2018). This conductive polymer is synthesized from monomeric aniline via electrochemical or chemical oxidative polymerization technique under acidic conditions (Fig. 2) (Gospodinova and Terlemezyan, 1998). The most commonly used initiators in the chemical method are potassium persulfate (KPS) and ammonium persulfate (APS) (Thomas and Visakh, 2011b; Visakh, 2018). The chemical technique allows the bulk production of polymer/polymer composites, whereas the electrochemical technique is appropriate only for small-scale production of polymer (Itoi et al., 2017). The electrochemical methods include co-deposition and electrode coating approaches (Menon and Mukherjee, 2004). In the former one, an insulating host material is dissolved in an electrolyte solution consisting of aniline. While in a later one, working, reference and counter electrodes are taken in a single compartment consisting of electrolyte and aniline solution.

Different nano-structured PANI, possessing specific characteristics, have been synthesized by numerous researchers (Shahadat et al., 2017; Zare et al., 2019). Improvement in properties of PANI with variation in nano size and their structure has been reported, and this behavior has been associated with high surface to volume ratio of nano polymer (Freitas et al., 2018). So, utmost care must be taken during the optimizing the synthesis conditions of PANI, since the sizes and specific morphologies of PANI plays a very crucial role in their utility in high-performance applications. Various techniques such as self-assembling, solution, electrochemical and heterophase interfacial polymerizations have been developed to synthesize and design PANI of different nanostructures, including nanorods, nanospheres, nano flowers, nanogranules, nano tubes and nanofibers (Dong et al., 2014; Freitas et al., 2018; Najafi Moghadam and Nazarzadeh Zareh, 2010; Peng et al., 2015; Pierini et al., 2017; Sim and Choi, 2015; Tian et al., 2014) (Fig. 3). In addition to it, other parameters such as oxidant

(initiator) concentration, pH medium, type of solvent, temperature, chemical oxidation process (interfacial reaction), additives, hard or soft nature of template, sonochemistry, electrochemistry and radiochemistry should be full considered and optimized for designing specific PANI nanostructures (Tian et al., 2014).

Efforts have been made by researchers to synthesize the PANI based nano composites to improve the weakness or qualities of pristine PANI (Kong et al., 2015; Zare and Lakouraj, 2014; Zhan et al., 2017). The most commonly utilized techniques for fabrication of PANI based conductive nano composites are in-situ polymerization of PANI in the presence of cellulose or main backbone, solvent casting and in situ nano particles formation in the presence of PANI polymers. Table 1 summarizes the details, advantages, and disadvantages of different methods (Kong et al., 2015; Moghadam et al., 2012; Zare and Lakouraj, 2014; Zhan et al., 2017).

### 2.2. Structure and physicochemical properties of polyaniline

PANI is made up of oxidized (1-y) and reduced (y) blocks ($1 \geq y \geq 0$) (Fig. 4) (Visakh, 2018). PANI may be found in one of three oxidation forms, depending on the redox state of the PANI structure, namely pernigraniline (when $y = 0$), leucoemeraldine (when $y = 1$), and emeraldine (when $y = 0.5$). Out of which, the Emeraldine form of PANI, depending upon basic or acidic conditions employed, further exists in the emeraldine base (EDB) and emeraldine-salt (EDS) forms (M. Kaur et al., 2015; G. Kaur et al., 2015). Out of various PANI forms, EDS is a conductive form of PANI. The electrical resistivity of PANI material depends upon several factors such as temperature, type of dopants used,

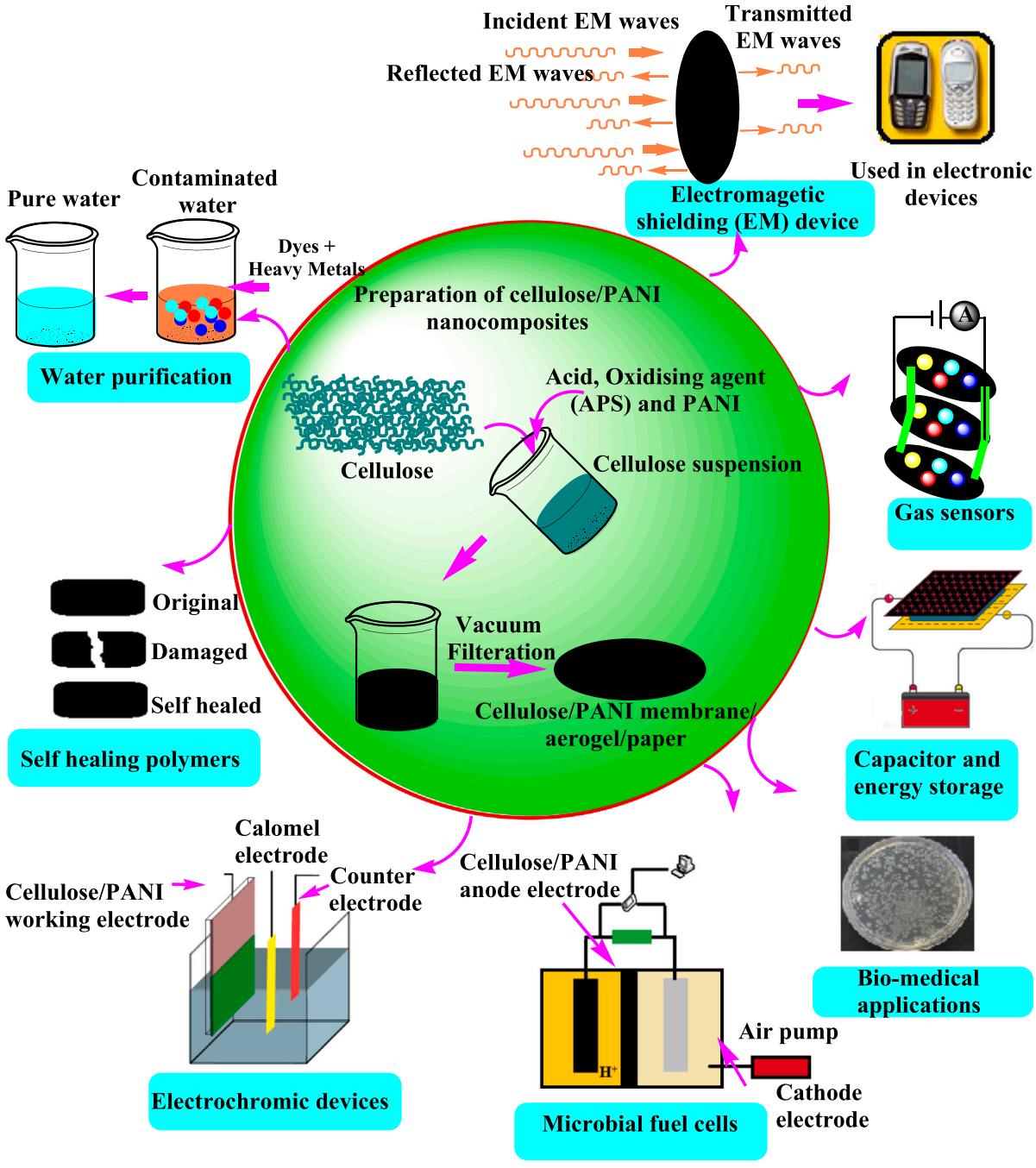


**Fig. 1.** Different applications of cellulose/PANI based nano composites.

redox state and degree of protonation (Thomas and Visakh, 2011b; Visakh, 2018).

EDB is an insulator possess $\sigma \leq 10^{-10}$ S/cm. After doping with suitable acids, it provides with the formation of highly conductive forms of PANI (EDS: $\sigma \geq 1$ S/cm) (Skotheim and Reynolds, 2006). Various organic acids such as *para*-toluene sulfonic, camphorsulfonic and dodecyl benzenesulfonic acids; inorganic acids like sulfuric, hydrochloric, phoshphoric and $HClO_4$ have been utilized for the doping of PANI, whereas a base like ammonium hydroxide is preferred for undoping of PANI (Kakde, 2017; Khalid et al., 2013; Visakh, 2018). Further, the electric properties of PANI-based nano composites rely on the length of PANI chain, the amount of doping, conjugation, molecular orientation and density of the synthesized materials. The physicochemical properties of PANI have been described in Table 2 (Ehsan et al., 2011; Gholami et al., 2017; M. Kaur et al., 2015; G. Kaur et al., 2015; Zare et al., 2020).

## 3. Structure, different forms, physicochemical properties and cost analysis of cellulose

Cellulose $(C_6H_{10}O_5)_n$ is one of the most abundant bio-polymer available on our planet, and its annual worldwide production is more than a thousand tons (Gupta et al., 2016; Singha et al., 2008; Varshney and Naithani, 2011). Out of which, only 5 % is extracted and devoured for applications (Klemm et al., 2005). Among the three main constituents of lignocellulosic biomass (cellulose, hemicelluloses and lignin), cellulose is the major component and it is extracted by employing nitric acid treatment (Klemm et al., 2005; O'sullivan, 1997). The different beneficial properties of cellulose, such as eco-friendly nature, easy availability, surface functionalization nature, low weight, biodegradability and good thermal and mechanical properties, make this material to be utilized in a wide range of assorted applications, including water treatment, biomedical instruments, building construction, automobiles spare parts, cosmetics and polymer composites (Habibi, 2014; Le Gars et al., 2019; Platnieks et al., 2021; Thakur et al., 2022; Zielińska et al., 2021). Cellulose is natural composite in pant biomass, in which lignin and hemicelluloses works as matrix and provides high mechanical strength and flexibility to it (Beluns et al., 2021; Rana et al., 2021d; Uppal et al., 2022; Usmani et al., 2020). Cellulose is made up of β-(1−4)-glycosidic linkage of β-D-glucopyranose $(C_6H_{12}O_6)$ units and contains three equatorial OH groups per unit(Ates et al., 2020; Briede et al., 2022; Le Gars et al., 2019). The monomeric unit of cellulose is cellobiose $(C_{12}H_{22}O_{11})$, which is formed when two glucose or β-D-glucopyranose $(C_6H_{10}O_5)$ units are joined to each other (Gupta et al., 2016; Klemm et al., 2005; Singha and Thakur, 2009; Singha and Thakur, 2009b, 2009c). The cellobiose, due to the presence of OH groups, forms sturdy hydrogen bonds with the contiguous glucose unit in the same chain and with various other surrounding chains and thus responsible for the tight packing of crystalline regions of cellulose fibrils(Thakur and Thakur, 2015; Thakur and Voicu, 2016). The presence of OH groups on its surface also provides the facility for researchers to functionalize cellulosic biomass for desired applications (Singha and Thakur, 2008).

Recently, keeping in view the alluring properties of nano materials, different nano forms of cellulose, such as CNC, CNFs and CNWs, have been synthesized/extracted from lignocellulosic biomass or cellulose by employing various physical, chemical and enzymatic treatments (Rana

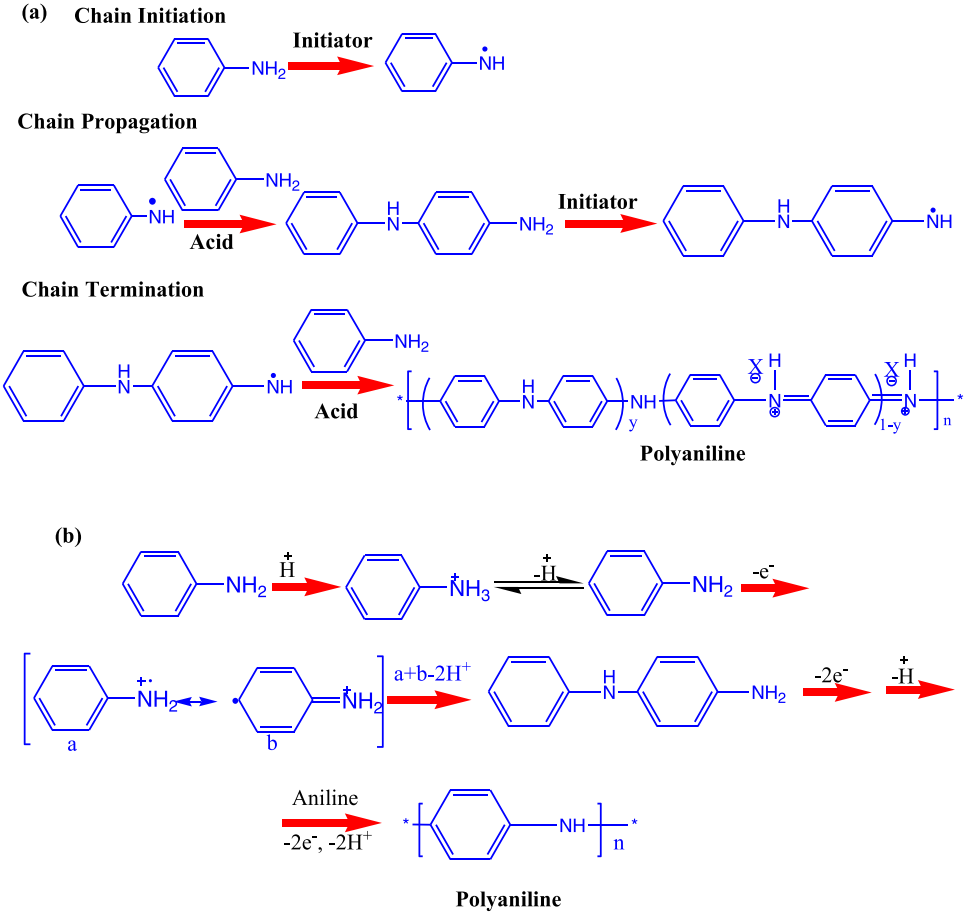


**Fig. 2.** Showing the mechanism pathway for (a) chemical and (b) electrochemical polymerization of PANI. Chemical polymerization is carried out in acidic medium using APS or KPS, whereas the electro-polymerization is carried out in the electrolyte solution of aniline and acid by applying a potential difference between the counter and electrode (Gospodinova and Terlemezyan, 1998). (Figure reproduced from Ref. (Gospodinova and Terlemezyan, 1998) Copyright (1998), Elsevier).

et al., 2021). Bacterial cellulose (BC) is another form of nano cellulose; in contrast to CNC and CNF, it is however produced either through microbial growth, or by using a cell-free enzyme system approach (Ullah et al., 2016, 2015; Volova et al., 2018). For the preparation of CNCs and CNFs top-down approach is used, whereas BC is synthesized via a bottom up approach (Volova et al., 2018). The properties of different nano forms and their extraction process have been given in Table 3 (Abitbol et al., 2016; Lavoine et al., 2012; Moon et al., 2011; Phanthong et al., 2018; Rana et al., 2021c; Rana et al., 2021; Yao et al., 2017; Zheng et al., 2019), and their SEM images have displayed in Fig. 5 (Anžlovar et al., 2018; Carlmark et al., 2012; Choi et al., 2017; Correia et al., 2017; Stanislawska, 2016; Zhou et al., 2020).

The microbial/bacterial technique for the preparation cellulose is however not effective, since it leads to low yields and needs expensive bioreactors and medium components(Manan et al., 2022). Additionally, an in-depth understanding of the biosynthetic process and the extracellular transport in microbial cells is necessary to carry out this microbial/bacterial technique. Through the use of genetic and metabolic modeling tools, efforts have been made to modify the functional characteristics, density, porosity, intrinsic structure, yield, and productivity (Manan et al., 2022). To design various bacterial strains, extensive genetic expertise is necessary. The bacterial strains can be designed either over expression, or the silencing of target genes. Additionally, it has been claimed that BC synthesized (bio-cellulose) made from cell-free enzyme method has superior physical, tensile strength and thermal qualities than BCs produced by microorganisms (Kim et al., 2019; Ullah et al., 2016). Cell free-enzyme techniques, which contrary to microbial cellulose is produced under anaerobic conditions, also yields higher than those from conventional microbial methods (Ullah et al., 2015).

The cost of materials plays an important role for large volumes productions. Production costs of CNC, CNF, and BC are approximately 3.632–4.420 (de Assis et al., 2017), 2.2472–13.6561 (Delgado Aguilar et al., 2015) and 25 USD/kg (Dourado et al., 2016; Zhong, 2020), respectively. Thus, mixing PANI with cellulose would not only reduce the price, but also enhance the general characteristics of PANIs. The production of microbial or bio cellulose from commercial synthetic sugar-based fermentation media is costly and accounts for 30 % of its total production costs. Therefore, efforts have been made to generate inexpensive BC by employing waste biomass to create a fermentation media for the formation of bacterial cellulose(Ul-Islam et al., 2020). These wastes are also rich in monosaccharides, polysaccharides, proteins, minerals and vitamins, and could also provide critical nutrients for microbial growth, as well as acting as carbon source for BC generation. Additionally, according to the ResearchMoz analysis(ResearchMoz QYResearch, 2017), the bacterial cellulose market is predicted to reach US S 497.76 millions by the end of 2022, and is projected to rise to US S 700 million by 2026. Therefore, further efforts are needed to use waste biomass in fermentation media at a rapid scale in this field, in order to lower the cost of producing bacterial cellulose.

## 4. Cellulose/polyaniline based nano composites

Various types of cellulose/PANI based composites have been synthesized and subsequently utilized in water purification, biosensors, electronic devices, etc. The complete details of their applications have been discussed below (Fig. 6). A possible mechanism for the interface

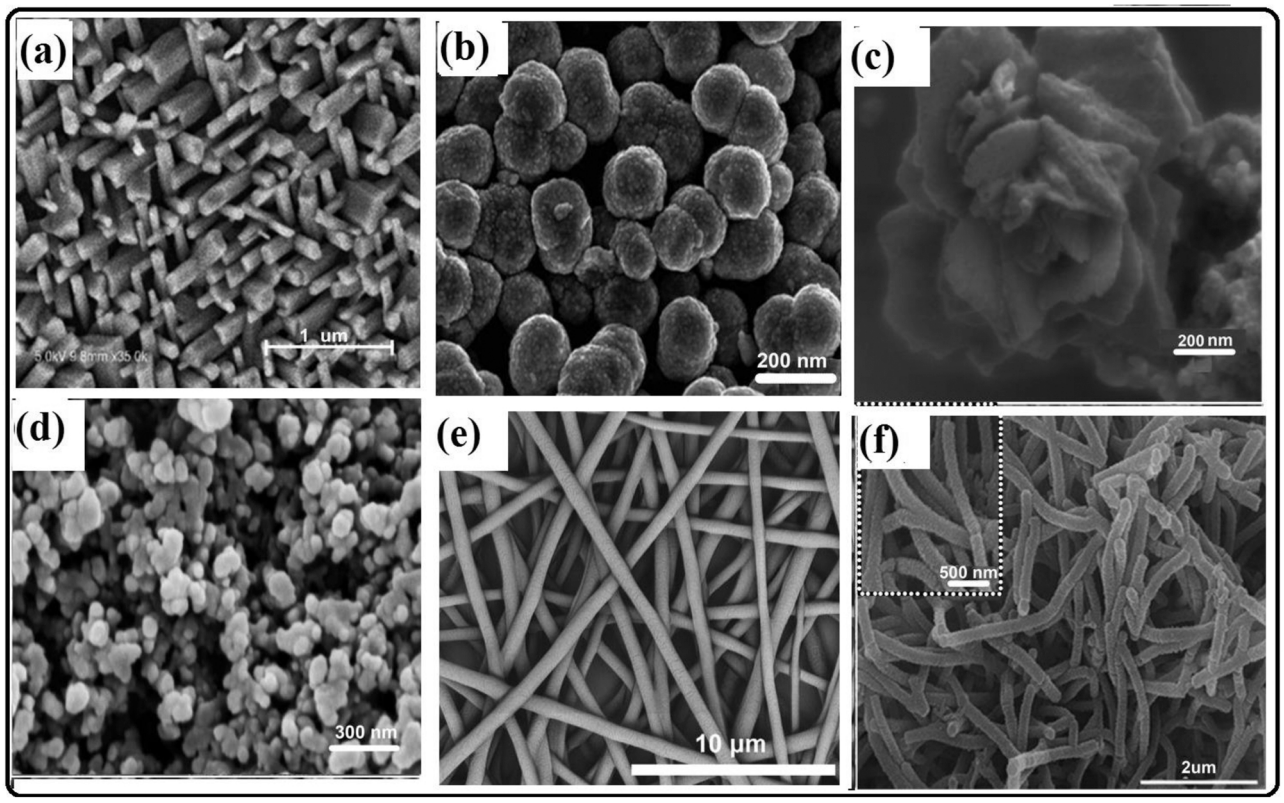


**Fig. 3.** (Dong et al., 2014). (Peng et al., 2015). (Freitas et al., 2018). (Moghadam et al., 2012). Copyright 2017 Hindawi) and (f) PANI nanofiber synthesized by the oxidation polymerization of aniline monomer at 0 °C in the acidic aqueous solution followed by the electrospinning in 50 ml of $CHCl_3$. Copyright 2015 Royal Chemical Society).

(a) Scanning electron microscope (SEM) images of (a) PANI nanorods, prepared by the ultrasonication technique (Reprinted with permission from Ref. (b) Copyright 2014 Royal Chemical Society), (b) PANI nanospheres prepared in the acidic medium (Reprinted with permission from Ref. (c) Copyright 2015 Royal Chemical Society), (c) PANI nanoflowers, prepared in toluene solvent via interfacial polymerization method (Reprinted with permission from Ref. (d) Copyright 2018 Elsevier), (d) PANI nanogranules, prepared in acidic medium utilizing sonochemistry technique, (e) PANI nanotubes, synthesized in oxalic acid solution utilizing micelle soft template procedure (Reprinted with permission from Ref. (e) (Reprinted with permission from Ref (Sim and Choi, 2015).

**Table 1**
Advantages, disadvantages and procedures of different techniques utilized for fabrication of cellulose/PANI based nano composites.

| Type of technique | Procedure | Advantages | Factors affect or disadvantages |
|---|---|---|---|
| *In-situ* polymerization of PANI in the presence of cellulose or other main backbone (Zare and Lakouraj, 2014) | Pristine nanofiller or surface-functionalized nanofillers are taken into monomer and then initiator and dopants are added to synthesize a desired polymer nanocomposite. | Polymer properties are improved in this method<br>No solvent is required<br>By using the dopant, the properties of final product can be controlled.<br>Mostly used technique<br>Excellent purity and homogeneity of resulted product | Amount of initiators, temperature, dopants, etc impact the resulted nano composites<br>Expensive technique<br>Limited amount of useable material may be obtained |
| Solvent Casting ( Kong et al., 2015; Moghadam et al., 2012) | Polymer is initially dissolved in a appropriate solvent and then a desired amount of cellulose or cellulose based nanofillers are added to the solution under constant stirring | Simplest method<br>No specific apparatus is required | Solvent type, temperature, polymer structure, molecular weight, stoichiometric amounts of polymer and frequency of stirring impact the solvent casting technique. |
| *In-situ* nano particles formation in the presence of PANI polymers (Zhan et al., 2017) | PANI solution, obtained after dissolving PANI in appropriate solvent, is used to dissolve nano cellulose, which is subsequently treated thermally or electrochemically to generate polymer nanocomposites. | Costly technique | Appropriate care must be taken during thermal (temperature) or electrochemical treatment |

interaction between PANI and cellulose is sketched in Fig. 7(Kaitsuka et al., 2016). The secondary interaction forces (i.e., hydrogen bonding between the cellulose OH and $NH_2$ groups of aniline) play a major role in the uniform doping of aniline hydrochloride molecules onto cellulose.

### 4.1. Water purification

Cellulose/PANI based nano composites have been successfully employed for adsorption of dyes and chromium (IV) ions from contaminated water. The details of their adsorption behavior and efficiency have been discussed below.

#### 4.1.1. Dye adsorption

The electrostatic interactions between dyes and adsorbing agent and the organic characteristics and structure of adsorbent and dyes play a significant role during the adsorption of dyes from waste water (Raizada et al., 2020; Sharma et al., 2021; Thakur et al., 2018; Verma et al., 2020). Since cellulose has a limited adsorption capacity and a slow removal rate, a number of attempts have lately been made by various researchers to improve its adsorption nature by altering it with amine groups (Anastopoulos and Kyzas, 2014; Qiu et al., 2014b). Low-cost PANI offers a wide range of applications in water treatment, including the removal of organic dyes and heavy metals from wastewaters (Bhaumik et al., 2014; Wang et al., 2013). The preference of PANI over other electrolytes may be attributed to its intrinsic benefits such as ease of synthesis, higher thermal strength (up to 250. 8 °C), quick oxidation–reduction process, and also due to the availability of conveniently accessible sites (nitrogen atoms) for binding a wide range of contaminants (Abbasian et al., 2012; Jaymand, 2013). Thus, combining or associating PANI with cellulose derivatives/different cellulose forms might improve their adsorption ability and removal rate (Ballav et al., 2015; Debnath et al., 2015b; Janaki et al., 2013; Mansour et al., 2011).

The dye adsorbing potential of cellulose/PANI based adsorbent against acidic and basic dyes has been depicted in Table 4 (Abbasian et al., 2017; Debnath et al., 2015a; Herrera et al., 2018; Lyu et al., 2018, 2021; MuDan et al., 2018; Zheng et al., 2012a). The cellulose/PANI based adsorbent showed maximum adsorption for anionic dyes [Congo Red, orange-II dye, orange-G (OG-G), acid red G (AR-G), direct red 23 (DR-23) and methyl orange] at lower pH values, whereas in the case of cationic dyes, maximum adsorption was seen in basic or neutral medium. At high pH, PANI/cellulose or cellulose derivatives based adsorbents exist in its base form with -ve surface charge because of the presence of basic amine and imine (Schiff base) groups and thus absorb strongly +ve charged dyes (Patra and Majhi, 2015). However, in the case of acidic medium, due to polaron and bipolaron sites, adsorbent presented high adsorbing potential towards anionic dyes (Zheng et al., 2012a). The mechanism for possible interaction between cellulose/PANI nano composites and dyes with varying pH has been displayed in Fig. 8 (Khadir et al., 2020; Samadi et al., 2021).

Using an in-situ chemical oxidation polymerization approach, Abbasian et al. (2017) synthesized a variety of cellulose/PANI derivatives using three distinct aniline-based organic molecules, namely PANI, poly(N-ethylaniline) (PNEANI), and poly(N-methylaniline) (PNMANI). The synthesized materials were successfully utilized for adsorption of DR23 and AR 4 dyes from simulated industrial effluents. Among different nano composite adsorbents, Cell/PANI sample showed maximum adsorption capacities (Qm) (117 mg/g and 56 mg/g in the case of AR4 and DR23, respectively), followed by Cell/PNEANI (73 mg/g and 39 mg/g in case of AR4 and DR23, respectively) and Cell/PNMANI nano composites (52 mg/g and 46 mg/g in case of AR4 and DR23, respectively). Further, through regeneration and reusability tests, it has been confirmed that the synthesized nano composites exhibit relatively good reusability after five repetitions of the adsorption–desorption cycles.

Lyu et al. (2021) used a two-step strategy (i.e. in-situ cross-linking followed by acid-induced polymerization) created a 3D PANI/Carbonylated nano fibers (CNFIB) aerogel (PCNFIBA) for the elimination of organic dye pollutants. The resulting PCNFIBA, through pi-pi stacking and electrostatic interactions, showed an impressive compressive strength of 48.2 kPa, and a superior Langmuir adsorption ability of 600.7 (at pH 2; temp-308 k) and 1369.6 mg/g (at pH 10; temp-318 k) against anionic AR-G and cationic MB dye, respectively. Furthermore, Lyu et al. (2018) used an environmentally friendly peroxydisulfate (PDS) process for synergistic regeneration of PCNFIBA adsorbent and oxidation of dyes with $^{\bullet}O_2$ reactive species for the radical deterioration of ARG and PCNFIBA-PDS* system for the nonradical deterioration of both MB and ARG dyes. After three consecutive regeneration cycles further multiple regeneration experiments confirmed that PCNFIBA maintain high adsorption capabilities (approx. 70 % against MB and 84 % for ARG). Additionally, through the adsorption and regeneration process mechanism, it has been confirmed that π-π stacking and electrostatic interactions were responsible for dyes adsorption. In contrast, nonradical reactions play an active role in the oxidation of dyes or contaminants and regeneration of PCNFIBA. The same group also doped PANI nano fibers with alkali-treated sawdust for the easy separation of ARG dyes (Lyu et al., 2018). Consistent with their earlier results, maximum adsorption (212.97 mg/g) was depicted at pH:2 and a temperature of 35 °C.

PANI/CFs were prepared using an in-situ approach and then doped with CdS to make CdS@PANI/CFs photo-nano catalyst. The capacity of

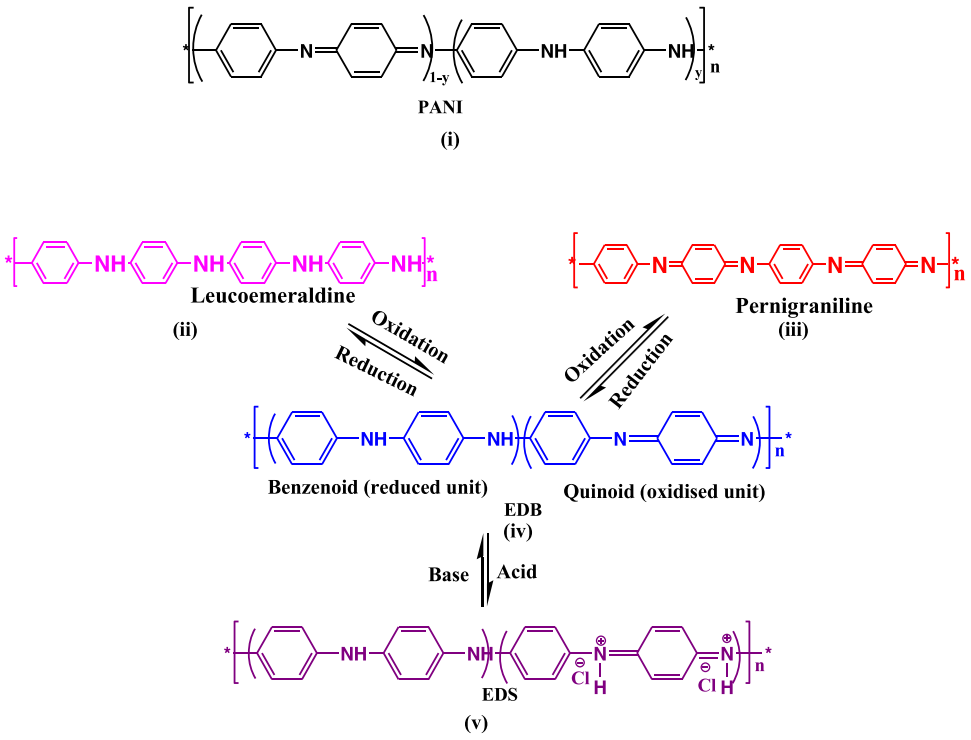


**Fig. 4.** Structure of different forms of PANI: PANI (i), leucoemeraldine (ii), pernigraniline (iii), EDB (iv) and EDS (v) (Gospodinova and Terlemezyan, 1998). (Figure reproduced from Ref. (Gospodinova and Terlemezyan, 1998) Copyright (1998), Elsevier).

**Table 2**
Various physicochemical properties of PANI.

| Properties | Description | Ref. |
|---|---|---|
| Electrical conductivity | Leucoemeraldine, pernigraniline and EDB: insulator; EDS: conductive ($10^{-2}$-100 S/cm) | (Nezakati et al., 2018; Skotheim and Reynolds, 2006; Zare et al., 2019) |
| Dopants commonly used | Organic dopants: *para*-toluene sulfonic acid, camphorsulfonic acid and dodecyl benzenesulfonic acid<br>Inorganic Dopants: $H_3PO_4$, $HClO_4$, HCl and $H_2SO_4$ | (M. Kaur et al., 2015; G. Kaur et al., 2015;Khalid et al., 2013;Visakh, 2018; Zare et al., 2019) |
| Stability in acidic/basic conditions | Highly structural and chemical resistant | (Visakh, 2018; Zare et al., 2019) |
| Solubility | EDS: insoluble in the common organic solvents), EDB soluble in dimethylformamide, tetrahydrofuran and dimethylsulphoxide | (Visakh, 2018; Zare et al., 2020, 2019) |
| Mechanical toughness | Young's Modulus: 1.91 GPa: % elongation: 5.88 | (Gholami et al., 2017; Zare et al., 2019) |
| Crystallinity | Depends upon the type of dopants used and conditions employed during synthesis | (Ehsan et al., 2011; Zare et al., 2019; Zare and Lakouraj, 2014) |
| Thermal stability | $T_g$ for cross linked PANI 250 °C and for uncross linked 70 °C | (Visakh, 2018; Zare et al., 2019) |
| Morphology | May be nanosphere, nanoflower, nanogranule, nanofiber, nanorod and nanotube | (Zare et al., 2019) |

the synthesized CdS@ PANI/CFs composite to degrade methylene blue dye under visible light was investigated, and it was discovered to be 1.5 times better than CdS @ CFs (MuDan et al., 2018). The effect of various reaction parameters on the degradation ratio of MB, such as MB concentration, catalyst dosage, and utilization durations, was explored. Maximum degradation of 90.37 % was achieved with 0.4 gm adsorbent dose, 5 hrs contact times, and 20 mg/L MB concentration. Furthermore, after three uses, the CdS@ PANI/CFs composite demonstrated good reusability with a degradation ratio of 80.36 % against MB. From the above results, we can interpret that cellulose/PANI based adsorbents have great potential to adsorb dyes, but all other factors such as pH, time, adsorbent dosage, type of dyes and dye concentration should be fully considered prior to their large scale applications.

#### 4.1.2. *Heavy metals removal*

The presence of heavy metals in the aquatic ecosystem is causing a severe threat to urban and rural populations worldwide (Hasija et al., 2020; Sudhaik et al., 2022). Different heavy metals such as lead, arsenic, cadmium, chromium and mercury are openly discharged from paint, leather and steel industries into local water bodies (Jahan et al., 2018; Ma et al., 2017; Rana et al., 2022; Wang et al., 2018). Among these metals, hexavalent chromium Cr(VI) is comparatively more toxic, carcinogenic, mutagenic, and teratogenic and thus researchers are prioritizing to eradicate it (Dayan and Paine, 2001; Olad et al., 2021). Cr (VI), in comparison to Cr (III), is highly soluble in an aqueous solution and can easily penetrate into the cell membrane in the form of oxyanions and thus may result in the destruction of lipids, cellular proteins and other organelles. Traditionally and conventionally, many techniques such as ion exchange, precipitation, electro-chemical, electro-coagulation, chemical reduction, reverse osmosis, electrochemical treatment, and membrane-based technologies have been developed and utilized to remove Cr(VI) or other heavy metals (Owlad et al., 2009). However, the major disadvantage of most of these techniques is their operational cost and disposal issue of toxic chemical sludge produced during treatment. Among various technologies, the adsorption technique is cheap, more versatile, energy-efficient and also allows the recovery of adsorbed metal species from the adsorbent by treating with mild acid or base, which can be subsequently reutilized and processed for different manufacturing applications (Jahan et al., 2018).

*In-situ* synthesized PANI-cellulose or cellulose derivatives based adsorbents have been widely utilized for the removal of various heavy metals such as Cr(VI) (Dayan and Paine, 2001; Hosseini and Mousavi, 2021; Jahan et al., 2018; Kumar et al., 2008; Li et al., 2014; Qiu et al., 2014b; Yu et al., 2021; Zheng et al., 2012b), Cu(II) (Jiang et al., 2012),

**Table 3**
Physicochemical properties of some most commonly utilized cellulose forms.

| Properties/ Dimensions | CNCs | CNFs | Cellulosic fiber | BC | Ref. |
|---|---|---|---|---|---|
| Shape | Rod like | Fiber | Fiber | Fiber | (Phanthong et al., 2018; Rana et al., 2021c; Rana et al., 2021) |
| Size | Diameter: 2–20 nm; Length: 100–500 nm; | Diameter:1–100 nm; Length:500–2000 nm; | Diameter: micron; Length: millimeter to meter size | BC Diameter: 25–80 nm in case of microbial cellulose and 70–232 nm in case of bio-cellulose; Length in millimeter | (Phanthong et al., 2018; Rana et al., 2021) |
| % Crystallinity | 54–88 | 45–80 | 44–78 | 45–89 (32.27 in case of bio-cellulose) | (Abitbol et al., 2016; Klemm et al., 2005; Lavoine et al., 2012; O'sullivan, 1997) |
| Extraction/ synthesis technique | Inorganic acid (hydrochloric acid/ phosphoric acid/sulfuric acid) or organic acid (oxalic acid/acetic acid/citric acid) hydrolysis or combination of both acids, deep eutectic solvents treatment, ionic liquids, etc | Mechanical techniques employed. However, to reduce the energy consumption during mechanical destruction, chemical pretreatments such as 2,2,6,6-tetramethylpiperi-dine-1-oxyl radical (TEMPO)-mediated, enzymatic hydrolysis, etc. have also been used. | Extracted from waste biomass via water retting or chemical retting process | Synthesized by bacteria in two stages, namely polymerization and crystallization. In the first stage, synthesis of β-1,4 glucan chains in the cytoplasm of bacteria from residues of glucose occurs, while in the later stage, these glucan chains undergo crystallization to give microfibrils. In addition, it can also be synthesized through cell-free enzyme systems | (Phanthong et al., 2018; Rana et al., 2021;Zheng et al., 2019) |
| Mechanically toughness | Tensile strength: 7500–7700 MPa; Elastic modulus (axial direction): 110–220 GPa | Tensile strength: 357.5 MPa; Elastic modulus: 22.9 GPa | Tensile strength (50 mm length):147–570 MPa | Tensile strength: 14.71 MPa for microbial BC and 17.63 MPa for bio-cellulose | (Moon et al., 2011; Yao et al., 2017) |
| Density (g/ $cm^3$) | 1.6 | 1.5 | 1.2–1.5 | 0.15 ± 0.01 | (Phanthong et al., 2018; Rana et al., 2021) |

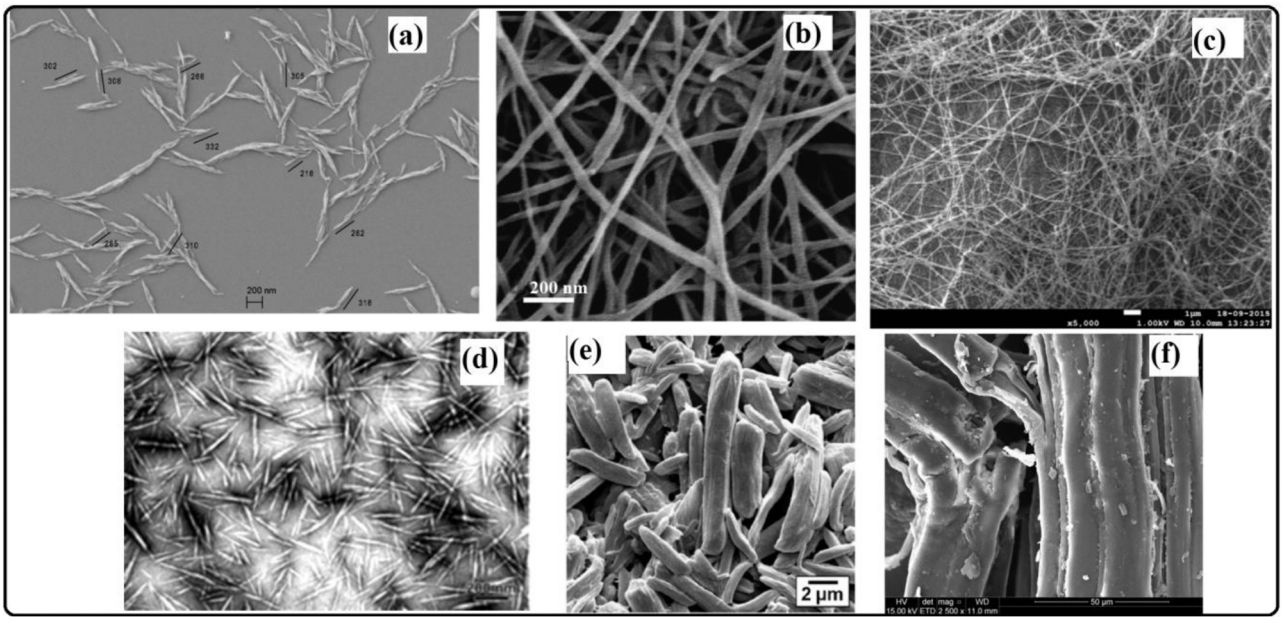


**Fig. 5.** SEM images of (a) CNCs (Anžlovar et al., 2018) (b) CNFs (Zhou et al., 2020), (c) BC (Stanislawska, 2016), (d) CNWs (Carlmark et al., 2012), (e) micro-crystalline cellulose (Choi et al., 2017) and (f) lignocellulosic jute fibers (Correia et al., 2017). All the images have been reproduced under CC licence.

Hg(II) (Ghorbani et al., 2011), Zn(II) (Ghorbani et al., 2012) and Pb(II) (Gapusan and Balela, 2020; Jiang et al., 2012) (Table 5). Most of these adsorption studies were carried out at temperature 25 or 30 ∘C under neutral or acidic conditions. The maximum Qm were found to be between 5 and 250 mg/g. The maximum adsorption for metal anions(e.g. Cr(VI) oxyanions) was observed at lower pH values because of the protonation of imine and amine groups in acidic media, whereas in case of metal cations, maximum adsorption was seen at high pH values (in between 6 and 10) due to the presence of amine groups or –ve charged basic imine (Schiff base). The unique chemical nature, high surface area, better morphology, and different functional groups present onto cellulose/PANI adsorbent play a very significant role in adsorption of heavy metals from contaminated water. Gapusan and Balela synthesized Kapok/PANI nased nano composite through in-situ grafting of PANI,

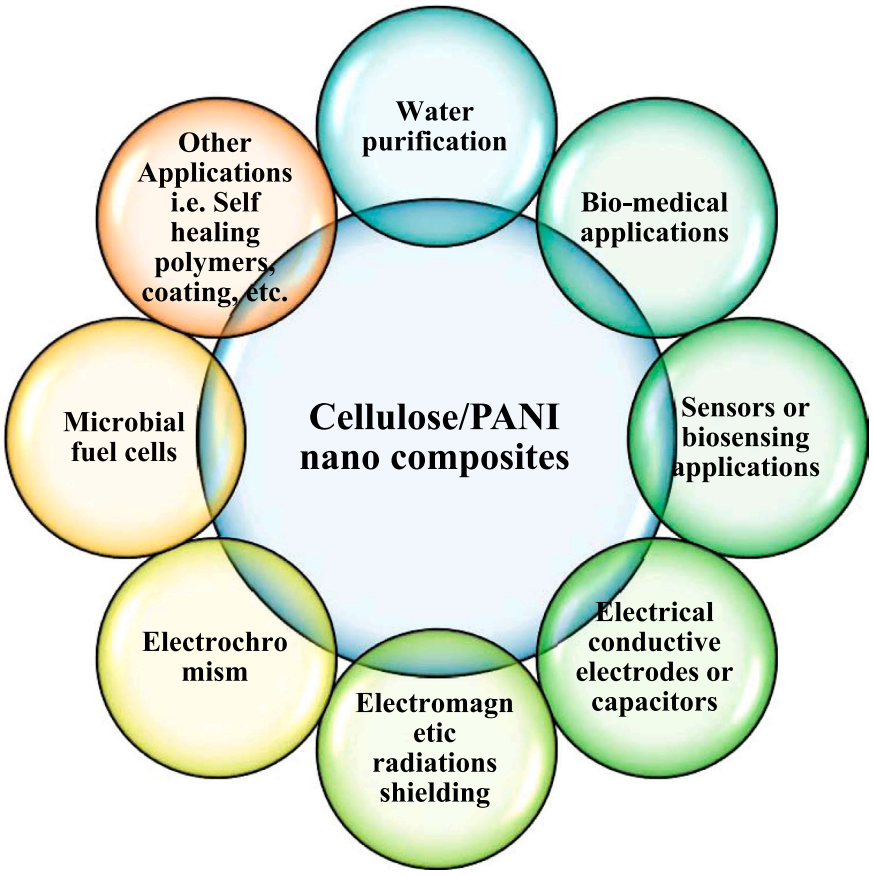


**Fig. 6.** Showing the different possible applications of cellulose/PANI nanocomposites.

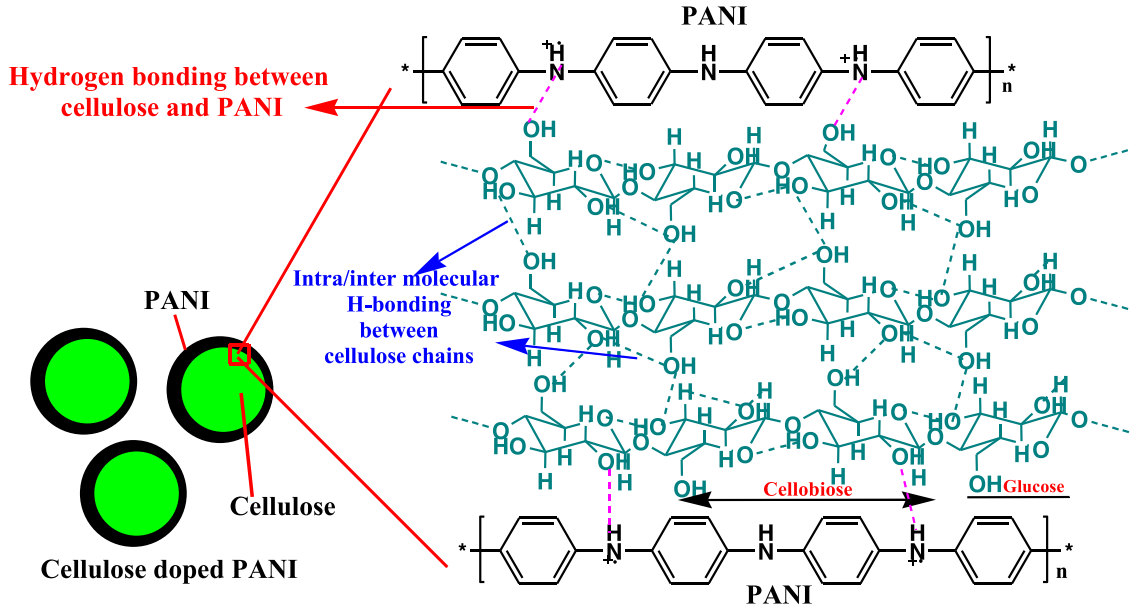


**Fig. 7.** A possible mechanism for interfacial interaction between cellulose and PANI(Kaitsuka et al., 2016).

using APS as oxidizing agent, onto sodium chlorite treated kapok fibers (Fig. 9) (Gapusan and Balela, 2020). The prime aim of using sodium chlorite was to remove the lignin contents or to enhance the hydrophilic character onto kapok fibers for better adsorption of PANI. The Kapok/PANI nano composites showed increase in adsorption ability towards Pd(II) ions with increase in pH (1−10) and temperature (25–65 °C) and was reported to be maximum (97.74 mg/g) at 65 °C. Pb (II) ions in aqueous phase known to exist in following four forms $Pb^{2+}$, $Pb(OH)_2$, $Pb(OH)^+$ and $Pb(OH)_3$ at different pH value. In acidic solution, Pb exist as $Pb^{2+}$, whereas at pH in between 7 and 10, $Pb(OH)_2$ and Pb $(OH)^+$ are the dominant species. Therefore, at lower pH, Pb(II) ions removal is not favorable because of the electrostatic repulsion between

**Table 4**
Dyes adsorption capacity of cellulose/PANI based adsorbents.

| Cellulose/PANI adsorbent (dosage amount) | pH | Time | Temperature (°C) | Dye (concentration) | Adsorption capacity (Q (mg/g) | Ref. |
|---|---|---|---|---|---|---|
| PANI/Kapok nano composite (40 mg) | 6 | 24 hrs | 25<br>45<br>65 | Methyl orange (200 ppm) | 136.75<br>166.25<br>218.26 | (Zheng et al., 2012a) |
| Cellulose/PANI (1 g/L) | 2 | 90 min | 25 | AR4 (10 ppm) | 117 | (Abbasian et al., 2017) |
| | | | | DR23(10 ppm) | 56 | |
| Cellulose/PNMANI(1 g/L) | 2 | 90 min | 25 | AR4 (10 ppm) | 52 | (Abbasian et al., 2017) |
| | | | | DR23(10 ppm) | 74 | |
| Cellulose/PNEANI(1 g/L) | 2 | 90 min | 25 | AR4 (10 ppm) | 73 | (Abbasian et al., 2017) |
| | | | | DR23(10 ppm) | 79 | |
| PANI/CNFs gel (1 g/L) | 2<br>10 | – | 35<br>45 | AR-G (500 mg/l)<br>Methylene blue (MB) (500 mg/l) | 600.7<br>1369.6 | (Lyu et al., 2021) |
| PANI-nano fibers/saw dust (2 g/l) | 2 | 120 min | 35 | AR-G (300 mg/l) | 212.97 | (Lyu et al., 2018) |
| PANI-kapok fiber (1 g/l) | 3 | 300 min | 30 | Congo red anionic dye (400 mg/L)<br>OG-II(400 mg/L)<br>OG-G (400 mg/L) | 40.8<br>188.7<br>132.3 | (Zheng et al., 2012a) |
| PANI-kapok fiber (30 mg) | 4.3 | 24 hrs | 25 | Methyl orange anionic dye (40–280 ppm)s | 75.76 | (Herrera et al., 2018) |
| PANI-lignocellulose (0.69 g/l) | 4.3 | 90 min | 25 | Congo red anionic dye (28.5 mg/l) | 1672.5 | (Debnath et al., 2015a) |
| CdS@ PANI/CFs composite (0.4 gm) | – | 5 hrs | – | MB (20 mg/L) | – | (MuDan et al., 2018) |

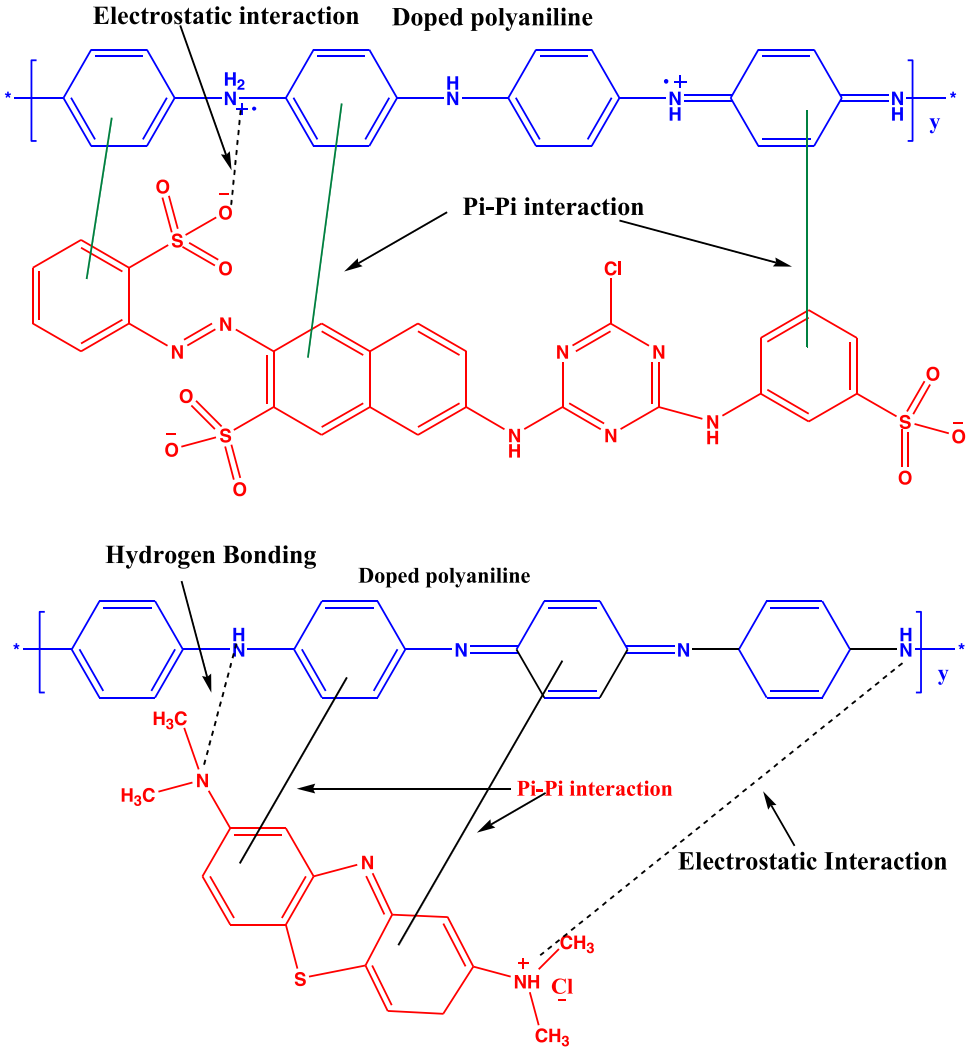


**Fig. 8.** Schematic illustration of the possible mechanisms for the adsorption of cationic (top) and anionic (below) organic dyes by using cellulose/PANI based adsorbents (Samadi et al., 2021). [Figure prepared from Ref. (Khadir et al., 2020; Samadi et al., 2021)].

**Table 5**
The adsorption capacity of cellulose/PANI adsorbents towards some heavy metals.

| Cellulose/PANI adsorbent | pH | Temperature (°C) | Pollutants removal | Qm (mg/g) | Ref. |
|---|---|---|---|---|---|
| PANI coated ethyl cellulose | 1 | – | Cr(VI) | 38.8 | (Qiu et al., 2014b) |
| PANI/ BC mat | 7 | 25 | Cr(VI) | – | (Jiang et al., 2012) |
| BC/PANI/SDBS | 7 | 25 | Cr(VI) | 189 | (Hosseini and Mousavi, 2021) |
| Carboxymethyl cellulose (CMC)/ PANI) interpenetrated network | 2 | 25 | Cr(VI) | 136.98 | (Dayan and Paine, 2001) |
| BC/PANI/SDS | 7 | 25 | Cr(VI) | 151 | (Hosseini and Mousavi, 2021) |
| TOCNFs-PABS | 3 | – | Cr(VI) | 5.263 | (Yu et al., 2021) |
| PANI/cell ulose acetate composite membrane | 2 | 30 | Cr(VI) | 94.34 | (Li et al., 2014) |
| PANI-kapok fiber | 4–5 | 30 | Cr(VI) | 66.2 | (Zheng et al., 2012b) |
| PANI/jute fiber | 3 | 20 | Cr(VI) | 62.9 | (Kumar et al., 2008) |
| PANI/CA | 3–7 | 25 | Cu(II)<br>Pb(II) | 68.0<br>251.3 | (Jiang et al., 2012) |
| PANI/RHA | 9 | 25 | Hg(II) | – | (Ghorbani et al., 2011) |
| PANI/RHA | 3 | 25 | Zn(II) | 24.3 | (Ghorbani et al., 2012) |
| PANI/Kapok | 10 | 25 | Pb(II) | 63.60 | (Gapusan and Balela, 2020) |

the positively charged EDS PANI and $Pb^{2+}$. However, removal is favorable at higher pH, because of simultaneous precipitation of Pb $(OH)_2$ and adsorption of Pb(OH)+ onto EDB or deprotonated PANI (Gapusan and Balela, 2020). Further adsorption was noticed to follow pseudo second order kinetics and best explained by Langmuir isothermal model.

Cellulose/PANI based adsorbents play a very significant role in the removal of Cr (IV) ions, which works by adsorbing negatively charged Cr (VI) complexes such as $Cr_2O_7^{2-}$, $HCrO^{4-}$ and $CrO_4^{2-}$ via protonated amine and imine groups present onto PANI chain and then reducing them to Cr (III) ions or by hydrogen bonding, van der Waals or electrostatic interaction with cellulose OH groups (Gu et al., 2012; Qiu et al., 2014b, 2014a). Out of three different forms of Cr(VI) metals, i.e., $Cr_2O_7^{2-}$, $HCrO^{4-}$ and $CrO_4^{2-}$, $Cr_2O_7^{2-}$ and $HCrO^{4-}$ forms exists at pH < 6; whereas $CrO_4^{2-}$ forms prevail at neutral pH (Zhang et al., 2019). The Cr(III) ions, generated after reduction, often revert back to the solution due to electrostatic repulsion from the adsorbent surface, posing further environmental and health risks. A high adsorption rate does not guarantee that all Cr ions have been eliminated; it is possible that Cr(VI) ions have been restored to the solution after being reduced to Cr (III) or that the desorption rate has been raised. Thus, to remove Cr(VI) from an aqueous solution, a correct balance or a comprehensive knowledge of the kinetics of adsorption, reduction, and desorption is required (Krishna et al., 2000; Miretzky and Cirelli, 2010; Mohan et al., 2006). Traditionally, attempts were made to adsorb Cr metals in an acidic medium using PANI based adsorbent (Jiang et al., 2018; Qiu et al., 2015). However, due to the degrading nature of cellulose in the cellulose/PANI blend at low pH, researchers are nowadays also attempting to remove the heavy metals at neutral pH.

Jahan et al. (2018) remove Cr(VI) ions from drinking water using a PANI/BC mat at neutral pH. In contrast to absorption in an acidic medium (where adsorption is the rate-determining phase), desorption of reduced Cr(III) from the PANI/BC adsorbent was observed to be the rate-determining step in this case and was confirmed through the Langmuir–Hinshelwood kinetic model for the adsorption–reduction–desorption processes. Hosseini and Mousavi (2021) used sodium dodecyl sulfate (SDS) and sodium dodecylbenzene-sulfonate (SDBS) surfactants to make BC/PANI-based aerogels with various surface morphologies. With SDS and SDBS, the synthesized BC/PANI displayed a cluster of grapes and thistle-like forms, respectively.

Further, between BC/PANI/SDBS (BPDB) and BC/PANI/SDS (BPDS) aerogels, the former showed the highest adsorption capacity (189 mg/g) than the later one (151 mg/g), when tested against Cr(VI) complexes for 24 h at neutral pH. The synthesized aerogels were recycled five times, and the re-adsorption capability of BPDB and BPDS was noticed to decrease by up to 68 % and 59 %, respectively. The better removal efficiencies of BC/PANI/SDBS than BC/PANI/SDS aerogels for Cr(VI) ions have been attributed to the higher ratio of amine to imine functional groups in BC/PANI/SDBS in comparison to BC/PANI/SDS nanoaerogels. With both the aerogels, the maximum adsorption efficiencies were recorded at pH 1, and as the pH values increased, the adsorption efficiencies decreased (Fig. 10). The figure displayed the variation in zeta potential and adsorption characteristics of BC/PANI/SDBS and BC/PANI/SDS aerogels towards Cr(IV) and Cr (III) at different pH. In contrast to Cr(VI) ions, adsorption effectiveness against Cr(III) ions has been found to increase with increase in pH up to 7. This behavior has been assigned because of the dominance of the anionic character onto aerogels at neutral pH and cationic character at low pH < 2.

Yu et al. (2021) graft copolymerized m-aminobezenesulfonate monomer (PABS), an aniline derivative, onto 6,6-tetramethylpiperidine-1-oxyl oxidized cellulose nano fibrils (TOCNFs). Prior to grafting onto TOCNFs, it was first activated to TOCNFs-Cl by treating with oxalyl chloride under a nitrogen atmosphere and then treated with PABS to produce the TOCNFs-PABS. The synthesized bio adsorbent, TOCNFs-PABS, was found to have almost cent percent adsorption ability against Cr(VI) ions at a pH < 3. Further, the adsorption was noticed to obey pseudo-second-order kinetics and follow the Langmuir adsorption model. The TOCNFs-PABS bio adsorbent showed ten times higher adsorption efficiency towards Cr(VI) in comparison to TOCNF, and also resulted in a reduction of Cr(VI) ions to Cr(III) ions during the adsorption process. TOCNFs-DABS could so detoxify and adsorb Cr(VI) synchronously. The improved adsorption at low pH is attributed to substantial protonation of amine groups to either $–NH^{2+}$ and $–NH^{3+}$ groups, which can boost the electrostatic attraction between +ve charged amine groups and -ve charged Cr anion species. Qiu et al. (2014b) coated PANI onto ethylcellulose and reported that the resulting polymer had a remarkable ability to remove Cr(VI) ions. From above discussion we can conclude that in addition to Cr(VI), cellulose/PANI plays a significant role in removing heavy metals from waste water.

#### 4.1.3. Other effluents

In addition to dyes and heavy metals, PANI@Ag doped regenerated cellulose fibers (CF) were utilized for the reduction of p-nitrophenol to p-aminophenol in contaminated water (Cheng et al., 2021). Cotton linter pulps were dissolved in NaOH/urea aqueous solvent systems using a scalable wet-spinning technique to create regenerated CFs with 3D micro- and nanoporous architectures. PANI was used as a reducing agent to dope Ag nano particles into the regenerated CFs. The synthesized CFs/PANI@Ag demonstrated great catalytic activity for the degradation

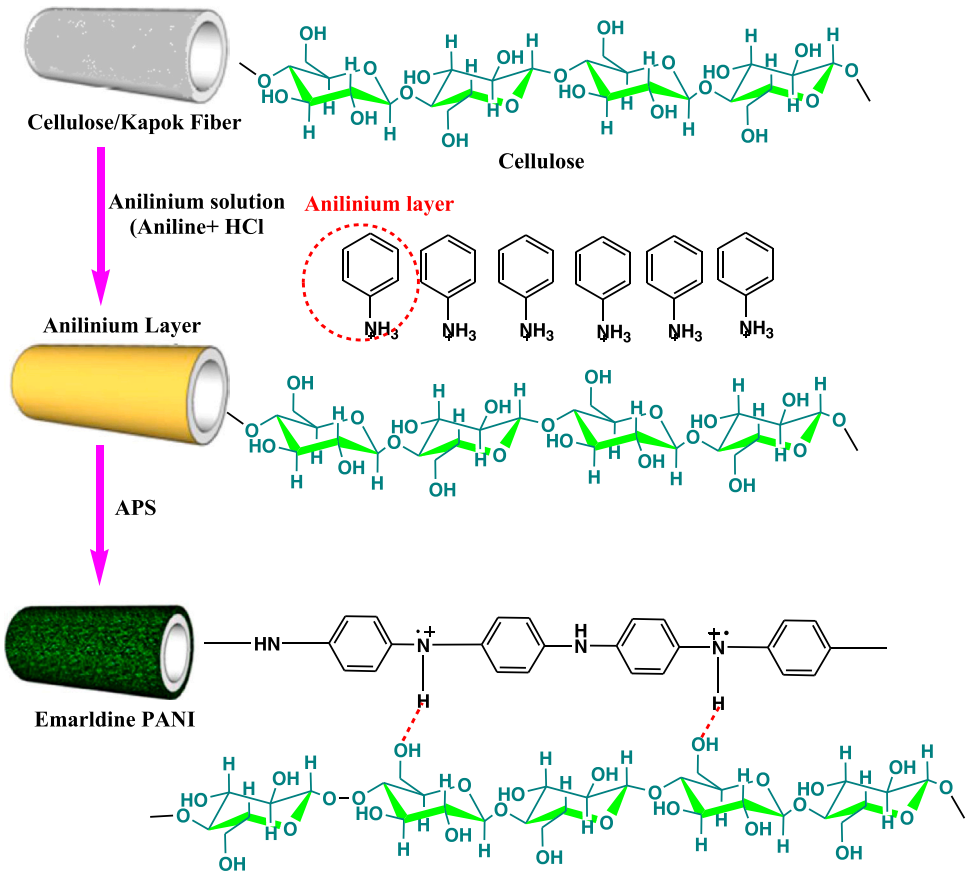


**Fig. 9.** *In-situ* oxidative polymerization mechanism of aniline on the surface of lignocellulosic kapok fiber. (Reproduced with permission from Ref. (Gapusan and Balela, 2020) Copyright 2020, Elsevier).

of p-nitrophenol to p-aminophenol.

### 4.2. Bio-medical applications

BC or nano cellulose has opened up the important and rapidly expanding fields of medicine and life sciences (Kumar et al., 2022; Yue et al., 2016). Nanocellulose (NC) showed a tremendous potential to monitor bio-potential signals upon blending with conductive PANI or as anti-bacterial material after subsequent doping with metal or metal oxide or metal nitrate nano particles (Chen et al., 2016; Zhang et al., 2018).

#### 4.2.1. Bio-potential monitoring

Traditional Ag/AgCl gel electrodes, which require a conductive gel for successful operation, are widely utilized in clinical bio-potential monitoring. However, the long term use of gel generally causes swelling, itchiness and reddening and thus may further lead to the trapping of bacteria on the skin. Therefore, due to the high risk of skin irritation, these electrodes are not suitable for long term monitoring (Zhang et al., 2018). Considering gel electrodes drawbacks, Zhang et al. (2018) developed a dry and flexible BC/PANI/$AgNO_3$ nano composite membrane for long term bio-potential signal monitoring. The purpose of doping of BC with PANI conductive material was to develop potential onto BC to monitor bio-potential signal, whereas subsequent doping of silver nitrate was done to enhance the antibacterial properties of BC/PANI for long term utility. The synthesized BC/PANI/$AgNO_3$ nano composite membrane showed skin-electrode contact impedance lower than the traditional Ag/AgCl gel electrode, hundred percent antibacterial activities against *S. aureus* and *E. coli* bacteria, and noise-free/stable electrocardiogram (ECG) waveforms signals. Further, flexible membrane electrodes provided high waveform fidelity of about 99.49 % after 800 ECG cardiac cycles. They maintained it to be 98.40 % when the membrane was born for 24 hrs and recorded for the same number of cardiac cycles. Due to low skin-electrode contact impedance, comparatively high fidelity for ECG monitoring, and significant anti-bacterial properties, the flexible BC/PANI/$AgNO_3$ membrane electrode has great potential than Ag/AgCl gel electrodes to be utilized in bio-potential monitoring. In light of the aforementioned advantages, we should consider the practical utility of BC/PANI/$AgNO_3$ membranes for long term medical practices.

#### 4.2.2. Antibacterial activities

Chitosan (CS)/hydroxylethyl cellulose (HEC)/PANI nanocomposites hydrogel loaded with 0, 1, 3 & 5% ratio of graphene oxide(GO)@Ag-nano particles were tested for their antibacterial activities against *Candida albicans*, *Staphylococcus aureus, Bacillus subtilis*, *Escherichia coli* and *Kelbsilla pneumonla* (Youssef et al., 2021). The antibacterial properties and electrical conductivities ($8.53 \times 10^{-2}$ S/cm) of fabricated nano composites were found to increase with an increase in percent ratio of GO@Ag-NPs. The best antibacterial property (inhibition zone) was found in the case of CS/HEC/PANI /5GO@Ag-NP against all the five microbes (*S. aureus:*$20 \pm 0.99$ mm, *B. subtilis:* $23 \pm 1$ mm, *E. coli:* $21 \pm 0.98$ mm, *K. pneumonla:* $17 \pm 0.98$ mm and *C. albicans*: $18 \pm 0.78$ mm, whereas CS/HEC/PANI /0GO@Ag-NP showed the lowest bacterial resistance ($4 \pm 0.82$ mm, $3 \pm 0.62$ mm, $3 \pm 0.25$ mm, $9 \pm 0.71$ mm and $5 \pm 0.67$ mm, respectively). The higher performance of CS/HEC/PANI /5GO@Ag-NP has been attributed to better loading of antibacterial Ag-NPs, which works either by inhibiting enzymatic systems on respiratory system and thus altering DNA synthesis, or by altering the bacterial cell wall structure, creating more hole and thus more accumulation of NPs leading to ultimately death of cells. The better loading of antibacterial Ag-NPs may also produce radicals upon

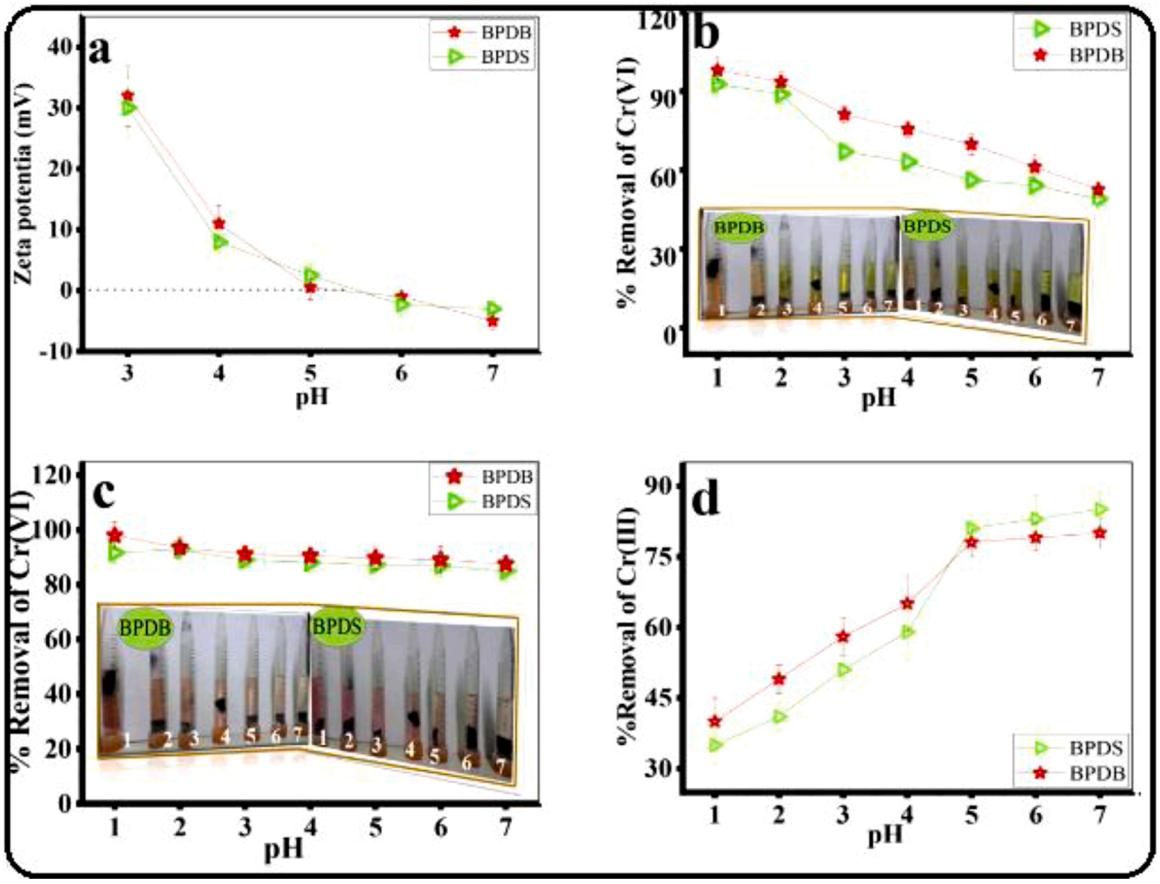


**Fig. 10.** (a) Zeta potential measurements, the influence of pH on removal rate of Cr(VI) after (b) 10 hrs, (c) 24 hrs, and (d) Cr(III) adsorption percentage for BPDB and BPDS. (Reprinted with permission from Ref. (Hosseini and Mousavi, 2021) Copyright 2021 Elsevier).

reaction with the microbes cells, leading to the generation of pits onto the cell wall and finally the death of the microbe (Durán et al., 2016; Wang et al., 2017).

Hosseini et al. (2020) found that depositing PANI onto the surface of BC/Ag-NP hydrogels polymerized in the presence of hydrochloric acid and polyethylene glycol medium, reduces significantly the antibacterial activity of parent BC/Ag-NPs hydrogels against *E. coli* and *S. aureus*. The poor performance of BC/Ag-NPs after deposition of PANI was attributed to a reduction in the effective contact of Ag with bacteria after the post-coating phase. Furthermore, no favorable impact of PANIs against gram +ve and -ve bacteria was demonstrated. Liu et al. (2018) coated both pre-synthesized nanofibrillated cellulose (NFC) /Ag/ PANI and NFC/PANI nano composites onto paper (75 g/cm$^2$) and subsequently tested the pristine paper and as-obtained materials for their antibacterial properties against *E. Coli*. The pristine paper showed zero % growth inhibition. However, when loaded with the NFC/PANI (8.1 g/m$^2$) and NFC /Ag/ PANI (8.1 g/m$^2$), the paper showed an increase of 47.1 % and 100 % in the growth inhibition of bacteria (Fig. 11).

Cellulose/PANI (Shalini et al., 2016) and cellulose/PANI/cobalt ferrite nano composites (Abou Hammad et al., 2019) membranes were developed and utilized for their antibacterial properties against *Staphylococcus aureus* (Inhibitory zone: 16 ± 0.43 mm) and *E. coli* (13 ± 0.45 mm). The antibacterial properties were also tested against *E. coli* (87.4 ± 1.2), *Bacillussubtilis* (78.3 ± 1.3) and *Candida albicans* (59.5 ± 1.0 mm). An increase in conductivity up to 3.5 × $10^{-3}$ S/cm was reported for cellulose/PANI/cobalt ferrite nano composites. From the above cited references, we can conclude that cellulose/PANI-based nano composites have remarkable capacities in terms of elimination of germs, or can significantly reduce the bacterial loads. Additionally, ternary nano fillers like silver nano particles have been proved to significantly

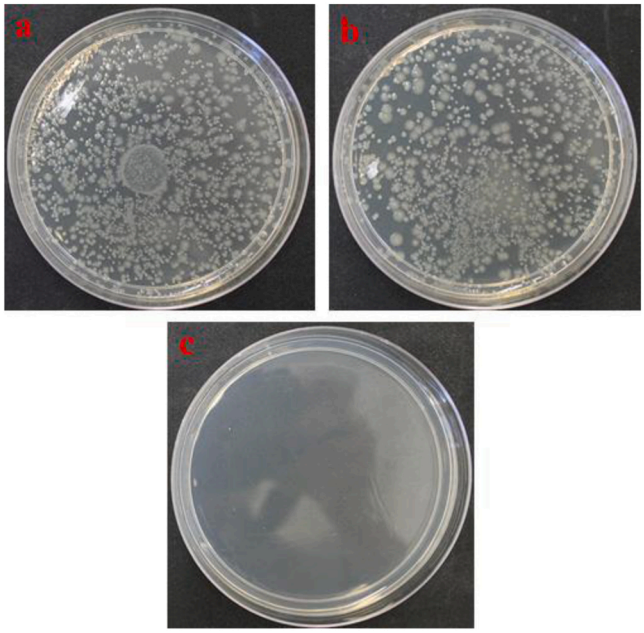


**Fig. 11.** Antibacterial activities of (a) the pristine paper and the paper coated with the (b) NFC/PANI and (c) NFC/Ag/PANI nanocomposites against *E. coli* (Liu et al., 2018). Copyright 2018 Elsevier).
(Reprinted with permission from Ref (Liu et al., 2018).

enhance the antibacterial activities of the cellulose/PANI based nano composites.

#### 4.2.3. Antioxidant properties

The ability of scavenging radicals or the antioxidant properties in packaging materials play an important role in the protection of food from deterioration. Efforts have been also made to develop PANI/cellulose based antioxidant packaging materials. PANI coated polymethylmethacrylate (MMA)/ CNCs (1, 3 & 5 wt%) composite membranes were evaluated for their antibacterial activities against *Bacillus cereus* and *Salmonella typhimurium* bacteria by measuring the optical density (OD) at 600 nm, as a measure of bacteria growth, as well for their antioxidant properties by evaluating the radical quenching activities against 2, 2-diphenyl-1-picryhydrazyl (DPPH) (Abdel Rehim et al., 2020). It has been noted that antibacterial activity of composite membranes rises with an increase in % proportions (1–5 wt%) of CNCs and was found to maximum when stacked with 5 wt% of CNCs, which reduces the viabilities of bacteria cells by about 25 %.

Further, the same pattern was seen when PANI coated membranes loaded with different amounts of CNCs were tested for antioxidant capabilities. When evaluated for 20 min, a maximum of 25 % inhibitory activity was recorded for 5 wt% CNCs stacked PANI-coated films, followed by 3 (15 %) and 1 % (12 %) CNCs stacked films, and was reported to increase up to 45 % with further increases in timing up to 240 min. We can infer from the above information that cellulose/PANI nanocomposites have significant abilities to be used in food packaging applications.

#### 4.2.4. Tissue engineering and biosensing

Poly(4-vinylaniline) (PVAN)/PANI functionalized BC membranes were developed and tested for their toxic nature against neural stem cells, isolated from the subventricular zone (SVZ) of postnatal mice, after growing in proliferation medium for possible applications in the neural sector. An increase in cell viability from 80% to 90% was observed with PVAN/PANI/BC membrane when compared to pristine BC (A. Rebelo et al., 2019; A.R. Rebelo et al., 2019). Cellulose/PANI based conductive hydrogel, having hierarchical nano/microstructure, was synthesized via interfacial polymerization methodology for the possible utilization as a scaffold material of neurons for sciatic nerve regeneration in rats (Xu et al., 2016). Because of its hierarchical structure, the resulted material showed increased electrical conductivity and a high potential for the extension of neurons, confirming a high potential for desired biomedical applications. For sensing cholesterol, PANI/NC/ionic liquid functionalized screen-printed electrode was developed by Abdi et al. (Abdi et al., 2019). The sensing electrode showed a detection limit of 0.48 u M and a sensitivity of 35.19 uA mM/cm$^{-2}$ in the range 1–12 mM.

#### 4.2.5. Drug delivery

Cellulose/PANI nano composites have also been used for developing drug delivery systems because of their attractive non-cytotoxic and electroactive properties. Li et al. (Department of Biomedical Engineering, College of Life Science and Technology, Huazhong University of Science and Technology, Wuhan 430074, PR China et al., 2018) diffused berberine hydrochloride (BH) drug onto pre synthesized BC/PANI hydrogel to develop a pH-electroactive controlled drug release system. When investigated under pH ranging from 2.2 to 11 in vitro, the synthesized electroactive hydrogels showed different drug release characteristics. Compared to acidic conditions (37 % drug release at pH: 2.2), a better drug release behavior was observed for hydrogels in a basic medium (69 % release at 11 pH). In contrast to Li et al., Jasim and co-workers preferred the reduction method for loading of BH drug and evaluated the antibacterial activity of synthesized BC/PANI/BH composite films against *Pseudomonas auroginosa* (*P. auroginasa*) and *E. coli*, and *Candida albicanis* utilizing the paper disk diffusion technique (Jasim, 2017). The zone of inhibition against *P. auroginasa*, *E. coli*, and *Candida albicanis* was found to be 5.8 mm, 7 and 7.3 mm, respectively. Further, no signs of cytotoxicity of BC/PANI/BH composite films for Hella cells and L-02 cells were reported by them. In order to develop efficient cellulose/PANI nanocomposites-based drug delivery systems, additional efforts must be put in place to provide an effective loading of drugs and to determine how the systems behave under different pH levels.

### 4.3. Sensors or biosensing applications

For the development of sensors, PANI was oxidatively polymerized onto cellulose or cellulose-based materials using HCl or a combination of other compounds such as sulfosalicylic acid (SSA) and poly(2-acrylamido-2-methyl-1-propane sulfonic acid) (PAMPS) or dodecylbenzene sulfonic acid (DBSA) and PAMPS, etc. as a doping agent. The prime aim to incorporate cellulose was to enhance the sensing ability of PANI as cellulose increases the porous nature of resulted composite materials (Yang et al., 2020).

Dubey and Arora (2021) employed SDBS and tetradecyltrimethylammonium bromide (TTAB) surfactants as soft templates for the fabrication of PANI/cellulose nano biosensors. Further, by utilizing cycling voltammetry (CV) measurements, it has been confirmed that synthesized composites are electrochemically active. PANI/cellulose/SDBS composite displayed maximum response at pH-5, whereas PANI/cellulose/TTAB was found to exhibit an irregular pattern. In addition, CV results of PANI/cellulose/surfactants at varying pH confirm its compatibility in different biosensing devices working at lower pH with a short response time.

Due to its porous 3D framework and thin ribbon-like microfibrils, BC possesses much higher tensile stability than plant cellulose and can also retain more significant amounts of water (about 99 % in weight) (Wang et al., 2019). Given the benefits of BC and its non-cytotoxic nature, the US Food and Drug Administration has approved it for a wide range of biomedical applications (Petersen and Gatenholm, 2011). The BC surface can be modified with new functionalities to acquire a certain range of electrical conductivity by grafting, blending, or mixing with metal or metal oxide nano particles, carbon nano tubes, ionic solutions, and ICPs like PANI, polypyrrole, and others (Lee et al., 2012; Poddar and Dikshit, 2021). PANI is the most adaptable conducting polymer among the several ICPs, with extensive applications in optics, bio-sensing, and electronics (Bhadra et al., 2009; Li, 2015). It exhibits conductivity ranging from $10^{-10}$ to $10^{5}$ S/cm, is environmentally stable, and has a reversible and straightforward doping chemistry that allows control over conductivity customization.

Rebelo and co-workers (A. Rebelo et al., 2019; A.R. Rebelo et al., 2019) surface-functionalized BC with a conductive bi-layer of PVAN/PANI by employing three-step reaction techniques for the prospective production of bio-sensors. In the first stage, they synthesized BC, then grafted 4-vinylaniline using a surface-initiated atom transfer radical polymerization approach in the second step. Finally, oxidative polymerization of aniline was carried out through in-situ approach. The PVAN interlayer was discovered to favor the synthesis of rod-like PANI structures, which ultimately improved the electrical conductivity of the resulting materials. The charge transfer redox processes taking place in the interface of the PVAN/PANI bilayer inside the BC framework have been attributed to the improved sensitivity of BC/PVAN/PANI composites to voltage changes. Due to the induced electrochemical activity of BC/PVAN/PANI composites, these materials have been used as a possible biosensor for the detection and analysis of a variety of biological structures. The non-cytotoxic functionalized BC nano composites have been effectively used in-vitro medical devices to detect and induce the neuronal development of neural stem cells NSCs, isolated from the SVZ of the brain in Neuron systems. As a result, these materials have been suggested as having the potential to cure a wide range of neurological disorders, such as Parkinson's (PD) and Alzheimer's (AD), as well as spinal cord injuries that necessitate certain neural cell types (Kim et al., 2015).

Jasim et al. (2017) used a two-step technique to create a BC-PANI/single-wall carbon nano tubes (SWCNTs) composite to improve the biocompatibility and electrical conductivity of BC for use as a bio-sensor. Their methodology includes in-situ polymerization of aniline on BC fibers followed by doping of SWCNTs onto the resulted BC-PANI composites. A considerable increase in electrical conductivity ($1.04 \times 10^{-3}$ S/cm) of BC after grafting of PANI was observed, which was further raised to 1.41 10–2 S/cm after doping with 0.1 mg/l of SWCNTs. The biocompatible and conductive polymeric membrane BC-PANI/SWCNTs has been stated to have great potential to utilize as biosensors.

#### 4.3.1. Humidity sensors

Kotresh et al. (2016) successfully used PANI coated CMC composite (PANI/CMC) and pure PANI after deposition onto glass substrate through spin coating process for humidity sensing at room temperature. An improvement in pi-electron delocalization and crystallinity of pure PANI after its grafting onto CMC was validated using the XRD technique. The impedance of composite films was measured at a selected frequency of 100 Hz, and a change of three orders of magnitudes in impedance was noted when relative humidity (RH) was varied from 25 % to 75 %, confirming the humidity sensing response of roughly 99 % for composite specimens. Further, for composite specimens, a recovery time of 90 s and response time of about 10 s were noted at 75 % RH. One month of testing confirmed the stability of composite specimens and their capacity to sense humidity.

Anju et al. developed nano fibrillated cellulose/PAN/polyvinyl alcohol (PVA) composite sensors for detecting humidity and ammonia gas The performance of the sensor was studied against varying concentrations of ammonia gas (0–100 ppm) and humidity (RH: 30–100 %) (Anju et al., 2019). An increase in resistance with a decrement in humidity has been observed. The sensors showed a sensitivity of 55 against ammonia, a response time of about 47 s, when RH was raised from 30 % to 100 % and a recovery time of 58 s, when RH is reversed from 100 % to 30 %. Thus, it can be anticipated that cellulose/PANI based nanocomposites could significantly contribute to the advancement of sensor technologies based on sustainable and environmentally friendly materials in the future.

#### 4.3.2. Ammonia gas sensors

$NH_3$ gas, due to its continue grow in its concentration in the open air in fertilizers factories and food process plants, is causing a serious threat to human respiratory as well as the immune system. It has been reported in the literature that acute exposure to 500 ppm $NH_3$ gas can result in irreversible lung injury, along with some other incurable injuries, including bronchitis, pulmonary effusion and skin burns (Maity and Kumar, 2018). Keeping in view its health hazards, time requires to develop sensitive, rapid and real-time ammonia gas sensors (Mani and Rayappan, 2015; Tabrizi and Chiniforoshan, 2017, p. 3).

CNCs, after coating with PANI, were tested for the sensing of ammonia gas by Wu et al. (2016). The gas sensing capabilities of composites were investigated by measuring the change in its resistance as a

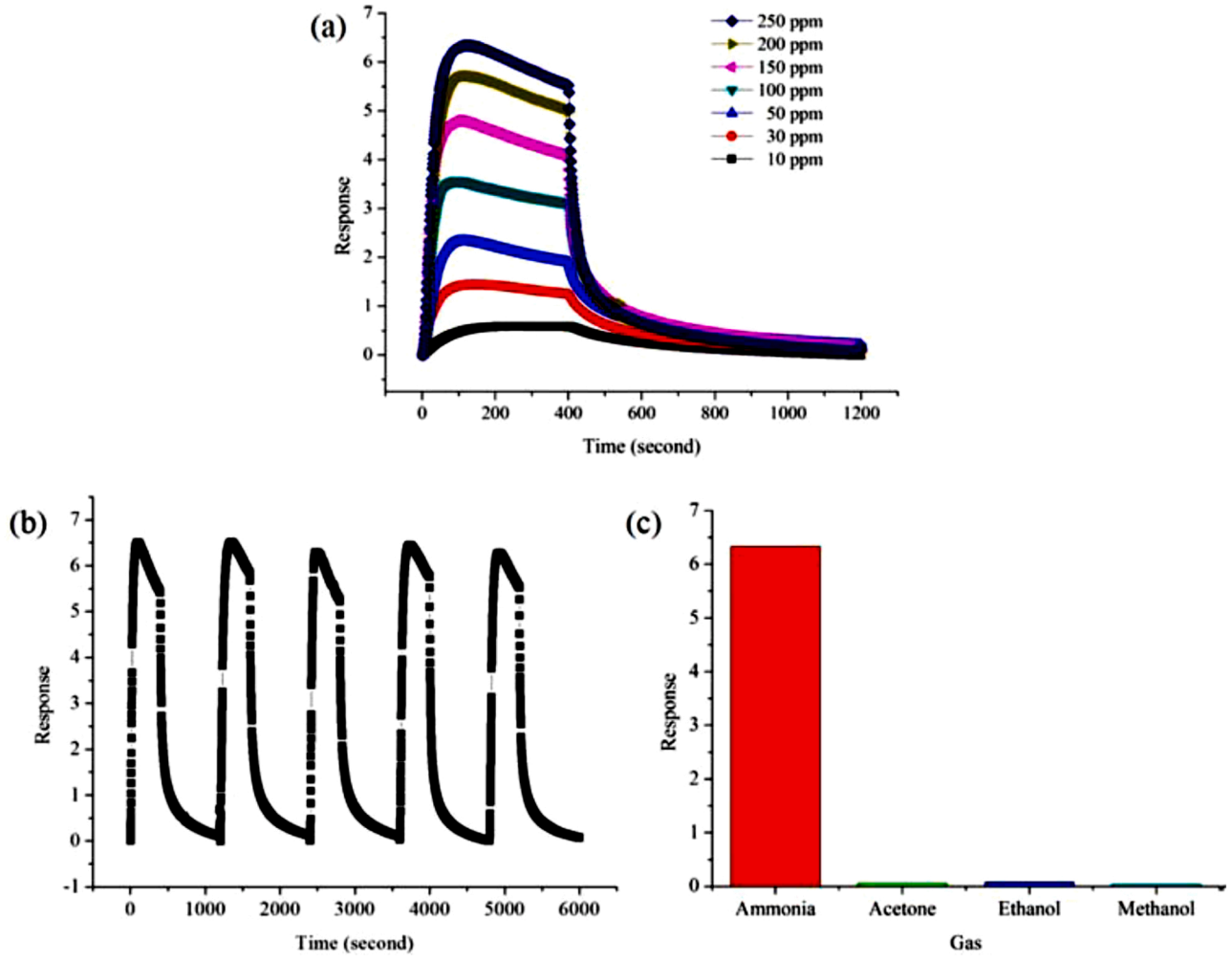


**Fig. 12.** Response of cellulose/$TiO_2$/PANI composite towards $NH_3$ (a) at different concentrations and (b) repeatability to 250 ppm and (c) selectivity against various gaseous (Pang et al., 2016). (Reprinted with permission from Ref. (Pang et al., 2016) Copyright 2016 Elsevier).

function of time at various concentrations of ammonia utilizing a digital multimeter. When composite specimens were exposed to ammonia gas, these materials displayed a rapid increase in $\Delta R/R_0$ (where $R_0$ is the initial resistance of composite specimens and $\Delta R$ is the difference between R, which is resistance after gas exposure, and $R_o$), which has been linked to PANI deprotonation. Furthermore, when the nanocomposite was exposed to ammonia vapor, it responded quickly, reaching a maximum value in $< 10$ s, with recovery times varying somewhat for $< 100$ ppm ammonia vapor.

Cellulose/$TiO_2$/PANI composite nanofibers were synthesized by Pang et al. (2016) and successfully employed for sensing ammonia gas (10–250 ppm) (Fig. 12). For synthesis purposes, they initially immersed cellulose nanofibers into $TiO_2$ sol to adsorb $TiO_2$ nano particles. The resulted cellulose/$TiO_2$ nano composites were then doped with PANI through in-situ polymerization of aniline to obtain the desired products. Further, ammonia gas sensing ability and response values (increased from 0.584 to 6.335, when ammonia gas concentration varied from 10 to 250 ppm) for cellulose/$TiO_2$/PANI nanofibers were reported to be better than Cellulose/PANI composite fibers. The behavior has been assigned (because of the formation of P–N hetero junctions at the interface of n-type $TiO_2$ and p-type PANI and the widening of its depletion layer upon exposure to ammonia gas, causing an increase in their resistance dramatically. Utilizing 3D interconnected BC as substrate, a flexible PANI-based ammonia gas sensor was prepared via co-doping of SSA and PAMPS (Yang et al., 2021). The prime aim of doping SSA was to enhance the intra-chain carrier mobility of PANI, whereas the simultaneous co-doping of PAMPS was carried out for efficient inter-chain charge transfer, leading to significant synergy in sensitivity enhancements and carrier mobility. The fabricated PANI-SSA/PAMPS-based sensor showed a quick response time of 4.1 s, a high response of 21.3 for 50 ppm $NH_3$ gas and a recovery time of 16 s. Additionally, synthesized materials also demonstrated remarkable ammonia gas selectivity among different adulterants/interfering agents and the limit sensing temperature $< -10$ °C.

Nano fibrillated cellulose/PAN/ PVA composite sensors showed an increase in sensitivity from 4.4 to 34 when the ammonia content was varied from 20 to 100 ppm (Anju et al., 2019). The greater response at high $NH_3$ concentration has been ascribed to the availability of a maximum number of active sites on the sensing material. Further, sensing materials showed a recovery time of 62 s and response time of 46 s at 60 ppm of ammonia concentration. They were found to vary to 35 s and 89 s, respectively, when the concentration of ammonia was decreased to 20 ppm. The increased response time with rising ammonia concentration has been attributed to the covering of all active sites on PANI by ammonia molecules, implying that all $H^+$ ions have been removed from the N atom of PANI, causing it to take too long to return to its previous energy levels.

Yang et al. (2020) co-doped BC/PANI nano composites with DBSA and PAMPS, via in-situ chemical oxidation polymerization process, to develop highly sensitive sensors for the detection of ammonia gas (20–150 ppm concentration). The synthesized sensor BC/PANI/DBSA-PAMPS displayed an excellent response, response time and recovery time of 6.1, 10.2 s and 8.6 s, respectively, at 100 ppm ammonia, compared to BC/PANI, with a detection limit of 200 ppb at room temperature. Such an increase in sensing ability has been assigned because of a change in PANI crystal structure after co-doping. The sensor was stated to maintain its ability to sense ammonia even after 60 days of multiple usages. Further, the impact of humidity (21–81 %) and temperature variation (0–85 °C) on the sensing ability of BC/PANI/DBSA-PAMPS sensor was evaluated at 100 ppm ammonia concentration. A slight increase in response has been reported when humidity was varied from 21 % to 81 % at room temperature. However, with variation in temperature, the response was found to increase up to 55 °C, and then a decreasing trend was obtained (Fig. 13). Fig. 13 displayed the sensing mechanism of sensors and response variation of sensors with temperature, humidity and against other volatile

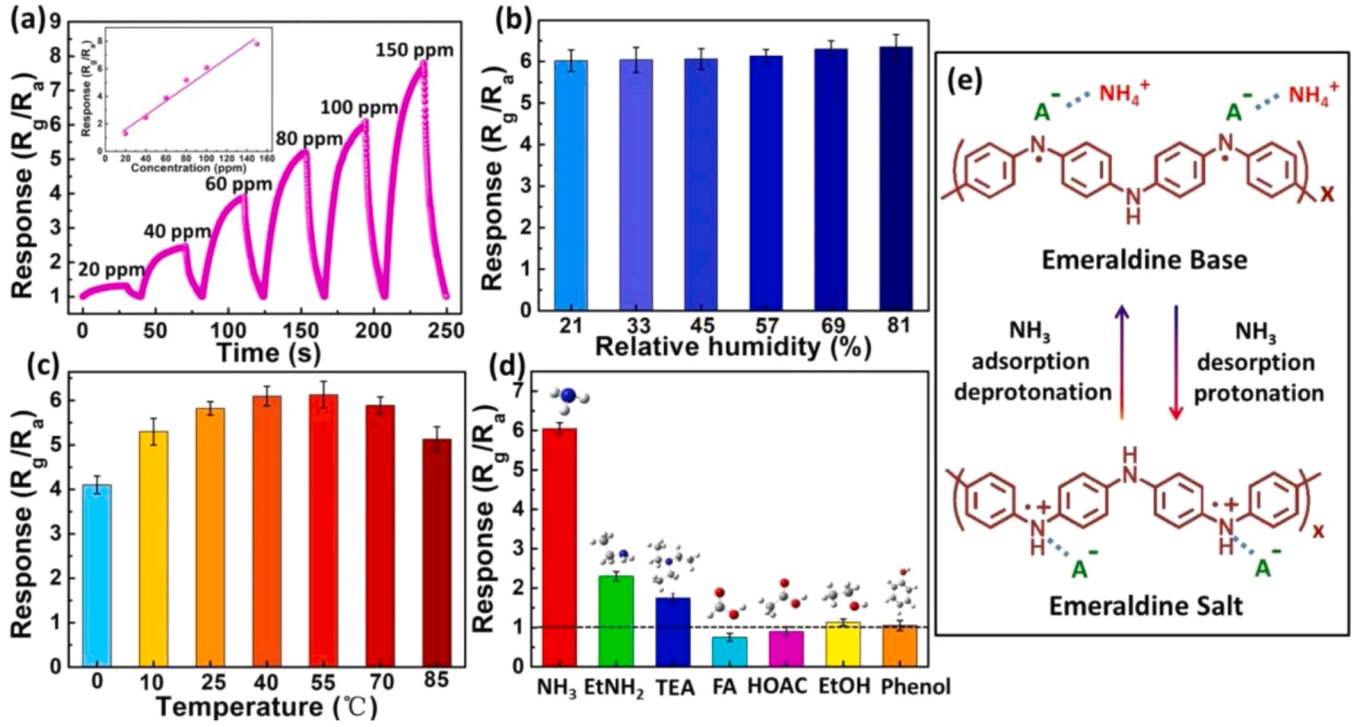


**Fig. 13.** a) Sensing performance of BC/PANI/DBSA-PAMPS composites toward different concentrations of $NH_3$, with a calibration plot of the response versus the concentration of NH3 in the range of 20–150 ppm (inset); The sensing respsonse of BC/PANI-DBSA/PAMPS composites at (b) different humidity conditions, (c) different temperatures, and (d) different types of gases. (e) Sensing mechanism of PANI-based sensors (A- is sulfonic anion).(Note here TEA-triethylamine; FA: Formic acid, HOAC-acetic acid) (Yang et al., 2020). Copyright 2020 Elsevier).
(Reprinted with permission from Ref (Yang et al., 2020).

gaseous/molecules.

#### 4.3.3. Carbon dioxide sensors

To detect $CO_2$, Abdali et al. (2019) fabricated BC/amino-functionalized graphene (AmG)/PANI nano composites via chemical modification of BC cellulose with AmG in the first step and in-situ polymerizations of PANI onto the surface of BC/AmG composites. The BC/AmG/PANI nano composites showed improved electrical-resistance at room temperature towards CO2 compared to pure BC/AmG nano composites and also possessed good response times (approx. 20 s) and high sensitivity towards $CO_2$ at a varying concentration ranging from 50 to 2000 ppm. However, no remarkable change in sensitivity of nanocomposites was observed upon varying percent humidity from 0 % to 80 %. Enhancement in resistance of BC/AmG/-PANI nano composites, when exposed to $CO_2$, has been attributed to an increase in thickness of depletion layer between the p-type PANI and n-type AmG junction in AmG/PANI Sensors. The observed increase in thickness of the depletion layer with the varying in concentration of CO2 from 50 to 2000 ppm has been assigned because of the liberation of electrons at the P-N junction interface. The higher the $CO_2$ concentration more will be the liberation of electrons at the P-N junction better will be resistance of nanocomposites.

#### 4.3.4. Acetone vapor sensor

Aparicio-Martínez et al. (2018) developed an electrochemical PANI/cellulose/$WO_3$ composite sensor for detection of acetone at room temperature. Here the PANI play the role of a P-type conductor, whereas $WO_3$ behave as N-type conductor and has been found to have a monoclinic phase. The synthesized materials displayed a conductivity of 13.9 S/cm against acetone and a detection limit of 10 ppm at room temperature. This sensor works through the process of electron transfer and chemisorptions. At low-temperature, oxygen ionic species such as $O^{2-}$and $O^{-}$ covers the surface of the sensor and prevents acetone from coming in contact with sensors or hindering chemisorptions and thus leads to low resistance. However, at higher temperatures these species react with acetone vapors leads to chemisorptions and causing an increase in resistance as well as the sensing ability of sensors considerably. The stacking of cellulose in composites has been found to enhance sensitivity of the sensor, because of generation of pores on the surface of sensors.

#### 4.3.5. Liquid petroleum gas sensors

Liquid petroleum gas is utilized both for industrial and domestic purposes. However, its leakages and accidents because of its explosion are pretty common nowadays and are causing severe destruction to property and human beings. Ravikiran et al. (2014) synthesized PANI and CMC/PANI composites through in chemical polymerization of aniline at room temperature for detection of liquid petroleum gas (LPG). The fabricated composites CMC/PANI showed a maximum of 32 % sensitivity factor, far higher than PANI (5 %), at 300 ppm LPG concentration, when the LPG concentration ranged from 50 to 500 ppm. Further, the sensitivity factor was found to increase linearly up to 250 ppm concentration of LPG, and afterwards, it becomes saturated. This behavior has been assigned due to the availability of a sufficient number of sensing sites at the film surface towards LPG at low concentrations. Further, the increase in sensing ability of composite or decrease in composite resistance upon an increase in LPG concentrations has been linked to the formation of a depletion layer on the surface of CMC after interaction with LPG gas leading to rapid inter particle electron transfer between CMC and PANI, resulting in improved sensitivity. In addition, the CMC/PANI sensor also showed a better response time and recovery time of 150 s and of 200 s, respectively, and maintained its sensitivity even after one month.

### 4.4. Electrical conductive electrodes or capacitors

The electrical conductivity data of PANI and its composites with various cellulosic forms/cellulose derivatives have been given in Table 6 (da S. Oliveira et al., 2018; El-Sayed et al., 2018; Gong et al., 2020; Huang et al., 2021; Ke et al., 2019; Lin et al., 2013; Liu et al., 2018; Nepomuceno et al., 2021; Park et al., 2016; Razalli et al., 2017; A. Rebelo et al., 2019; A.R. Rebelo et al., 2019; Shim et al., 2019; Tan et al., 2021; Tian et al., 2017; Tissera et al., 2018; Ummami et al., 2021; Wan et al., 2018; Wang et al., 2016, 2020; Yatsu and Goto, 2021; Youssef et al., 2021; Zhang et al., 2013). From the table, we can interpret that PANI coating plays a significant role to enhance the electrical conductivity of resulted materials. The dopant type and its concentration also play a crucial role in enhancing electrical properties. Different authors have optimized its amount to gain maximum electrical conductivity. Further, synthesized nano composites were also used as electrodes in capacitors and showed promising results. Due to such an increase in electrical conductivity, cellulose/PANI nano composites, in addition to the capacitor, have also been used in electromagnetic shielding, electrochromic resistance, sensors, etc. Gong et al. (Gong et al., 2020) prepared flash light-emitting diode using cellulose-g-β-cyclodextrin/PANI nano composites; they observed a flash time of 2 min

### 4.5. Electromagnetic radiations shielding

To shield the workspace from harmful radiations transmitted out from computers and telecommunication equipment, there is a growing demand for lightweight electromagnetic shielding materials for the safety of sensitive circuits (Zamanian and Hardiman, 2005). Electromagnetic waves transmitted out from the sensitive electronic equipment are either absorbed or reflected by the human body, thus causing a serious threat to human beings. Efforts were made by a couple of researchers to tackle this situation by developing various lightweight polypyrrole, ployacetylene and PANI based electromagnetic shielding materials (Zhang et al., 2015). However, among them, PANI based shielding materials have gained a huge amount of interest because of their environmental-friendly and controllable electrical properties nature, which can be controlled through the protonation/deprotonation process in PANI (Bhadra et al., 2009). CNFs were doped with PANI via in-situ polymerization technique to develop light, flexible and highly conductive cellulose nano (CNFs/PANI) papers for possible adsorption of electromagnetic radiations (Gopakumar et al., 2018). An electromagnetic shielding (EMS) of ca. − 23 dB (having attenuation higher than 99 %) against 8.2 GHz Microwave radiations (X-band) was achieved with a 1 mm thick nanopaper. Further, the direct current conductivity of CNF/PANI nanopaper was noticed to be 0.314 S/cm, which is a primary requirement for developing effective electromagnetic shielding devices and makes them suitable for utilization in electronic gadgets. Zhang et al. (2022) synthesized CNF through electrospinning techniques in the first step and subsequently doped it with PANI through in-situ polymerization technique. The fabricated CNFs/PANI composite displayed an excellent electromagnetic radiations adsorption tendency (showed 34.93 dB shielding efficiency in the whole X-band) because of their strong conductive loss, interfacial polarization and optimal impedance matching nature. Further, a minimum reflection loss was found to be − 49.24 dB, and effective absorption bandwidth [reflection loss (RL) < −10 dB] reaches 6.90 GHz. Zhang et al. (2019), in a different approach, synthesized CNFs by employing chemicals followed by intense ultrasonication technique, which were then coated with PANI via in-situ polymerization technique and converted into membrane utilizing vacuum induced process. They prepared different CNF/PANI nano composites membranes containing different % amounts (20 %, 30 %, 40 %, 50 % and 60 %) of PANI. A maximum electromagnetic shielding interference (EMI) of about 25.2 dB was achieved, when tested against microwave radiations (ranged from 8.2 to 12.4 GHz), with composites of thickness 0.28 mm containing 50 % PANI.

**Table 6**
A comparative data on electrical and mechanical properties of cellulose/PANI based nanocomposites.

| Sample Name/electrode type | Technique of Polymerization of PANI | Oxidizing agent/ dopant utilized for polymerization of PANI | Resistivity, KΩ·cm | Conductivity, S/cm | Electrode Capacitance ($F/cm^2$) | *All-Solid-State Supercapacitor* Capacitance (F/g) | Mechanical Properties | Ref. |
|---|---|---|---|---|---|---|---|---|
| CNCs/PANI | *In- situ* polymerization | 1.0 M HCl | $1.3 \times 10^2$ | $7.8 \times 10^{-5}$ | | | | (Zhang et al., 2013) |
| Cellulose/PANI composite | *In- situ* polymerization | 1.0 M HCl | Resistance: 4.49 Ω | Cross section: 36.79 ± 4.7; longitudinal: 23.2 ± 1.7 | Gravimetric specific capacitance: 218.75 F/g Areal specific capacitance: 0.41 $F/cm^2$ | Gravimetric specific capacitance: 112.48 F/g Areal specific capacitance: 0.12 $F/cm^2$ | | (Ke et al., 2019) |
| Wood/PANI composite | *In -situ* polymerization | 1.0 M HCl | Resistance: 7.55 Ω | Cross section: 11.8 ± 3.2; longitudinal: 6.3 ± 0.2 | Gravimetric specific capacitance: 99.79; Areal specific capacitance: 0.25 $F/cm^2$ | – | | (Ke et al., 2019) |
| Pristine graphene/BC/ PANI composite | *In-situ* polymerization | $H_2SO_4$ | Interfacial charge resistance decline from 150 to 28 Ω, when graphene contents were varies from 0 to 20 wt% | – | Areal capacitance: 3.65 $F/cm^2$ | Areal Capacitance: 1.389 $F/cm^2$, | | (Tan et al., 2021) |
| CNCs/PANI composites | *In- situ* polymerization controlled by open circuit potential adjustment | 1.0 M p-toluenesulfonic acid monohydrate | – | $8.9 \times 10^{-1}$ | – | – | | ( Nepomuceno et al., 2021) |
| Pure PANI | – | 1.0 M p-toluenesulfonic acid monohydrate | | 3.63 | – | – | | ( Nepomuceno et al., 2021) |
| Polylactic acid/PANI/ nanocrystalline cellulose | Solution casting method | HCl | | 2.16–1.5, when contents of nanocrystalline cellulose varied from 1 to 4 wt% | – | – | Tensile strength: 20.4, 24.0, 25.7 and 26.1 MPa, when loaded with 1, 2, 3 and 4 wt% of nanocrystalline cellulose | (Wang et al., 2020) |
| BC/SiNPs/PANI composites | *In -situ* polymerization | 0.5 N HCl | Resistance: ≤ 239 Ω | 0.017 | – | – | | (Park et al., 2016) |
| PANI/Ag/Cellulose | Solution casting method | – | | 23–34, when contents of PANI/Ag were varied from 10 to 50 wt% | – | – | | (da S. Oliveira et al., 2018) |
| BC/graphene/PANI | *In -situ* polymerization | 1.0 M HCl | – | 1.7 ± 0.1 | – | – | Tensile Strength: 1.3 ± 0.1; Percent elongation: 11.8 ± 0.7 | (Wan et al., 2018) |
| BC/PANI (0.025 mol/L) concentration of oxidizing agent used) | *In- situ* polymerization | 1.0 M HCl | Resistance: 40.1 Ω on PANI side and 1.65 ± 0.09) × 108 on BC side | – | – | – | Tensile Strength: 19.4 ± 1.0 MPa: % Elongation: 1.91 ± 0.06 | (Lin et al., 2013) |
| PANI/tosylcellulose stearate (TCS) composites | *In-situ* polymerization | APS/HCl | – | $3.24 \times 10^{-3}$ S/cm, at 75:25 wt % loading of PANI and TCS | – | – | Young's Modulus: 71.83; Stress at break: 1.86 Mpa | (El-Sayed et al., 2018) |
| Cellulose/PANI composites (contents of dopant HCl was | *In -situ* polymerization | 3, 5 M HCl | | $4{,}70 \times 10^{-4}$ S/cm, when 3.5 M | – | – | | (Ummami et al., 2021) |

(*continued on next page*)

**Table 6** (*continued*)

| Sample Name/electrode type | Technique of Polymerization of PANI | Oxidizing agent/ dopant utilized for polymerization of PANI | Resistivity, KΩ·cm | Conductivity, S/cm | Electrode Capacitance ($F/cm^2$) | *All-Solid-State Supercapacitor* Capacitance (F/g) | Mechanical Properties | Ref. |
|---|---|---|---|---|---|---|---|---|
| optimized to give maximum conductivity) | | | | HCl was optimized | | | | |
| CS/ HEC/PANI/GO@Ag) | *In- situ* polymerization | HCl | – | $8.53 \times 10^{-2}$, when loaded with 5% of GO | – | – | – | (Youssef et al., 2021) |
| Cellulose/ polyphenylacetylene/ PANI triple-layered composite membrane | *In -situ* polymerization | 0.5 g H2SO4 | – | $6.5 \times 10^{-4}$ S/cm (increases to $6.0 \times 10^{-3,}$ when further doped with m-cresol | – | – | – | (Yatsu and Goto, 2021) |
| Porous cellulose scaffolds/PANI/Ag nano composite | *In -situ* polymerization | 0.1 M HCl | – | 0.94 S/C m; | Gravimetric specific Conductance: 217 F/g at a current density of 0.1 A/g | – | – | (Tian et al., 2017) |
| BC/PVA/PANI composite membrane | *In -situ* polymerization | 1.0 M HCl | – | $4.5 \pm 1.7)x10^{-2}$ S/cm at 0.7 M concentration of aniline | – | – | – | (A. Rebelo et al., 2019; A.R. Rebelo et al., 2019) |
| CNCs/PANI composite | *In- situ* polymerization | 1.3 M HCl | – | 104.7 S/m | – | – | Tensile Strength: 26.7 Mpa | (Wang et al., 2016) |
| Screen printed electrode doped with CNCs/PANI | *In- situ* polymerization | 1.0 M HCl | Charge transfer resistance: 148 $\Omega/cm^2$ | – | Double layer conductance: 151 $mF/cm^2$ | – | – | (Razalli et al., 2017) |
| Paper coated with NFC/ Ag/PANI nanocomposite | *In -situ* polymerization | 1.0 M HCl | | Maximum of 0.0167 S/m, when amount of coating was 25.2 $g/m^2$ | – | – | – | (Liu et al., 2018) |
| BC/PANI nano composites | Enzyme catalyzed in-situ polymerization | Potassium hexacyanoferrate (II) trihydrate (PHCFT) and sodium bis (2 −ethyl hexyl) sulfosuccinate (AOT) | | $7 \times 10^{-4}$ (7. E-4) S/m | – | – | – | (Shim et al., 2019) |
| Cellulose-g-β-cyclodextrin/PANI nanocomposites (Here, the cellulose and cyclodextrin were taken in 1:3,1:4 and 1:5 relative mass ratio | *In-situ* polymerization | 1.0 M HCl | – | – | – | Maximum of 1003.50 $mF/cm^2$ with a 1:3 relative ratio | – | (Gong et al., 2020) |
| Cellulose paper coated with CNC/PANI composites | Emulsion polymerization | 1.0 M HCl | – | 5.64 S/m with 8 wt% coated paper | – | – | Tensile strength: 75 and 40 Nm/g in machine and cross direction | (Huang et al., 2021) |
| Cotton textiles/PANI nano composites | *In-situ* polymerization | 1.0–3.0 M HCl | Minimum electrical resistance: 1.2 ± 0.2 K Ω/cm | – | – | – | – | (Tissera et al., 2018) |

Omura et al. (2019) prepared chlorine and (±)− 10-camphorsulfonic acid-coated CNF/PANI based flexible membrane and studied their EMS effectiveness in a wide range of 0.45–15 GHz frequency, including the X-band the range. The CNF/PANI paper (thickness 55 μm) coated with (±)− 10-camphorsulfonic acid has shown a maximum of 38.5 S/cm electrical conductivity and EMS of − 30 dB (−545 dB/mm), whereas in case of chlorine coated CNF/PANI flexible membrane (87.5 ± 14.0 μm thickness), comparatively a lesser amount EMS (−3 dB) was observed. Similar to Omura et al., two more research groups, Gopakumar et al. (2018) and Marins et al. (2014), also studied the EMS effectiveness of chlorine doped CNF/PANI and BC/PANI, respectively. A maximum of − 23 Db and − 5 Db EMS effectiveness was observed for Cl doped CNF/PANI (1.0 mm) and BC/PANI (0.080 mm) conductive materials, respectively, when tested against a varied frequency ranging from 8.2 to 12.4 GHz.

Yatsu and Goto (2021) fabricated cellulose-polyphenylacetylene

**Table 7**
A comparatively view of techniques/assembly utilized by various researchers for developing ECDs and their performance data.

| Name of materials | Cycle | Detail about electrochromic device assembly | Contrast ratio | Response time | | Coloration efficiency ($cm^2/C$) | Ref. |
|---|---|---|---|---|---|---|---|
| | | | | **Colored state (s)** | **Bleached state (s)** | | |
| ITO/NCPANI/ Gel Polymeric electrolyte (GPE)/ Poly(3,4-ethylenedioxythiophene) PEDOT:PSS:PSS/ITO | Ist | **Three electrode system utilized**<br>**Substrate:** Indium tin oxide (ITO) coated glass<br>**Composite film electrode:** Naneocellulose/PANI dip-coated substrate.<br>**Complementary counter electrode**: Poly(3,4-ethylenedioxythiophene) PEDOT:polystyrene sulfonate (PSS) dip-coated ITO substrates<br>**Gel polymeric electrolyte (GPE)**:Made up of LiClO4/ dehydrated poly (methyl methacrylate)PMMA/ propylene carbonates<br>**Operation voltage:** − 1.0 to + 0.8 V<br>**ECD assembly:** | 42.6 | 1.5 | 1.1 | 172 | (Zhang et al., 2017b) |
| | 500 | Same as above | 40.6 | 1.4 | 0.9 | 170 | (Zhang et al., 2017b) |
| ITO/NCPANI/ GPE/NCPEDOT/ITO | Ist | **Three electrode system utilized**<br>**Substrate:** Indium tin oxide coated glass<br>**Composite film electrode:** NC/PANI dip-coated substrate.<br>**Complementary counter electrode:** NC/PEDOT)<br>**GPE:** Made up of PMMA and LiClO4 dissolved in propylene carbonate<br>**ECD assembly:** Same as above<br>**Operation voltage:** − 1.0 V and þ1.0 V | 19.6% | 1.5 | 1.9 | 241.6 | (Zhang et al., 2017a) |
| NC/PANI (40%) | 1–5 th cycle | **Three electrode system utilized**<br>**Substrate:** Indium tin oxide coated glass<br>**Composite film electrode:** NC/PANI dip coated substrate<br>**Reference electrode:** Calomel electrode<br>**Counter electrode:** Platinum<br>**Electrolyte:** 0.25 M HCl solution<br>**Operation voltage:** − 0.2 V and + 0.8 V<br>**ECD assembly:** | 62.9 | 1.0 | 1.5 | 206.2 | (Zhang et al., 2017c) |
| | 501–505 | | 49.5 | 1.2 | 1.6 | 176.3 | (Zhang et al., 2017c) |

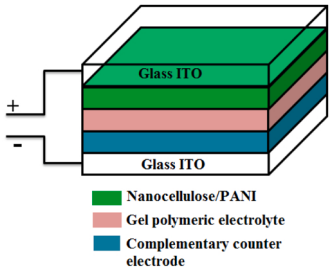


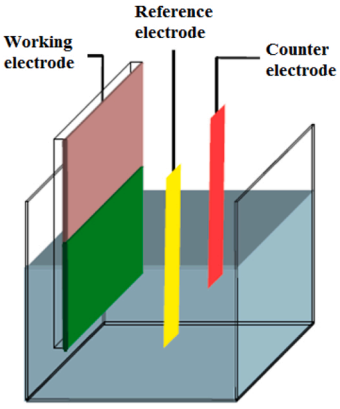


**Figure Reproduced with permission from Ref. 199. Copyright ACS (2017).**

(*continued on next page*)

**Table 7** (*continued*)

| Name of materials | Cycle | Detail about electrochromic device assembly | Contrast ratio | Response time | | Coloration efficiency ($cm^2$/C) | Ref. |
|---|---|---|---|---|---|---|---|
| | | | | **Colored state (s)** | **Bleached state (s)** | | |
| Pure PANI | 1–5 | **Detail about assembly: Same as discussed for** NC/PANI (40%) samples | 37.4 | 1.5 | 1.5 | 28.4 | (Tong et al., 2016) |
| | 501–505 | | 22.5 | 2.0 | 2.0 | 22.2 | (Tong et al., 2016) |

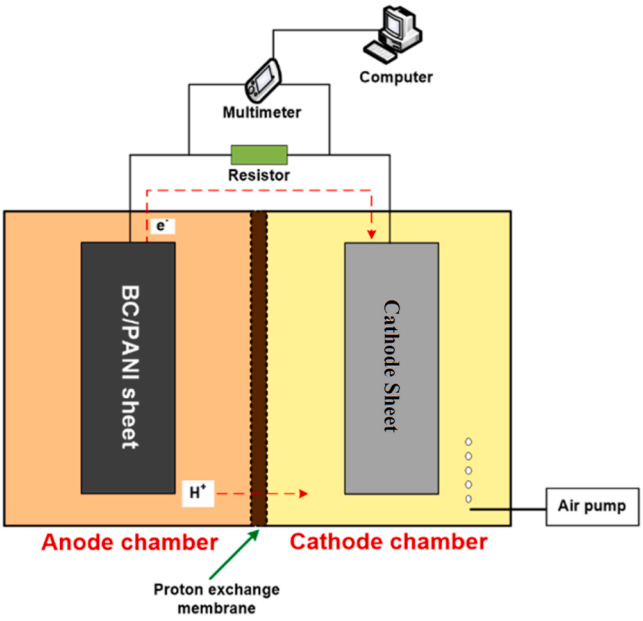


**Fig. 14.** Schematic construction of dual-chamber MFC (Truong et al., 2021). Copyright 2021 Elsevier).
(Reprinted with permission from Ref (Truong et al., 2021).

(PPA)/PANI composite membrane via one-pot synthesis step and subsequently utilized it for shielding of multi-wave noise emitted from circularly polarized Tesla coil. The value of the electric field after shielding by employing a composite membrane was found to be half at a distance of 10 cm when compared to an unshielded one and almost 100% at a distance of 50 cm.

### 4.6. Electrochromism

Electrochromic materials have piqued the curiosity of researchers all over the world because of their practical benefits in anti-glare mirrors, smart windows, smart paper and screens (Cummins et al., 2000; Kateb et al., 2016). The role of transition metal oxide films in this field have been extremely investigated due to their remarkable color contrast ratio (Song et al., 2015; Tong et al., 2016). Many of these inorganic materials, on the other hand, are expensive to produce, have poor cycle stability and require 15–60 s to achieve a good contrast (Song et al., 2015). Thus, researchers are now focussing their efforts for developing organic based electrochromic devices (ECD) owing to their fast response time, improved color contrast, low operation potential and long stability (Zhang et al., 2017b,a,c).

Various kinds of conducting organic polymers such as PANI, polypyrrole, polythiophene and their derivatives have been tested for their ability to design ECD and showed rapid response time, better contrast ratio, good switching capability and multiple color possibilities (Nicho, 2004; Zhao et al., 2009). However, PANI stands out as the most

**Table 8**
Comparative view of the set up of different fuel cells and their performance.

| Type of MFC | Fuel Cell bio-anode | Cathode | The filler used in Anode compartment/ chamber | The filler used in Cathode compartment/ chamber | Proton exchange membrane | Exoelectrogenic bacteria name | Maximum Power density ($mW/m^2$)/ current density mA/ $cm^2$ | Ref. |
|---|---|---|---|---|---|---|---|---|
| Double-chamber MFC | BC/PANI-HCl (1.0 M) | Carbon tissue | culture media of yeast extract (5 g/L), glucose (10 g/L), sodium chloride (10 g/L) and tryptone (10 g/L) | Solution of $K_3Fe[CN]_6$ in phosphate buffer | Nafion 115 | *E. Coli* | 0.009 mA/$cm^2$(in 144 hrs) | (Trindade et al., 2020) |
| Double-chamber MFC having three-electrode system in which bioanode and reference electrode (KCl saturated Ag/AgCl) was taken in anode compartment | BC/PANI (0.4 M)–HCl (0.5 M) | Graphite plate | 0.5 M phosphate buffer media consisted of 10 g of glucose, 3 g of yeast extract and 1 g of peptone | Phosphate buffer solution (pH:7) | Nafion 117 after treatment with 3% $H_2O_2$, D.I water and 0.5 M $H_2SO_4$ | – | 117.76 /616 | (Mashkour et al., 2016) |
| Double-chamber MFC Double-chamber MFC | BC/ PANI/ $TiO_2$/APS BC/ PANI/ APS | Graphite sheet | LB broth medium in isotonic saline phosphate-buffer | 0.1 M $K_3Fe[CN]_6$ solution in 0.5 M Sorensen phosphate buffer (pH:7) | Nafion 117 | *Shewanella xiamenensis* | 179.4/116.72 A/$m^3$ (8–28 hrs) 137.4 (23.95–29.30 W/ $m^3$) | (Truong et al., 2021) |

promising among them since it is simple to make, environmentally benign, and less expensive than other conducting polymers. Because of the presence of OH groups, cellulose has a strong affinity for a wide range of conducting polymers. Its combination with PANI plays an essential role in the synthesis of nanocomposite films with potential utility in ECD (Wu et al., 2016). A comparatively view of technique-s/assembly employed by different researchers for developing ECDs by using NC/PANI electrochromic materials and results obtained were displayed in Table 7. From the table we can interpret that the addition of cellulose remarkably increases the film-forming abilities of PANI and, ultimately, the functioning of ECD (Tong et al., 2016; Zhang et al., 2017b,a,c).

### 4.7. Microbial fuel cells

Microbial fuel cells (MFC) are gaining much attention these days since they can cleanse/treat organic waste materials while also generating electricity (Logan et al., 2015). These cells use active microbes as biocatalysts to oxidize organic molecules like glucose and release protons and electrons simultaneously. Furthermore, the simultaneous movement of electrons from anode to cathode in the external circuit and protons, from anode to cathode after crossing the proton exchange membrane leads to the conversion of chemical energy into electricity (Santoro et al., 2017; Truong et al., 2021) (Fig. 14). Numerous factors, such as proton exchange membrane, electrode materials, operating conditions, charge transfer rate and internal resistance impact the overall performance of MFC (Trindade et al., 2020). Extensive research has been performed to develop renewable and more efficient electrodes. For an improved performance of MFCs, the anode should be chemically stable, bio-compatible, corrosion-resistant, have a large surface area, have low resistance and appropriate mechanical toughness (Ucar et al., 2017; Zhou et al., 2011). Conductive polymers like PANIs have gained significant interest in the field of renewable energies and particularly in the development of fuel cells. This is because of their intrinsic conductive nature, that leads to good electrical conductivity, chemical and thermal stability, and oxidation/reduction capacity (Khandelwal et al., 2018; Sapurina and Stejskal, 2008; Truong et al., 2021) (Table 8).

Trindade et al. (2020) synthesized carbon fiber (CF)-embedded in BC/PANI-HCl (1.0 M) and CF/ BC/PANI-HCl (0.5 M) nanocomposite anode electrodes and further evaluated their ability to generate potential in MFC. 0.5 mg/cm$^2$ carbon tissue was utilized as cathode, and a solution of $K_3Fe[CN]_6$ in phosphate buffer was used as an electrolyte in the cathodic compartment. Whereas, in the anodic compartment, a culture media of yeast extract (5 g/L), glucose (10 g/L), sodium chloride (10 g/L) and tryptone (10 g/L) was used for the growth of exoelectrogenic (*E. Coli*) bacteria. A maximum of 0.009 mA/cm$^2$ conductivity was demonstrated by the BC/PANI-HCl (1.0 M) nanocomposite electrode when operated for 144 h. However, in the case of BC/PANI-HCl (0.5 M) nanocomposite anode, only 0.006 mA/cm$^2$ conductivity was observed. The above result demonstrated a great potential of CF/BC/PANI anode in MFC fabrication, which also supports the formation of microbial biofilm.

Mashkour et al. (2016) developed BC/PANI-HCl (0.5 M) bioanode with varying amount (0.1, 0.2, 0.3 and 0.4 M) of aniline. An increase in current, as well as power density with an increase in the amount of aniline, has been reported by them. Truong et al. (2021) synthesized BC/PANI/$TiO_2$ bio-anode. Still, instead of HCl, they used two different types of oxidizing agents such as APS and chloride hexahydrate of iron (III) to carry out polymerization of aniline. Maximum current/power density was found with APS. Further, among BC/PANI/$TiO_2$ bio-anode and BC/PANI, better results were obtained with the former one.

### 4.8. Other applications

Borsoi et al. (2016) functionalized CNWs with PANI. Subsequently, they utilized the prepared nanocomposites for the development of epoxy-based polymeric coatings, cross-linked by amino-propylytriethoxysilane and applied for carbon steel protection. Improvement in bonding to polymer coatings after the incorporation of CNWs/PANI nanocomposites has been reported by those authors. Furthermore, hardness and flexibility have been enhanced when APS cross-linkers and Zirconium conversion coatings were used along with CNW/PANI nanocomposites.

Song et al. (2020) synthesized self-healing polymers utilizing CNCs/PANI nanocomposites. Their technique includes the preparation of multi-branched CNCs by grafting citric and ascorbic acid in the first step, followed by a coating of PANI and subsequent utilization as a stacking material for enhancing the mechanical toughness and self-healing/sensing properties of PVA and borax based hydrogels. Due to the hierarchical structure and dynamic interactions/bridge between multi CNCs and dynamic borax, the multi CNCs/PANI/PVA hydrogel offered good self-adhesive properties, exceptional good viscoelasticity, ultra-stretching (1085 %), breaking strength of 171.52 KPa, quick self-healing characteristics and high sensitivity to human motions such as fingers, elbow, throat vocalization, wrist and knee joints movements.

## 5. Conclusion and future prospective

The current review paper covers a wide range of topics related to cellulose/PANI biocompatible nanocomposites, including production methods, electrical characteristics, biosensing, and their applications in various fields. Because of their low cost, ease of fabrication, high conductivity, and exceptional mechanical strength, these nanocomposites are gaining popularity among researchers. PANI/cellulose-based scaffolds demonstrated excellent cell growth and regeneration ability. Although pure PANI is cytotoxic by nature, promising results were obtained when blended with cellulose, resulting in the development of new technologies or innovative pathways for the development of biodegradable conducting materials that do not contain nerve growth factors.

Conducting and eco-friendly cellulose/ PANI based nanocomposites were found to be very beneficial for biomedical applications such as tissue engineering, regenerative nerve medicine, repairing tissue cells and drug delivery and have also been utilized for cholesterol sensors. However, further research is needed to better understand the behavior and long term life of materials within the body to develop novel biomaterials that can bring a breakthrough in diseases control.

We have also discovered that cellulose/PANI-based adsorbents effectively remove dyes and heavy ions such as Cr(VI) ion from polluted water (Herrera et al., 2018; Patra and Majhi, 2015). However, efforts to improve the adsorption capability of PANI-based nanocomposites are still needed, either by combining it with a ternary nano nonmaterial or chemically changing the surface of additives. Furthermore, van der Waals forces, electrostatic interactions, pi-pi interactions, and/or hydrogen bonding were discovered to be important factors in contaminant adsorption.

The shape of the adsorbent, which is vital for the adsorption, can be regulated by using a suitable PANI synthesis technique. PANIs have been produced with reinforcements possessing various surface morphologies, including nanofibres, nanotubes, nanorods, nanopowders, and nanoflakes. However, a large proportion of pollutants can be removed by altering the pore size of cellulose/PANI based adsorbents. Efforts have also been undertaken to regenerate cellulose/PANI based nano adsorbents by changing the pH. Scientists however still face a significant hurdle in regenerating exhausted adsorbents. In future, efforts should be made to develop inexpensive regeneration technologies for recycling exhausted adsorbents.

Nanosensors made of cellulose/PANI also showed promise to sense gas presences like ammonia LPG, $CO_2$ and humidity. PANI-based nanosensors should also be developed to further detect formalin, phenols, and other volatile organic chemicals. In comparison to carbonaceous and traditional ceramic sensors, the literature on cellulose/PANI based gaseous or humidity detecting materials is still in its early stages.

As a result, more research is required to fully comprehend the gaseous/humidity sensing pathways for cellulose/PANI based composites. By applying complementary experimental approaches, experimental work assisted by computational analyses is expected to attain this goal in the future.

Efforts are also needed to enhance the sensing abilities of cellulose/PANI nanocomposites by incorporating ternary nano particles like GO, $TiO_2$ and reduced oxide carbon nanotubes at different proportions, because of the tremendous impact of these nanomaterials due to their unique electrical properties. The understanding of the mechanisms leading to optimum synergy between ternary nano materials and cellulose/PANI will also constitute a significant challenge for researchers, since that synergy depends upon a variety of variables: type and amount of ternary dopants, and the cellulose/PANI relative ratio. All these questions represent a major challenge to design reliable ammonia, carbon dioxide and LPG gas sensors with superior sensing performance.

The role of cellulose/PANI based electrodes in supercapacitors and fuel cells has been thoroughly discussed. One of the most difficult challenges facing scientists is the development of materials with the ability to store energy. Exceptional efforts have been made in this area, but more work is needed to improve cellulose/PANI based nanocomposites in this field. Without a doubt, low electrical potential differences were obtained when cellulose/PANI based electrodes were used as anodes in fuel cells, but this justifies the ability of PANI based anodes in fuel cells. The ability of the cellulose/PANI electrode to adhere to microorganisms also validates its biocompatibility, which is a crucial criterion for using it in a microbial fuel cell. Since, the fuel cell has been found to have short term potential, so optimization of cellulose/PANI electrodes is highly anticipated in the near future. Instead of synthetic sugars, waste biomass should be tested to develop culture media for bacterial growth in the anionic compartment of fuel cells, and their long-term stability should also be examined. Future research should also focus on how nanofillers like graphene oxide, reduced carbon nanotubes and boron nitride nanotubes may affect the performance of the resulting nanofillers-doped cellulose/PANI electrodes.

We can see from the above discussion that cellulose, in combination with PANI, plays an important role in multidimensional applications, particularly in energy storage devices and green electronics. However, there are some obstacles that scientists must overcome to expand the range of cellulose applications. For example, the techniques used to prepare nano cellulose are usually expensive and deliver low yields due to cellulose damage. Thus, initiatives in this field are required to minimize the destruction of cellulose and to strengthen the crystallinity and the overall electrochemical properties of cellulose/PANI nanocomposites. Furthermore, proper dispersion of NC or nanoparticles is highly recommended during the synthesis of cellulose/PANI nanocomposites, because it will result in better electrochemical properties.

A methodology for integrating several conductive compounds should also be devised. Furthermore, when we combine cellulose, which is a non-conductive substance, with conductive PANI, we can expect weak electrical contacts or gaps in conductive particles. As a result, researchers must pay close attention to improving the current transfer rate through the inevitable gaps between various types of conductive materials. Light-emitting diodes have also been created using cellulose/PANI nanocomposites, but more research is needed in this area. PANI-based nanocomposites to adsorb electromagnetic radiation were also produced and showed promising results, but further improving their adsorption capacity and large-scale application in electronics devices may be explored in the future.

## Declaration of Competing Interest

The authors declare that they have no known competing financial interests or personal relationships that could have appeared to influence the work reported in this paper.

## Data availability

No data was used for the research described in the article.

## References


Abbasian, M., Jaymand, M., Shoja Bonab, S.E., 2012. Synthesis and characterization of a terpolymer derived from styrene, methyl styrene, and polyaniline and its organoclay nanocomposite. J. Appl. Polym. Sci. 125 https://doi.org/10.1002/app.35391.

Abbasian, M., Niroomand, P., Jaymand, M., 2017. Cellulose/polyaniline derivatives nanocomposites: synthesis and their performance in removal of anionic dyes from simulated industrial effluents. J. Appl. Polym. Sci. 134, 45352 https://doi.org/10.1002/app.45352.

Abdali, H., Heli, B., Ajji, A., 2019. Cellulose nanopaper cross-linked amino graphene/polyaniline sensors to detect $CO_2$ gas at room temperature. Sensors 19, 5215. https://doi.org/10.3390/s19235215.

Abdel Rehim, M.H., Yassin, M.A., Zahran, H., Kamel, S., Moharam, M.E., Turky, G., 2020. Rational design of active packaging films based on polyaniline-coated polymethyl methacrylate/nanocellulose composites. Polym. Bull. 77, 2485–2499. https://doi.org/10.1007/s00289-019-02866-0.

Abdi, M.M., Razalli, R.L., Tahir, P.M., Chaibakhsh, N., Hassani, M., Mir, M., 2019. Optimized fabrication of newly cholesterol biosensor based on nanocellulose. Int. J. Biol. Macromol. 126, 1213–1222. https://doi.org/10.1016/j.ijbiomac.2019.01.001.

Abitbol, T., Rivkin, A., Cao, Y., Nevo, Y., Abraham, E., Ben-Shalom, T., Lapidot, S., Shoseyov, O., 2016. Nanocellulose, a tiny fiber with huge applications. Curr. Opin. Biotechnol. 39, 76–88.

Abou Hammad, A.B., Abd El-Aziz, M.E., Hasanin, M.S., Kamel, S., 2019. A novel electromagnetic biodegradable nanocomposite based on cellulose, polyaniline, and cobalt ferrite nanoparticles. Carbohydr. Polym. 216, 54–62. https://doi.org/10.1016/j.carbpol.2019.03.038.

Abu Hassan Shaari, H., Ramli, M.M., Mohtar, M.N., Abdul Rahman, N., Ahmad, A., 2021. Synthesis and conductivity studies of poly (Methyl Methacrylate)(PMMA) by co-polymerization and blending with polyaniline (PANi). Polymers 13, 1939.

Anastopoulos, I., Kyzas, G.Z., 2014. Agricultural peels for dye adsorption: a review of recent literature. J. Mol. Liq. 200, 381–389. https://doi.org/10.1016/j.molliq.2014.11.006.

Anju, V.P., Jithesh, P.R., Narayanankutty, S.K., 2019. A novel humidity and ammonia sensor based on nanofibers/polyaniline/polyvinyl alcohol. Sens. Actuators A: Phys. 285, 35–44. https://doi.org/10.1016/j.sna.2018.10.037.

Anžlovar, A., Kunaver, M., Krajnc, A., Žagar, E., 2018. Nanocomposites of LLDPE and surface-modified cellulose nanocrystals prepared by melt processing. Molecules 23, 1782. https://doi.org/10.3390/molecules23071782.

Aparicio-Martínez, E., Osuna, V., Dominguez, R.B., Márquez-Lucero, A., Zaragoza-Contreras, E.A., Vega-Rios, A., 2018. Room temperature detection of acetone by a PANI/Cellulose/$WO_3$ electrochemical sensor. J. Nanomater. 2018, 1–9. https://doi.org/10.1155/2018/6519694.

de Assis, C.A., Houtman, C., Phillips, R., Bilek, E.M., Rojas, O.J., Pal, L., Peresin, M.S., Jameel, H., Gonzalez, R., 2017. Conversion economics of forest biomaterials: risk and financial analysis of CNC manufacturing. Biofuels, Bioprod. Bioref. 11, 682–700.

Ates, B., Koytepe, S., Ulu, A., Gurses, C., Thakur, V.K., 2020. Chemistry, structures, and advanced applications of nanocomposites from biorenewable resources. Chem. Rev. 120, 9304–9362. https://doi.org/10.1021/acs.chemrev.9b00553.

Ballav, N., Debnath, S., Pillay, K., Maity, A., 2015. Efficient removal of reactive black from aqueous solution using polyaniline coated ligno-cellulose composite as a potential adsorbent. J. Mol. Liq. 209, 387–396. https://doi.org/10.1016/j.molliq.2015.05.051.

Beluns, S., Gaidukovs, S., Platnieks, O., Gaidukova, G., Mierina, I., Grase, L., Starkova, O., Brazdausks, P., Thakur, V.K., 2021. From wood and hemp biomass wastes to sustainable nanocellulose foams. Ind. Crops Prod. 170, 113780 https://doi.org/10.1016/j.indcrop.2021.113780.

Bhadra, S., Khastgir, D., Singha, N.K., Lee, J.H., 2009. Progress in preparation, processing and applications of polyaniline. Prog. Polym. Sci. 34, 783–810. https://doi.org/10.1016/j.progpolymsci.2009.04.003.

Bhaumik, M., Choi, H.J., McCrindle, R.I., Maity, A., 2014. Composite nanofibers prepared from metallic iron nanoparticles and polyaniline: high performance for water treatment applications. J. Colloid Interface Sci. 425, 75–82. https://doi.org/10.1016/j.jcis.2014.03.031.

Blaker, J.J., Lee, K.-Y., Walters, M., Drouet, M., Bismarck, A., 2014. Aligned unidirectional PLA/bacterial cellulose nanocomposite fibre reinforced PDLLA composites. React. Funct. Polym. 85, 185–192. https://doi.org/10.1016/j.reactfunctpolym.2014.09.006.

Borsoi, C., Zattera, A.J., Ferreira, C.A., 2016. Effect of cellulose nanowhiskers functionalization with polyaniline for epoxy coatings. Appl. Surf. Sci. 364, 124–132. https://doi.org/10.1016/j.apsusc.2015.12.140.

Briede, S., Barkane, A., Jurinovs, M., Thakur, V.K., Gaidukovs, S., 2022. Acrylation of biomass: a review of synthesis process: know-how and future application directions. Curr. Opin. Green. Sustain. Chem. 35, 100626 https://doi.org/10.1016/j.cogsc.2022.100626.

Carlmark, A., Larsson, E., Malmström, E., 2012. Grafting of cellulose by ring-opening polymerisation – a review. Eur. Polym. J. 48, 1646–1659. https://doi.org/10.1016/j.eurpolymj.2012.06.013.

Chen, X., Yuan, F., Zhang, H., Huang, Y., Yang, J., Sun, D., 2016. Recent approaches and future prospects of bacterial cellulose-based electroconductive materials. J. Mater. Sci. 51, 5573–5588. https://doi.org/10.1007/s10853-016-9899-2.

Cheng, Q., Li, Q., Yuan, Z., Li, S., Xin, J.H., Ye, D., 2021. Bifunctional regenerated cellulose/polyaniline/nanosilver fibers as a catalyst/bactericide for water decontamination. ACS Appl. Mater. Interfaces 13, 4410–4418. https://doi.org/10.1021/acsami.0c20188.

Choi, K., Gao, C., Nam, J., Choi, H., 2017. Cellulose-based smart fluids under applied electric fields. Materials 10, 1060. https://doi.org/10.3390/ma10091060.

Correia, C.A., Oliveira, L.M., de, Valera, T.S., 2017. The influence of bleached jute fiber filler on the properties of vulcanized natural rubber. Mater. Res. 20, 466–471.

Cummins, D., Boschloo, G., Ryan, M., Corr, D., Rao, S.N., Fitzmaurice, D., 2000. Ultrafast electrochromic windows based on redox-chromophore modified nanostructured semiconducting and conducting films. J. Phys. Chem. B 104, 11449–11459. https://doi.org/10.1021/jp001763b.

da S. Oliveira, R., Bizeto, M.A., Camilo, F.F., 2018. Production of self-supported conductive films based on cellulose, polyaniline and silver nanoparticles. Carbohydr. Polym. 199, 84–91. https://doi.org/10.1016/j.carbpol.2018.06.049.

Das, T.K., Prusty, S., 2012. Review on conducting polymers and their applications. Polym. -Plast. Technol. Eng. 51, 1487–1500.

Dayan, A.D., Paine, A.J., 2001. Mechanisms of chromium toxicity, carcinogenicity and allergenicity: review of the literature from 1985 to 2000. Hum. Exp. Toxicol. 20, 439–451. https://doi.org/10.1191/096032701682693062.

Debnath, S., Ballav, N., Maity, A., Pillay, K., 2015a. Development of a polyaniline-lignocellulose composite for optimal adsorption of Congo red. Int. J. Biol. Macromol. 75, 199–209. https://doi.org/10.1016/j.ijbiomac.2015.01.011.

Debnath, S., Ballav, Niladri, Maity, A., Pillay, K., 2015b. Single stage batch adsorber design for efficient Eosin yellow removal by polyaniline coated ligno-cellulose. Int. J. Biol. Macromol. 72, 732–739. https://doi.org/10.1016/j.ijbiomac.2014.09.018.

Delgado Aguilar, M., González Tovar, I., Tarrés Farrés, J.A., Alcalà Vilavella, M., Pèlach Serra, M.À., Mutjé Pujol, P., 2015. Approaching a low-cost production of cellulose nanofibers for papermaking applications. Bioresources 10 (núm. 3, p. 5435-5355).

Dong, Y., Zhou, Y., Ding, Y., Chu, X., Wang, C., 2014. Sensitive detection of Pb(II) at gold nanoparticle/polyaniline/graphene modified electrode using differential pulse anodic stripping voltammetry. Anal. Methods 6, 9367–9374. https://doi.org/10.1039/C4AY01908C.

Dourado, F., Fontão, A., Leal, M., Rodrigues, A.C., Gama, M., 2016. Process modeling and techno-economic evaluation of an industrial bacterial nanocellulose fermentation process. In: Bacterial Nanocellulose. Elsevier, pp. 199–214.

Dubey, N., Arora, S., 2021. Surfactant assisted synthesis of pH responsive polyaniline-cellulose biocomposite for sensor applications. Polym. -Plast. Technol. Mater. 60, 1135–1147. https://doi.org/10.1080/25740881.2021.1888985.

Dufresne, A., 2020. Preparation and properties of cellulose nanomaterials. Pap. Biomater. 5, 1–13.

Durán, N., Durán, M., de Jesus, M.B., Seabra, A.B., Fávaro, W.J., Nakazato, G., 2016. Silver nanoparticles: a new view on mechanistic aspects on antimicrobial activity. Nanomed. Nanotechnol. Biol. Med. 12, 789–799. https://doi.org/10.1016/j.nano.2015.11.016.

Dzulkurnain, N.A., Mokhtar, M., Rashid, J.I.A., Knight, V.F., Wan Yunus, W.M.Z., Ong, K. K., Mohd Kasim, N.A., Mohd Noor, S.A., 2021. A review on impedimetric and voltammetric analysis based on polypyrrole conducting polymers for electrochemical sensing applications. Polymers 13, 2728.

Ehsan, N.Z., Peyman, N.M., Elham, A., Iman, S., 2011. Conductive and biodegradable polyaniline/starch blends and their composites with polystyrene. Iran. Polym. J. 20, 319–328.

El-Bery, H.M., Salah, M.R., Ahmed, S.M., Soliman, S.A., 2021. Efficient non-metal based conducting polymers for photocatalytic hydrogen production: comparative study between polyaniline, polypyrrole and PEDOT. RSC Adv. 11, 13229–13244.

El-Sayed, N.S., Abd El-Aziz, M.E., Kamel, S., Turky, G., 2018. Synthesis and characterization of polyaniline/tosylcellulose stearate composites as promising semiconducting materials. Synth. Met. 236, 44–53. https://doi.org/10.1016/j.synthmet.2018.01.001.

Foyle, L.D., Hicks, G.E., Pollit, A.A., Seferos, D.S., 2021. Polyacetylene revisited: a computational study of the molecular engineering of N-type polyacetylene. J. Phys. Chem. Lett. 12, 7745–7751.

Freitas, T.V., Sousa, E.A., Fuzari Jr., G.C., Arlindo, E.P.S., 2018. Different morphologies of polyaniline nanostructures synthesized by interfacial polymerization. Mater. Lett. 224, 42–45. https://doi.org/10.1016/j.matlet.2018.04.062.

Fu, J., Pang, Z., Yang, J., Huang, F., Cai, Y., Wei, Q., 2015. Fabrication of polyaniline/carboxymethyl cellulose/cellulose nanofibrous mats and their biosensing application. Appl. Surf. Sci. 349, 35–42. https://doi.org/10.1016/j.apsusc.2015.04.215.

Gapusan, R.B., Balela, M.D.L., 2020. Adsorption of anionic methyl orange dye and lead (II) heavy metal ion by polyaniline-kapok fiber nanocomposite. Mater. Chem. Phys. 243, 122682 https://doi.org/10.1016/j.matchemphys.2020.122682.

Gholami, H., Shakeri, A., Saadattalab, V., 2017. Investigation of physical and mechanical properties of polyaniline/MMT nanocomposites. Curr. Chem. Lett. 6, 151–158.

Ghorbani, M., Lashkenari, M.S., Eisazadeh, H., 2011. Application of polyaniline nanocomposite coated on rice husk ash for removal of Hg(II) from aqueous media. Synth. Met. 161, 1430–1433. https://doi.org/10.1016/j.synthmet.2011.05.016.

Ghorbani, M., Eisazadeh, H., Ghoreyshi, A.A., 2012. Removal of zinc ions from aqueous solution using polyaniline nanocomposite coated on rice husk. Iran. J. Energy Environ. 3, 83–88.

Gong, Q., Li, Y., Liu, X., Xia, Z., Yang, Y., 2020. A facile preparation of polyaniline/cellulose hydrogels for all-in-one flexible supercapacitor with remarkable enhanced performance. Carbohydr. Polym. 245, 116611.

Gopakumar, D.A., Pai, A.R., Pottathara, Y.B., Pasquini, D., Carlos de Morais, L., Luke, M., Kalarikkal, N., Grohens, Y., Thomas, S., 2018. Cellulose nanofiber-based polyaniline flexible papers as sustainable microwave absorbers in the X-band. ACS Appl. Mater. Interfaces 10, 20032–20043. https://doi.org/10.1021/acsami.8b04549.

Gospodinova, N., Terlemezyan, L., 1998. Conducting polymers prepared by oxidative polymerization: polyaniline. Prog. Polym. Sci. 23, 1443–1484.

Gu, H., Rapole, S.B., Sharma, J., Huang, Y., Cao, D., Colorado, H.A., Luo, Z., Haldolaarachchige, N., Young, D.P., Walters, B., Wei, S., Guo, Z., 2012. Magnetic polyaniline nanocomposites toward toxic hexavalent chromium removal. RSC Adv. 2, 11007. https://doi.org/10.1039/c2ra21991c.

Gupta, V.K., Carrott, P.J.M., Singh, R., Chaudhary, M., Kushwaha, S., 2016. Cellulose: a review as natural, modified and activated carbon adsorbent. Bioresour. Technol. 216, 1066–1076.

Habibi, Y., 2014. Key advances in the chemical modification of nanocelluloses. Chem. Soc. Rev. 43, 1519–1542.

Hasanin, M., Mwafy, E.A., Youssef, A.M., 2021. Electrical properties of conducting tertiary composite based on biopolymers and polyaniline. J. Bio- Tribo-Corros. 7, 1–10.

Hasija, V., Raizada, P., Sudhaik, A., Singh, P., Thakur, V.K., Khan, A.A.P., 2020. Fabrication of Ag/AgI/WO3 heterojunction anchored P and S co-doped graphitic carbon nitride as a dual Z scheme photocatalyst for efficient dye degradation. Solid State Sci. 100, 106095 https://doi.org/10.1016/j.solidstatesciences.2019.106095.

Herrera, M.U., Futalan, C.M., Gapusan, R., Balela, M.D.L., 2018. Removal of methyl orange dye and copper (II) ions from aqueous solution using polyaniline-coated kapok (Ceiba pentandra) fibers. Water Sci. Technol. 78, 1137–1147. https://doi.org/10.2166/wst.2018.385.

Hosseini, H., Mousavi, S.M., 2021. Bacterial cellulose/polyaniline nanocomposite aerogels as novel bioadsorbents for removal of hexavalent chromium: experimental and simulation study. J. Clean. Prod. 278, 123817 https://doi.org/10.1016/j.jclepro.2020.123817.

Hosseini, H., Zirakjou, A., Goodarzi, V., Mousavi, S.M., Khonakdar, H.A., Zamanlui, S., 2020. Lightweight aerogels based on bacterial cellulose/silver nanoparticles/polyaniline with tuning morphology of polyaniline and application in soft tissue engineering. Int. J. Biol. Macromol. 152, 57–67. https://doi.org/10.1016/j.ijbiomac.2020.02.095.

Hu, W., Chen, S., Yang, Z., Liu, L., Wang, H., 2011. Flexible electrically conductive nanocomposite membrane based on bacterial cellulose and polyaniline. J. Phys. Chem. B 115, 8453–8457. https://doi.org/10.1021/jp204422v.

Huang, M., Tang, Y., Wang, X., Zhu, P., Chen, T., Zhou, Y., 2021. Preparation of polyaniline/cellulose nanocrystal composite and its application in surface coating of cellulosic paper. Prog. Org. Coat. 159, 106452 https://doi.org/10.1016/j.porgcoat.2021.106452.

Itoi, H., Hayashi, S., Matsufusa, H., Ohzawa, Y., 2017. Electrochemical synthesis of polyaniline in the micropores of activated carbon for high-performance electrochemical capacitors. Chem. Commun. 53, 3201–3204. https://doi.org/10.1039/C6CC08822H.

Jahan, K., Kumar, N., Verma, V., 2018. Removal of hexavalent chromium from potable drinking using a polyaniline-coated bacterial cellulose mat. Environ. Sci.: Water Res. Technol. 4, 1589–1603. https://doi.org/10.1039/C8EW00255J.

Janaki, V., Vijayaraghavan, K., Oh, B.-T., Ramasamy, A.K., Kamala-Kannan, S., 2013. Synthesis, characterization and application of cellulose/polyaniline nanocomposite for the treatment of simulated textile effluent. Cellulose 20, 1153–1166. https://doi.org/10.1007/s10570-013-9910-x.

Jasim, A., 2017. Synthesis and characterization of bacterial cellulose/PAni composite for antibacterial and biomedical application. Synthesis 54.

Jasim, A., Ullah, M.W., Shi, Z., Lin, X., Yang, G., 2017. Fabrication of bacterial cellulose/polyaniline/single-walled carbon nanotubes membrane for potential application as biosensor. Carbohydr. Polym. 163, 62–69. https://doi.org/10.1016/j.carbpol.2017.01.056.

Jaymand, M., 2013. Recent progress in chemical modification of polyaniline. Prog. Polym. Sci. 38, 1287–1306. https://doi.org/10.1016/j.progpolymsci.2013.05.015.

Jiang, N., Xu, Y., Dai, Y., Luo, W., Dai, L., 2012. Polyaniline nanofibers assembled on alginate microsphere for Cu2+ and Pb2+ uptake. J. Hazard. Mater. 215–216, 17–24. https://doi.org/10.1016/j.jhazmat.2012.02.026.

Jiang, Y., Liu, Z., Zeng, G., Liu, Yujie, Shao, B., Li, Z., Liu, Yang, Zhang, W., He, Q., 2018. Polyaniline-based adsorbents for removal of hexavalent chromium from aqueous solution: a mini review. Environ. Sci. Pollut. Res. 25, 6158–6174. https://doi.org/10.1007/s11356-017-1188-3.

Kaitsuka, Y., Hayashi, N., Shimokawa, T., Togawa, E., Goto, H., 2016. Synthesis of polyaniline (PANI) in nano-reaction field of cellulose nanofiber (CNF), and carbonization. Polymers 8, 40. https://doi.org/10.3390/polym8020040.

Kakde, K., 2017. Synthesis and characterization of polyaniline doped with HCl H. Indian J. Sci. Technol. 10, 20.

Kateb, M., Safarian, S., Kolahdouz, M., Fathipour, M., Ahamdi, V., 2016. ZnO–PEDOT core–shell nanowires: an ultrafast, high contrast and transparent electrochromic display. Sol. Energy Mater. Sol. Cells 145, 200–205. https://doi.org/10.1016/j.solmat.2015.10.014.

Kaur, G., Adhikari, R., Cass, P., Bown, M., Gunatillake, P., 2015. Electrically conductive polymers and composites for biomedical applications. RSC Adv. 5, 37553–37567. https://doi.org/10.1039/C5RA01851J.

Kaur, M., Malik, B., Garg, T., Rath, G., Goyal, A.K., 2015. Development and characterization of guar gum nanoparticles for oral immunization against tuberculosis. Drug Deliv. 22, 328–334. https://doi.org/10.3109/10717544.2014.894594.

Ke, S., Ouyang, T., Zhang, K., Nong, Y., Mo, Y., Mo, Q., Wei, Y., Cheng, F., 2019. Highly conductive cellulose network/polyaniline composites prepared by wood fractionation and in situ polymerization of aniline. Macromol. Mater. Eng. 304, 1900112. https://doi.org/10.1002/mame.201900112.

Khadir, A., Negarestani, M., Ghiasinejad, H., 2020. Low-cost sisal fibers/polypyrrole/polyaniline biosorbent for sequestration of reactive orange 5 from aqueous solutions. J. Environ. Chem. Eng. 8, 103956.
Khalid, M., Tumelero, M.A., Brandt, I., Zoldan, V.C., Acuña, J.J., Pasa, A.A., 2013. Electrical conductivity studies of polyaniline nanotubes doped with different sulfonic acids. Indian J. Mater. Sci. 2013.
Khandelwal, V., Sahoo, S.K., Kumar, A., Manik, G., 2018. Electrically conductive green composites based on epoxidized linseed oil and polyaniline: an insight into electrical, thermal and mechanical properties. Compos. Part B: Eng. 136, 149–157. https://doi.org/10.1016/j.compositesb.2017.10.030.
Kherroub, D.E., Bouhadjar, L., Medjahdi, M., 2021. Development of novel conductive copolymer based on furan with improved solubility and thermal properties. J. Mol. Struct. 1225, 129174.
Kim, T.-H., Yea, C.-H., Chueng, S.-T.D., Yin, P.T.-T., Conley, B., Dardir, K., Pak, Y., Jung, G.Y., Choi, J.-W., Lee, K.-B., 2015. Large-scale nanoelectrode arrays to monitor the dopaminergic differentiation of human neural stem cells. Adv. Mater. 27, 6356–6362. https://doi.org/10.1002/adma.201502489.
Kim, Y., Ullah, M.W., Ul-Islam, M., Khan, S., Jang, J.H., Park, J.K., 2019. Self-assembly of bio-cellulose nanofibrils through intermediate phase in a cell-free enzyme system. Biochem. Eng. J. 142, 135–144. https://doi.org/10.1016/j.bej.2018.11.017.
Klemm, D., Heublein, B., Fink, H.-P., Bohn, A., 2005. Cellulose: fascinating biopolymer and sustainable raw material. Angew. Chem. Int. Ed. 44, 3358–3393.
Kong, I., Tshai, K.Y., Hoque, M.E., 2015. Manufacturing of natural fibre-reinforced polymer composites by solvent casting method. In: Salit, M.S., Jawaid, M., Yusoff, N. B., Hoque, M.E. (Eds.), Manufacturing of Natural Fibre Reinforced Polymer Composites. Springer International Publishing, Cham, pp. 331–349. https://doi.org/10.1007/978-3-319-07944-8_16.
Kotresh, S., Ravikiran, Y.T., Raj Prakash, H.G., Ramana, Ch.V.V., Vijayakumari, S.C., Thomas, S., 2016. Humidity sensing performance of spin coated polyaniline–carboxymethyl cellulose composite at room temperature. Cellulose 23, 3177–3186. https://doi.org/10.1007/s10570-016-1035-6.
Krishna, B.S., Murty, D.S.R., Jai Prakash, B.S., 2000. Thermodynamics of chromium(VI) anionic species sorption onto surfactant-modified montmorillonite clay. J. Colloid Interface Sci. 229, 230–236. https://doi.org/10.1006/jcis.2000.7015.
Kumar, P.A., Chakraborty, S., Ray, M., 2008. Removal and recovery of chromium from wastewater using short chain polyaniline synthesized on jute fiber. Chem. Eng. J. 141, 130–140. https://doi.org/10.1016/j.cej.2007.11.004.
Kumar, A., Sood, A., Han, S.S., 2022. Potential of magnetic nano cellulose in biomedical applications: Recent Advances. Biomaterials and Polymers Horizon 1, 32–47.
Lavoine, N., Desloges, I., Dufresne, A., Bras, J., 2012. Microfibrillated cellulose – its barrier properties and applications in cellulosic materials: a review. Carbohydr. Polym. 90, 735–764.
Le Gars, M., Douard, L., Belgacem, N., Bras, J., 2019. Cellulose nanocrystals: from classical hydrolysis to the use of deep eutectic solvents. Smart Nanosystems for Biomedicine, Optoelectronics and Catalysis. IntechOpen,.
Le Hoang, S., Vu, C.M., Pham, L.T., Choi, H.J., 2018. Preparation and physical characteristics of epoxy resin/ bacterial cellulose biocomposites. Polym. Bull. 75, 2607–2625. https://doi.org/10.1007/s00289-017-2162-4.
Lee, H.-J., Chung, T.-J., Kwon, H.-J., Kim, H.-J., Tze, W.T.Y., 2012. Fabrication and evaluation of bacterial cellulose-polyaniline composites by interfacial polymerization. Cellulose 19, 1251–1258. https://doi.org/10.1007/s10570-012-9705-5.
Li, R., Liu, L., Yang, F., 2014. Removal of aqueous Hg(II) and Cr(VI) using phytic acid doped polyaniline/cellulose acetate composite membrane. J. Hazard. Mater. 280, 20–30. https://doi.org/10.1016/j.jhazmat.2014.07.052.
Li, Y., 2015. Conducting polymers. In: Li, Y. (Ed.), Organic Optoelectronic Materials, Lecture Notes in Chemistry. Springer International Publishing, Cham, pp. 23–50. https://doi.org/10.1007/978-3-319-16862-3_2.
Lin, Z., Guan, Z., Huang, Z., 2013. New bacterial cellulose/polyaniline nanocomposite film with one conductive side through constrained interfacial polymerization. Ind. Eng. Chem. Res. 52, 2869–2874. https://doi.org/10.1021/ie303297b.
Liu, D.Y., Sui, G.X., Bhattacharyya, D., 2014. Synthesis and characterisation of nanocellulose-based polyaniline conducting films. Compos. Sci. Technol. 99, 31–36. https://doi.org/10.1016/j.compscitech.2014.05.001.
Liu, K., Nasrallah, J., Chen, L., Huang, L., Ni, Y., Lin, S., Wang, H., 2018. A facile template approach to preparing stable NFC/Ag/polyaniline nanocomposites for imparting multifunctionality to paper. Carbohydr. Polym. 194, 97–102. https://doi.org/10.1016/j.carbpol.2018.04.015.
Logan, B.E., Wallack, M.J., Kim, K.-Y., He, W., Feng, Y., Saikaly, P.E., 2015. Assessment of microbial fuel cell configurations and power densities. Environ. Sci. Technol. Lett. 2, 206–214. https://doi.org/10.1021/acs.estlett.5b00180.
Lyu, W., Yu, M., Feng, J., Yan, W., 2018. Highly crystalline polyaniline nanofibers coating with low-cost biomass for easy separation and high efficient removal of anionic dye ARG from aqueous solution. Appl. Surf. Sci. 458, 413–424. https://doi.org/10.1016/j.apsusc.2018.07.074.
Lyu, W., Li, J., Zheng, L., Liu, H., Chen, J., Zhang, W., Liao, Y., 2021. Fabrication of 3D compressible polyaniline/cellulose nanofiber aerogel for highly efficient removal of organic pollutants and its environmental-friendly regeneration by peroxydisulfate process. Chem. Eng. J. 414, 128931 https://doi.org/10.1016/j.cej.2021.128931.
Ma, Y., Lv, L., Guo, Y., Fu, Y., Shao, Q., Wu, T., Guo, S., Sun, K., Guo, X., Wujcik, E.K., Guo, Z., 2017. Porous lignin based poly (acrylic acid)/organo-montmorillonite nanocomposites: swelling behaviors and rapid removal of Pb (II) ions. Polymer 128, 12–23. https://doi.org/10.1016/j.polymer.2017.09.009.
Mahato, N., Jang, H., Dhyani, A., Cho, S., 2020. Recent progress in conducting polymers for hydrogen storage and fuel cell applications. Polymers 12, 2480.
Maity, D., Kumar, R.T.R., 2018. Polyaniline anchored MWCNTs on fabric for high performance wearable ammonia sensor. ACS Sens. 3, 1822–1830. https://doi.org/10.1021/acssensors.8b00589.
Manan, S., Ullah, M.W., Ul-Islam, M., Shi, Z., Gauthier, M., Yang, G., 2022. Bacterial cellulose: molecular regulation of biosynthesis, supramolecular assembly, and tailored structural and functional properties. Prog. Mater. Sci. 129, 100972 https://doi.org/10.1016/j.pmatsci.2022.100972.
Mani, G.K., Rayappan, J.B.B., 2015. A highly selective and wide range ammonia sensor — nanostructured ZnO:Co thin film. Mater. Sci. Eng.: B 191, 41–50. https://doi.org/10.1016/j.mseb.2014.10.007.
Mansour, M.S., Ossman, M.E., Farag, H.A., 2011. Removal of Cd (II) ion from waste water by adsorption onto polyaniline coated on sawdust. Desalination 272, 301–305. https://doi.org/10.1016/j.desal.2011.01.037.
Marins, J.A., Soares, B.G., Fraga, M., Müller, D., Barra, G.M.O., 2014. Self-supported bacterial cellulose polyaniline conducting membrane as electromagnetic interference shielding material: effect of the oxidizing agent. Cellulose 21, 1409–1418. https://doi.org/10.1007/s10570-014-0191-9.
Mashkour, Mehrdad, Rahimnejad, M., Mashkour, Mahdi, 2016. Bacterial cellulose-polyaniline nano-biocomposite: a porous media hydrogel bioanode enhancing the performance of microbial fuel cell. J. Power Sources 325, 322–328. https://doi.org/10.1016/j.jpowsour.2016.06.063.
Menon, R., Mukherjee, A.K., 2004. Polyaniline fractal nanocomposites. In: Encyclopedia of Nanoscience and Nanotechnology. American Scientific Publishers, pp. 715–729.
Miretzky, P., Cirelli, A.F., 2010. Cr(VI) and Cr(III) removal from aqueous solution by raw and modified lignocellulosic materials: a review. J. Hazard. Mater. 180, 1–19. https://doi.org/10.1016/j.jhazmat.2010.04.060.
Moghadam, P.N., Zare, E.N., Amiri, H., Lakouraj, M.M., 2012. Preparation of conductive nanocomposites based on poly (aniline-co- butyl 3-aminobenzoate) and poly (aniline-co-ethyl 3-aminobenzoate) by solution blending method. Compos. Interfaces 19, 475–488. https://doi.org/10.1080/15685543.2012.760263.
Mohan, D., Singh, K., Singh, V., 2006. Trivalent chromium removal from wastewater using low cost activated carbon derived from agricultural waste material and activated carbon fabric cloth. J. Hazard. Mater. 135, 280–295. https://doi.org/10.1016/j.jhazmat.2005.11.075.
Moon, R.J., Martini, A., Nairn, J., Simonsen, J., Youngblood, J., 2011. Cellulose nanomaterials review: structure, properties and nanocomposites. Chem. Soc. Rev. 40, 3941–3994.
MuDan, Y., XueRen, Q., WanPeng, Z., 2018. Photocatalytic activity of CdS@ polyaniline/cellulose fibers composite. Chem. Ind. For. Prod. 38, 115–121.
Najafi Moghadam, P., Nazarzadeh Zareh, E., 2010. Synthesis of conductive nanocomposites based on polyaniline/poly(styrene-alt-maleic anhydride)/polystyrene. e-Polym. 10 https://doi.org/10.1515/epoly.2010.10.1.588.
Nepomuceno, N.C., Seixas, A.A.A., Medeiros, E.S., Mélo, T.J.A., 2021. Evaluation of conductivity of nanostructured polyaniline/cellulose nanocrystals (PANI/CNC) obtained via in situ polymerization. J. Solid State Chem. 302, 122372 https://doi.org/10.1016/j.jssc.2021.122372.
Nezakati, T., Seifalian, A., Tan, A., Seifalian, A.M., 2018. Conductive polymers: opportunities and challenges in biomedical applications. Chem. Rev. 118, 6766–6843. https://doi.org/10.1021/acs.chemrev.6b00275.
Nicho, M., 2004. Synthesis of derivatives of polythiophene and their application in an electrochromic device. Sol. Energy Mater. Sol. Cells 82, 105–118. https://doi.org/10.1016/j.solmat.2004.01.009.
Norouzian, R.-S., Lakouraj, M.M., Zare, E.N., 2014. Novel conductive PANI/hydrophilic thiacalix [4] arene nanocomposites: synthesis, characterization and investigation of properties. Chin. J. Polym. Sci. 32, 218–229.
O'sullivan, A.C., 1997. Cellulose: the structure slowly unravels. Cellulose 4, 173–207.
Oberhaus, F.V., Frense, D., 2021. Fast, simple, and gentle method for removal of polythiophene and other conductive polymer films from gold electrodes. J. Electroanal. Chem. 895, 115466.
Olad, A., Bastanian, M., Aber, S., Zebhi, H., 2021. Ion-crosslinked carboxymethyl cellulose/polyaniline bio-conducting interpenetrated polymer network: preparation, characterization and application for an efficient removal of Cr(VI) from aqueous solution. Iran. Polym. J. 30, 105–119. https://doi.org/10.1007/s13726-020-00877-7.
Omura, T., Chan, C.H., Wakisaka, M., Nishida, H., 2019. Organic thin paper of cellulose nanofiber/polyaniline doped with (±)-10-camphorsulfonic acid nanohybrid and its application to electromagnetic shielding. ACS Omega 4, 9446–9452. https://doi.org/10.1021/acsomega.9b00708.
Owlad, M., Aroua, M.K., Daud, W.A.W., Baroutian, S., 2009. Removal of hexavalent chromium-contaminated water and wastewater: a review. Water Air Soil Pollut. 200, 59–77. https://doi.org/10.1007/s11270-008-9893-7.
Palza, H., Zapata, P.A., Angulo-Pineda, C., 2019. Electroactive smart polymers for biomedical applications. Materials 12, 277.
Pang, Z., Yang, Z., Chen, Y., Zhang, J., Wang, Q., Huang, F., Wei, Q., 2016. A room temperature ammonia gas sensor based on cellulose/TiO 2 /PANI composite nanofibers. Colloids Surf. A: Physicochem. Eng. Asp. 494, 248–255. https://doi.org/10.1016/j.colsurfa.2016.01.024.
Pappu, A., Pickering, K.L., Thakur, V.K., 2019. Manufacturing and characterization of sustainable hybrid composites using sisal and hemp fibres as reinforcement of poly (lactic acid) via injection moulding. Ind. Crops Prod. 137, 260–269. https://doi.org/10.1016/j.indcrop.2019.05.040.
Park, M., Lee, D., Shin, S., Kim, H.-J., Hyun, J., 2016. Flexible conductive nanocellulose combined with silicon nanoparticles and polyaniline. Carbohydr. Polym. 140, 43–50. https://doi.org/10.1016/j.carbpol.2015.12.046.

Patra, B.N., Majhi, D., 2015. Removal of anionic dyes from water by potash alum doped polyaniline: investigation of kinetics and thermodynamic parameters of adsorption. J. Phys. Chem. B 119, 8154–8164. https://doi.org/10.1021/acs.jpcb.5b00535.
Peng, H., Ma, G., Sun, K., Mu, J., Zhou, X., Lei, Z., 2015. A novel fabrication of nitrogen-containing carbon nanospheres with high rate capability as electrode materials for supercapacitors. RSC Adv. 5, 12034–12042. https://doi.org/10.1039/C4RA11889H.
Petersen, N., Gatenholm, P., 2011. Bacterial cellulose-based materials and medical devices: current state and perspectives. Appl. Microbiol Biotechnol. 91, 1277–1286. https://doi.org/10.1007/s00253-011-3432-y.
Phanthong, P., Reubroycharoen, P., Hao, X., Xu, G., Abudula, A., Guan, G., 2018. Nanocellulose: extraction and application. Carbon Resour. Convers. 1, 32–43.
Pierini, F., Lanzi, M., Nakielski, P., Kowalewski, T.A., 2017. Electrospun polyaniline-based composite nanofibers: tuning the electrical conductivity by tailoring the structure of thiol-protected metal nanoparticles. J. Nanomater. 2017.
Platnieks, O., Sereda, A., Gaidukovs, S., Thakur, V.K., Barkane, A., Gaidukova, G., Filipova, I., Ogurcovs, A., Fridrihsone, V., 2021. Adding value to poly (butylene succinate) and nanofibrillated cellulose-based sustainable nanocomposites by applying masterbatch process. Ind. Crops Prod. 169, 113669 https://doi.org/10.1016/j.indcrop.2021.113669.
Poddar, M.K., Dikshit, P.K., 2021. Recent development in bacterial cellulose production and synthesis of cellulose based conductive polymer nanocomposites. Nano Sel. 2, 1605–1628. https://doi.org/10.1002/nano.202100044.
Pradhan, S.H., Mulenos, M.R., Steele, L.R., Gibb, M., Ede, J.D., Ong, K.J., Shatkin, J.A., Sayes, C.M., 2020. Physical, chemical, and toxicological characterization of fibrillated forms of cellulose using an in vitro gastrointestinal digestion and co-culture model. Toxicol. Res. 9, 290–301. https://doi.org/10.1093/toxres/tfaa026.
Prajapati, D.G., Kandasubramanian, B., 2019. Progress in the development of intrinsically conducting polymer composites as biosensors. Macromol. Chem. Phys. 220, 1800561.
Qiu, B., Xu, C., Sun, D., Wei, H., Zhang, X., Guo, J., Wang, Q., Rutman, D., Guo, Z., Wei, S., 2014a. Polyaniline coating on carbon fiber fabrics for improved hexavalent chromium removal. RSC Adv. 4, 29855 https://doi.org/10.1039/C4RA01700E.
Qiu, B., Xu, C., Sun, D., Yi, H., Guo, J., Zhang, X., Qu, H., Guerrero, M., Wang, X., Noel, N., Luo, Z., Guo, Z., Wei, S., 2014b. Polyaniline coated ethyl cellulose with improved hexavalent chromium removal. ACS Sustain. Chem. Eng. 2, 2070–2080. https://doi.org/10.1021/sc5003209.
Qiu, B., Xu, C., Sun, D., Wang, Q., Gu, H., Zhang, X., Weeks, B.L., Hopper, J., Ho, T.C., Guo, Z., Wei, S., 2015. Polyaniline coating with various substrates for hexavalent chromium removal. Appl. Surf. Sci. 334, 7–14. https://doi.org/10.1016/j.apsusc.2014.07.039.
Raizada, P., Thakur, P., Sudhaik, A., Singh, P., Thakur, V.K., Hosseini-Bandegharaei, A., 2020. Fabrication of dual Z-scheme photocatalyst via coupling of BiOBr/Ag/AgCl heterojunction with P and S co-doped g-C3N4 for efficient phenol degradation. Arab. J. Chem. 13, 4538–4552. https://doi.org/10.1016/j.arabjc.2019.10.001.
Rana, Ashvinder K., Gupta, V.K., Saini, A.K., Voicu, S.I., Abdellattifaand, M.H., Thakur, V.K., 2021a. Water desalination using nanocelluloses/cellulose derivatives based membranes for sustainable future. Desalination 520, 115359.
Rana, Ashvinder K., Mishra, Y.K., Gupta, V.K., Thakur, V.K., 2021b. Sustainable materials in the removal of pesticides from contaminated water: perspective on macro to nanoscale cellulose. Sci. Total Environ. 797, 149129 https://doi.org/10.1016/j.scitotenv.2021.149129.
Rana, Ashvinder K., Potluri, P., Thakur, V.K., 2021c. Cellulosic Grewia optiva fibres: towards chemistry, surface engineering and sustainable materials. J. Environ. Chem. Eng., 106059
Rana, Ashvinder K., Thakur, V.K., Singha, A.S., 2021d. Towards the use of acrylic acid graft-copolymerized plant biofiber in sustainable fortified composites: manufacturing and characterization. e-Polym. 21, 881–896. https://doi.org/10.1515/epoly-2021-0080.
Rana, Ashvinder Kumar, Frollini, E., Thakur, V.K., 2021. Cellulose nanocrystals: pretreatments, preparation strategies, and surface functionalization. Int. J. Biol. Macromol. 182, 1554–1581.
Rana, D.S., Thakur, N., Thakur, S., Singh, D., 2022. Electrochemical determination of hydrazine by using MoS2 nanostructure modified gold electrode. Nanofabrication 7. https://doi.org/10.37819/nanofab.007.190.
Ravikiran, Y.T., Kotresh, S., Vijayakumari, S.C., Thomas, S., 2014. Liquid petroleum gas sensing performance of polyaniline-carboxymethyl cellulose composite at room temperature. Curr. Appl. Phys. 14, 960–964.
Razalli, R.L., Abdi, M.M., Tahir, P.M., Moradbak, A., Sulaiman, Y., Heng, L.Y., 2017. Polyaniline-modified nanocellulose prepared from Semantan bamboo by chemical polymerization: preparation and characterization. RSC Adv. 7, 25191–25198. https://doi.org/10.1039/C7RA03379F.
Rebelo, A., Liu, Y., Liu, C., Schäfer, K.-H., Saumer, M., Yang, G., 2019. Poly(4-vinylaniline)/polyaniline bilayer functionalized bacterial cellulose membranes as bioelectronics interfaces. Carbohydr. Polym. 204, 190–201. https://doi.org/10.1016/j.carbpol.2018.10.017.
Rebelo, A.R., Liu, C., Schäfer, K.-H., Saumer, M., Yang, G., Liu, Y., 2019. Poly(4-vinylaniline)/polyaniline bilayer-functionalized bacterial cellulose for flexible electrochemical biosensors. Langmuir 35, 10354–10366. https://doi.org/10.1021/acs.langmuir.9b01425.
ResearchMoz QYResearch, 2017. Available online at: ⟨https://www.researchmoz.us/globalmicrobial-and-bacterial-cellulose-market-research-report-2017-report.html⟩.
Samadi, A., Xie, M., Li, J., Shon, H., Zheng, C., Zhao, S., 2021. Polyaniline-based adsorbents for aqueous pollutants removal: a review. Chem. Eng. J. 418, 129425 https://doi.org/10.1016/j.cej.2021.129425.
Santoro, C., Arbizzani, C., Erable, B., Ieropoulos, I., 2017. Microbial fuel cells: from fundamentals to applications. A review. J. Power Sources 356, 225–244. https://doi.org/10.1016/j.jpowsour.2017.03.109.
Sapurina, I., Stejskal, J., 2008. The mechanism of the oxidative polymerization of aniline and the formation of supramolecular polyaniline structures. Polym. Int. 57, 1295–1325. https://doi.org/10.1002/pi.2476.
Shaghaleh, H., Xu, X., Wang, S., 2018. Current progress in production of biopolymeric materials based on cellulose, cellulose nanofibers, and cellulose derivatives. RSC Adv. 8, 825–842.
Shahadat, M., Khan, M.Z., Rupani, P.F., Embrandiri, A., Sultana, S., Ahammad, S.Z., Ali, S.W., Sreekrishnan, T.R., 2017. A critical review on the prospect of polyaniline-grafted biodegradable nanocomposite. Adv. Colloid Interface Sci. 249, 2–16.
Shalini, A., Nishanthi, R., Palani, P., Jaisankar, V., 2016. One pot synthesis, characterization of polyaniline and cellulose/polyaniline nanocomposites: application towards in vitro measurements of antibacterial activity. Mater. Today.: Proc. 3, 1633–1642. https://doi.org/10.1016/j.matpr.2016.04.053.
Sharma, B., Thakur, S., Mamba, G., Prateek, Gupta, R.K., Gupta, V.K., Thakur, V.K., 2021. Titania modified gum tragacanth based hydrogel nanocomposite for water remediation. J. Environ. Chem. Eng. 9, 104608 https://doi.org/10.1016/j.jece.2020.104608.
Sheng, L., Jiang, R., Zhu, Y., Ji, Y., 2014. Electrospun cellulose nanocrystals/polycaprolactone nanocomposite fiber mats. J. Macromol. Sci. Part B 53, 820–828. https://doi.org/10.1080/00222348.2013.861311.
Shim, E., Noro, J., Cavaco-Paulo, A., Silva, C., Kim, H.R., 2019. Effect of additives on the in situ laccase-catalyzed polymerization of aniline onto bacterial cellulose. Front. Bioeng. Biotechnol. 7, 264. https://doi.org/10.3389/fbioe.2019.00264.
Sim, B., Choi, H.J., 2015. Facile synthesis of polyaniline nanotubes and their enhanced stimuli-response under electric fields. RSC Adv. 5, 11905–11912. https://doi.org/10.1039/C4RA13635G.
Singha, A.S., Kumar Thakur, V., 2008. Saccaharum cilliare fiber reinforced polymer composites. E-J. Chem. 5, 782–791. https://doi.org/10.1155/2008/941627.
Singha, A.S., Thakur, V.K., 2009a. Fabrication and characterization of H. sabdariffa fiber-reinforced green polymer composites. Polym. -Plast. Technol. Eng. 48, 482–487. https://doi.org/10.1080/03602550902725498.
Singha, A.S., Thakur, V.K., 2009b. Mechanical, thermal and morphological properties of grewia optiva fiber/polymer matrix composites. Polym. -Plast. Technol. Eng. 48, 201–208. https://doi.org/10.1080/03602550802634550.
Singha, A.S., Thakur, V.K., 2009c. Fabrication and characterization of S. cilliare fibre reinforced polymer composites. Bull. Mater. Sci. 32, 49–58. https://doi.org/10.1007/s12034-009-0008-x.
Singha, A.S., Shama, A., Thakur, V.K., 2008. X-ray diffraction, morphological, and thermal studies on methylmethacrylate graft copolymerized saccharum ciliare fiber. Int. J. Polym. Anal. Charact. 13, 447–462. https://doi.org/10.1080/10236660802399747.
Singha, Amar Singh, Thakur, V.K., 2008. Fabrication of Hibiscus sabdariffa fibre reinforced polymer composites. Iran. Polym. J. 17, 541–553.
Singha, Amar Singh, Thakur, V.K., 2009. Morphological, thermal, and physicochemical characterization of surface modified pinus fibers. Int. J. Polym. Anal. Charact. 14, 271–289. https://doi.org/10.1080/10236660802666160.
Skotheim, T.A., Reynolds, J., 2006. Conjugated Polymers: Theory, Synthesis, Properties, and Characterization. CRC press.
Song, M., Yu, H., Zhu, J., Ouyang, Z., Abdalkarim, S.Y.H., Tam, K.C., Li, Y., 2020. Constructing stimuli-free self-healing, robust and ultrasensitive biocompatible hydrogel sensors with conductive cellulose nanocrystals. Chem. Eng. J. 398, 125547 https://doi.org/10.1016/j.cej.2020.125547.
Song, X., Dong, G., Gao, F., Xiao, Y., Liu, Q., Diao, X., 2015. Properties of NiO x and its influence upon all-thin-film ITO/NiO x /LiTaO 3 /WO 3 /ITO electrochromic devices prepared by magnetron sputtering. Vacuum 111, 48–54. https://doi.org/10.1016/j.vacuum.2014.09.007.
Stanislawska, A., 2016. Bacterial nanocellulose as a microbiological derived nanomaterial. Adv. Mater. Sci. 16, 45.
Sudhaik, A., Raizada, P., Khan, A.A.P., Singh, A., Singh, P., 2022. Graphitic carbon nitride-based upconversion photocatalyst for hydrogen production and water purification. Nanofabrication 7. https://doi.org/10.37819/nanofab.007.189.
Tabrizi, L., Chiniforoshan, H., 2017. High-performance room temperature gas sensor based on gold(III) pincer complex with high sensitivity for NH3. Sens. Actuators B: Chem. 245, 815–820. https://doi.org/10.1016/j.snb.2017.01.193.
Tan, H., Xiao, D., Navik, R., Zhao, Y., 2021. Facile fabrication of polyaniline/pristine graphene–bacterial cellulose composites as high-performance electrodes for constructing flexible all-solid-state supercapacitors. ACS Omega 6, 11427–11435. https://doi.org/10.1021/acsomega.1c00442.
Thakur, S., Sharma, B., Verma, A., Chaudhary, J., Tamulevicius, S., Thakur, V.K., 2018. Recent progress in sodium alginate based sustainable hydrogels for environmental applications. J. Clean. Prod. 198, 143–159. https://doi.org/10.1016/j.jclepro.2018.06.259.
Thakur, S., Verma, A., Kumar, V., Jin Yang, X., Krishnamurthy, S., Coulon, F., Thakur, V. K., 2022. Cellulosic biomass-based sustainable hydrogels for wastewater remediation: chemistry and prospective. Fuel 309, 122114. https://doi.org/10.1016/j.fuel.2021.122114.
Thakur, V.K., Thakur, M.K., 2015. Recent advances in green hydrogels from lignin: a review. Int. J. Biol. Macromol. 72, 834–847. https://doi.org/10.1016/j.ijbiomac.2014.09.044.
Thakur, V.K., Voicu, S.I., 2016. Recent advances in cellulose and chitosan based membranes for water purification: a concise review. Carbohydr. Polym. 146, 148–165. https://doi.org/10.1016/j.carbpol.2016.03.030.

Thakur, V.K., Singha, A.S., Thakur, M.K., 2013. Fabrication and physico-chemical properties of high-performance pine needles/green polymer composites. Int. J. Polym. Mater. Polym. Biomater. 62, 226–230. https://doi.org/10.1080/00914037.2011.641694.
Thomas, S., Visakh, P.M., 2011a. Handbook of Engineering and Speciality Thermoplastics: Polyethers and Polyesters. Wiley Online Library,.
Thomas, S., Visakh, P.M., 2011b. Handbook of Engineering and Specialty Thermoplastics, Volume 4: Nylons. John Wiley & Sons.
Tian, J., Peng, D., Wu, X., Li, W., Deng, H., Liu, S., 2017. Electrodeposition of Ag nanoparticles on conductive polyaniline/cellulose aerogels with increased synergistic effect for energy storage. Carbohydr. Polym. 156, 19–25. https://doi.org/10.1016/j.carbpol.2016.09.005.
Tian, Z., Yu, H., Wang, L., Saleem, M., Ren, F., Ren, P., Chen, Y., Sun, R., Sun, Y., Huang, L., 2014. Recent progress in the preparation of polyaniline nanostructures and their applications in anticorrosive coatings. RSC Adv. 4, 28195 https://doi.org/10.1039/c4ra03146f.
Tissera, N.D., Wijesena, R.N., Rathnayake, S., de Silva, R.M., de Silva, K.M.N., 2018. Heterogeneous in situ polymerization of polyaniline (PANI) nanofibers on cotton textiles: improved electrical conductivity, electrical switching, and tuning properties. Carbohydr. Polym. 186, 35–44. https://doi.org/10.1016/j.carbpol.2018.01.027.
Tong, Z., Li, N., Lv, H., Tian, Y., Qu, H., Zhang, X., Zhao, J., Li, Y., 2016. Annealing synthesis of coralline V2O5 nanorod architecture for multicolor energy-efficient electrochromic device. Sol. Energy Mater. Sol. Cells 146, 135–143. https://doi.org/10.1016/j.solmat.2015.11.008.
Trindade, E.C.A., Antônio, R.V., Brandes, R., Souza, L., Neto, G., Vargas, V.M.M., Carminatti, C.A., Oliveira Souza Recouvreux, D., 2020. Carbon fiber embedded bacterial cellulose/polyaniline nanocomposite with tailored for microbial fuel cells electrode. J. Appl. Polym. Sci. 137, 49036 https://doi.org/10.1002/app.49036.
Truong, D.H., Dam, M.S., Bujna, E., Rezessy-Szabo, J., Farkas, C., Vi, V.N.H., Csernus, O., Nguyen, V.D., Gathergood, N., Friedrich, L., Hafidi, M., Gupta, V.K., Nguyen, Q.D., 2021. In situ fabrication of electrically conducting bacterial cellulose-polyaniline-titanium-dioxide composites with the immobilization of Shewanella xiamenensis and its application as bioanode in microbial fuel cell. Fuel 285, 119259. https://doi.org/10.1016/j.fuel.2020.119259.
Ucar, D., Zhang, Y., Angelidaki, I., 2017. An overview of electron acceptors in microbial fuel cells. Front. Microbiol. 8 https://doi.org/10.3389/fmicb.2017.00643.
Ul-Islam, M., Ullah, M.W., Khan, S., Park, J.K., 2020. Production of bacterial cellulose from alternative cheap and waste resources: a step for cost reduction with positive environmental aspects. Korean J. Chem. Eng. 37, 925–937. https://doi.org/10.1007/s11814-020-0524-3.
Ullah, M.W., Ul-Islam, M., Khan, S., Kim, Y., Park, J.K., 2015. Innovative production of bio-cellulose using a cell-free system derived from a single cell line. Carbohydr. Polym. 132, 286–294. https://doi.org/10.1016/j.carbpol.2015.06.037.
Ullah, M.W., Ul-Islam, M., Khan, S., Kim, Y., Park, J.K., 2016. Structural and physico-mechanical characterization of bio-cellulose produced by a cell-free system. Carbohydr. Polym. 136, 908–916. https://doi.org/10.1016/j.carbpol.2015.10.010.
Ummami, R., Busroni, B., Piluharto, B., 2021. Synthesis and characterization of bacterial cellulose-polyaniline composite with variation of dopant concentration. B. SAINSTEK 9, 69. https://doi.org/10.19184/bst.v9i2.18120.
Uppal, N., Pappu, A., Gowri, V.K.S., Thakur, V.K., 2022. Cellulosic fibres-based epoxy composites: from bioresources to a circular economy. Ind. Crops Prod. 182, 114895 https://doi.org/10.1016/j.indcrop.2022.114895.
Usmani, Z., Sharma, M., Awasthi, A.K., Sivakumar, N., Lukk, T., Pecoraro, L., Thakur, V. K., Roberts, D., Newbold, J., Gupta, V.K., 2020. Bioprocessing of waste biomass for sustainable product development and minimizing environmental impact. Bioresour. Technol., 124548 https://doi.org/10.1016/j.biortech.2020.124548.
Vaghela, C., Kulkarni, M., Haram, S., Karve, M., Aiyer, R., 2016. Biopolymer-polyaniline composite for a wide range ammonia gas sensor. IEEE Sens. J. 16, 4318–4325.
Varshney, V.K., Naithani, S., 2011. Chemical functionalization of cellulose derived from nonconventional sources. In: Cellulose Fibers: Bio-and Nano-Polymer Composites. Springer, pp. 43–60.
Verma, A., Thakur, S., Mamba, G., Prateek, Gupta, R.K., Thakur, P., Thakur, V.K., 2020. Graphite modified sodium alginate hydrogel composite for efficient removal of malachite green dye. Int. J. Biol. Macromol. 148, 1130–1139. https://doi.org/10.1016/j.ijbiomac.2020.01.142.
Visakh, P.M., 2018. Polyaniline: Structure and Properties Relationship in Polyaniline Blends, Composites and Nanocomposites.
Volova, T.G., Prudnikova, S.V., Sukovatyi, A.G., Shishatskaya, E.I., 2018. Production and properties of bacterial cellulose by the strain Komagataeibacter xylinus B-12068. Appl. Microbiol. Biotechnol. 102, 7417–7428.
Wan, Y., Li, J., Yang, Z., Ao, H., Xiong, L., Luo, H., 2018. Simultaneously depositing polyaniline onto bacterial cellulose nanofibers and graphene nanosheets toward electrically conductive nanocomposites. Curr. Appl. Phys. 18, 933–940. https://doi.org/10.1016/j.cap.2018.05.008.
Wang, J., Pan, K., Giannelis, E.P., Cao, B., 2013. Polyacrylonitrile/polyaniline core/shell nanofiber mat for removal of hexavalent chromium from aqueous solution: mechanism and applications. RSC Adv. 3, 8978. https://doi.org/10.1039/c3ra40616d.
Wang, J., Tavakoli, J., Tang, Y., 2019. Bacterial cellulose production, properties and applications with different culture methods – a review. Carbohydr. Polym. 219, 63–76. https://doi.org/10.1016/j.carbpol.2019.05.008.
Wang, L., Hu, C., Shao, L., 2017. The antimicrobial activity of nanoparticles: present situation and prospects for the future. Int. J. Nanomed. 12, 1227–1249. https://doi.org/10.2147/IJN.S121956.
Wang, S., Wei, C., Gong, Y., Lv, J., Yu, C., Yu, J., 2016. Cellulose nanofiber-assisted dispersion of cellulose nanocrystals@polyaniline in water and its conductive films. RSC Adv. 6, 10168–10174. https://doi.org/10.1039/C5RA19346J.
Wang, X., Tang, Y., Zhu, X., Zhou, Y., Hong, X., 2020. Preparation and characterization of polylactic acid/polyaniline/nanocrystalline cellulose nanocomposite films. Int. J. Biol. Macromol. 146, 1069–1075. https://doi.org/10.1016/j.ijbiomac.2019.09.233.
Wang, Y.-P., Zhou, P., Luo, S.-Z., Guo, S., Lin, J., Shao, Q., Guo, X., Liu, Z., Shen, J., Wang, B., Guo, Z., 2018. In situ polymerized poly(acrylic acid)/alumina nanocomposites for $Pb^{2+}$ adsorption. Adv. Polym. Technol. 37, 2981–2996. https://doi.org/10.1002/adv.21969.
Wu, Q., Qin, Y.-F., Chen, L., Qin, Z.-Y., 2016. Conductive polyaniline/cellulose nanocrystals composite for ammonia gas detection. Computer Science and Engineering Technology (CSET2015), Medical Science and Biological Engineering (MSBE2015). Presented at the The Joint Conferences of 2015 International Conference on Computer Science and Engineering Technology (CSET2015) and 2015 International Conference on Medical Science and Biological Engineering (MSBE2015). World Scientific, Hong Kong, pp. 670–675. https://doi.org/10.1142/9789814651011_0093.
Xu, D., Fan, L., Gao, L., Xiong, Y., Wang, Y., Ye, Q., Yu, A., Dai, H., Yin, Y., Cai, J., Zhang, L., 2016. Micro-nanostructured polyaniline assembled in cellulose matrix via interfacial polymerization for applications in nerve regeneration. ACS Appl. Mater. Interfaces 8, 17090–17097. https://doi.org/10.1021/acsami.6b03555.
Yang, L., Xu, X., Liu, M., Chen, C., Cui, J., Chen, X., Wu, K., Sun, D., 2021. Wearable and flexible bacterial cellulose/polyaniline ammonia sensor based on a synergistic doping strategy. Sens. Actuators B: Chem. 334, 129647 https://doi.org/10.1016/j.snb.2021.129647.
Yang, Luyu, Yang, Lei, Wu, S., Wei, F., Hu, Y., Xu, X., Zhang, L., Sun, D., 2020. Three-dimensional conductive organic sulfonic acid co-doped bacterial cellulose/polyaniline nanocomposite films for detection of ammonia at room temperature. Sens. Actuators B: Chem. 323, 128689 https://doi.org/10.1016/j.snb.2020.128689.
Yao, J., Chen, S., Chen, Y., Wang, B., Pei, Q., Wang, H., 2017. Macrofibers with high mechanical performance based on aligned bacterial cellulose nanofibers. ACS Appl. Mater. Interfaces 9, 20330–20339.
Yatsu, A., Goto, H., 2021. Preparation of a cellulose-polyphenylacetylene-polyaniline composite. J. Text. Inst. 112, 1883–1889. https://doi.org/10.1080/00405000.2020.1867414.
Youssef, A.M., Hasanin, M.S., El-Aziz, M.E.A., Turky, G.M., 2021. Conducting chitosan/hydroxylethyl cellulose/polyaniline bionanocomposites hydrogel based on graphene oxide doped with Ag-NPs. Int. J. Biol. Macromol. 167, 1435–1444. https://doi.org/10.1016/j.ijbiomac.2020.11.097.
Yu, Y.H., An, L., Bae, J.H., Heo, J.W., Chen, J., Jeong, H., Kim, Y.S., 2021. A novel biosorbent from hardwood cellulose nanofibrils grafted with poly(m-aminobenzene sulfonate) for adsorption of Cr(VI). Front. Bioeng. Biotechnol. 9, 682070 https://doi.org/10.3389/fbioe.2021.682070.
Yue, L., Zheng, Y., Xie, Y., Liu, S., Guo, S., Yang, B., Tang, T., 2016. Preparation of a carboxymethylated bacterial cellulose/polyaniline composite gel membrane and its characterization. RSC Adv. 6, 68599–68605. https://doi.org/10.1039/C6RA07646G.
Zamanian, A., Hardiman, C., 2005. Electromagnetic radiation and human health: a review of sources and effects. High Frequency. Electronics 4, 16–26.
Zare, E.N., Lakouraj, M.M., 2014. Biodegradable polyaniline/dextrin conductive nanocomposites: synthesis, characterization, and study of antioxidant activity and sorption of heavy metal ions. Iran. Polym. J. 23, 257–266. https://doi.org/10.1007/s13726-014-0221-3.
Zare, E.N., Makvandi, P., Ashtari, B., Rossi, F., Motahari, A., Perale, G., 2019. Progress in conductive polyaniline-based nanocomposites for biomedical applications: a review. J. Med. Chem. 63, 1–22.
Zare, E.N., Abdollahi, T., Motahari, A., 2020. Effect of functionalization of iron oxide nanoparticles on the physical properties of poly (aniline-co-pyrrole) based nanocomposites: experimental and theoretical studies. Arab. J. Chem. 13, 2331–2339. https://doi.org/10.1016/j.arabjc.2018.04.016.
Zhan, C., Yu, G., Lu, Y., Wang, L., Wujcik, E., Wei, S., 2017. Conductive polymer nanocomposites: a critical review of modern advanced devices. J. Mater. Chem. C 5, 1569–1585. https://doi.org/10.1039/C6TC04269D.
Zhang, D., Zhang, L., Wang, B., Piao, G., 2013. Nanocomposites of polyaniline and cellulose nanocrystals prepared in lyotropic chiral nematic liquid crystals. J. Mater. 2013, 1–6.
Zhang, N., Yue, L., Xie, Y., Samuel, O.W., Omisore, O.M., Pei, W., Xing, X., Lin, C., Zheng, Y., Wang, L., 2018. A novel antibacterial membrane electrode based on bacterial cellulose/polyaniline/$AgNO_3$ composite for bio-potential signal monitoring. IEEE J. Transl. Eng. Health Med. 6, 1–10. https://doi.org/10.1109/JTEHM.2018.2863388.
Zhang, S., Fu, R., Du, Z., Jiang, M., Zhou, M., Gu, Y., Chen, S., 2017a. High-performance electrochromic device based on nanocellulose/polyaniline and nanocellulose/poly (3,4-ethylenedioxythiophene) composite thin films. Opt. Eng. 56, 077101 https://doi.org/10.1117/1.OE.56.7.077101.
Zhang, S., Fu, R., Gu, Y., Dong, L., Li, J., Chen, S., 2017b. Preparation of nanocellulose-based polyaniline composite film and its application in electrochromic device. J. Mater. Sci. Mater. Electron. 28, 10158–10165. https://doi.org/10.1007/s10854-017-6778-9.
Zhang, S., Sun, G., He, Y., Fu, R., Gu, Y., Chen, S., 2017c. Preparation, characterization, and electrochromic properties of nanocellulose-based polyaniline nanocomposite films. ACS Appl. Mater. Interfaces 9, 16426–16434. https://doi.org/10.1021/acsami.7b02794.
Zhang, W., Wang, H., Hu, X., Feng, H., Xiong, W., Guo, W., Zhou, J., Mosa, A., Peng, Y., 2019. Multicavity triethylenetetramine-chitosan/alginate composite beads for

enhanced Cr(VI) removal. J. Clean. Prod. 231, 733–745. https://doi.org/10.1016/j.jclepro.2019.05.219.
Zhang, Y., Wang, Z., Zhang, B., Zhao, G.-L., Guo, S.M., 2015. The electromagnetic interference shielding effectiveness of high aspect-ratio SiC nanofibers/epoxy composites. RSC Adv. 5, 93499–93506. https://doi.org/10.1039/C5RA16007C.
Zhang, Z., Wang, G., Gu, W., Zhao, Y., Tang, S., Ji, G., 2022. A breathable and flexible fiber cloth based on cellulose/polyaniline cellular membrane for microwave shielding and absorbing applications. J. Colloid Interface Sci. 605, 193–203. https://doi.org/10.1016/j.jcis.2021.07.085.
Zhao, Lu, Zhao, Liang, Xu, Y., Qiu, T., Zhi, L., Shi, G., 2009. Polyaniline electrochromic devices with transparent graphene electrodes. Electrochim. Acta 55, 491–497. https://doi.org/10.1016/j.electacta.2009.08.063.
Zheng, D., Zhang, Y., Guo, Y., Yue, J., 2019. Isolation and characterization of nanocellulose with a novel shape from walnut (Juglans regia L.) shell agricultural waste. Polymers 11, 1130.
Zheng, Y., Liu, Y., Wang, A., 2012a. Kapok fiber oriented polyaniline for removal of sulfonated dyes. Ind. Eng. Chem. Res. 51, 10079–10087. https://doi.org/10.1021/ie300246m.
Zheng, Y., Wang, W., Huang, D., Wang, A., 2012b. Kapok fiber oriented-polyaniline nanofibers for efficient Cr(VI) removal. Chem. Eng. J. 191, 154–161. https://doi.org/10.1016/j.cej.2012.02.088.
Zhong, C., 2020. Industrial-scale production and applications of bacterial cellulose. Front. Bioeng. Biotechnol. 8, 605374 https://doi.org/10.3389/fbioe.2020.605374.
Zhou, M., Chi, M., Luo, J., He, H., Jin, T., 2011. An overview of electrode materials in microbial fuel cells. J. Power Sources 196, 4427–4435. https://doi.org/10.1016/j.jpowsour.2011.01.012.
Zhou, S., Apostolopoulou-Kalkavoura, V., Tavares da Costa, M.V., Bergström, L., Strømme, M., Xu, C., 2020. Elastic aerogels of cellulose nanofibers@metal–organic frameworks for thermal insulation and fire retardancy. Nano-Micro Lett. 12, 9. https://doi.org/10.1007/s40820-019-0343-4.
Zielińska, D., Rydzkowski, T., Thakur, V.K., Borysiak, S., 2021. Enzymatic engineering of nanometric cellulose for sustainable polypropylene nanocomposites. Ind. Crops Prod. 161, 113188 https://doi.org/10.1016/j.indcrop.2020.113188.